APPLICATION OF BORON/EPOXY REINFORCED ALUMINUM STRINGERS FOR THE CH-54B HELICOPTER TAIL CONE

PHASE I: DESIGN, ANALYSIS, FABRICATION AND TEST

Final Report

by

R. T. Welge

July 1971

Prepared under Contract No. NAS1-10459

for

Langley Research Center
NATIONAL AERONAUTICS AND SPACE ADMINISTRATION

by

Sikorsky Aircraft
Division of United Aircraft Corporation

NASA-CR-111929

APPLICATION OF BORON/EPOXY REINFORCED ALUMINUM STRINGERS FOR THE CH-54B HELICOPTER TAIL CONE

PHASE I: DESIGN, ANALYSIS, FABRICATION AND TEST

Final Report

by

R. T. Welge

July 1971

Prepared under Contract No. NAS1-10459

by

Sikorsky Aircraft
Division of United Aircraft Corporation

for

Langley Research Center
NATIONAL AERONAUTICS AND SPACE ADMINISTRATION

-o00o-

FOREWORD

This summary technical report was prepared by Sikorsky Aircraft, Division of United Aircraft Corporation, under NASA Contract NAS1-10459, and covers the work performed during the period of February 1971 through May 1971 on Phase I of a two-phase contract.

This report contains the account of the experimental hardware phase of this study which incorporates the design, fabrication and tests of boron/epoxy reinforced stringers. The detailed structural analysis of the aircraft is contained in a separate report entitled "CH-54B Boron/Epoxy Reinforced Tail Cone Detailed Structural Substantiation." A copy of this report is on file with NASA, U.S. Army Air Mobility Research and Development Laboratory (Eustis Directorate) and the Federal Aviation Agency.

Technical monitor for this program was Richard A. Pride of the Structural Materials Division, NASA Langley Research Center.

The individuals who made technical contributions to the program and their areas of activity are as follows:

R. T. Welge	Program Manager
D. W. Lowry	Structures
S. W. Ciardullo	Structures
J. B. Sainsbury-Carter, Ph.D.	Analysis
K. M. Adams	Fabrication
S. C. Svensson	Fabrication
C. Kowalkowski	Manufacturing
J. Barto	Manufacturing
H. Kearny	Test

TABLE OF CONTENTS

FIGURES

TABLES

LIST OF SYMBOLS

A	Area, $Inches^2$
D	Drag Load, Pounds
E	Percent of Area (when used in computer shear and bending analysis)
E	Young's Modulus, $Pounds/Inches^2$
F	Stringer Stress, $Pounds/Inches^2$
IY	Area Moment of Inertia About the Lateral Axis, $Inches^4$
IYZ	Product of Inertia About Centroidal Axes, $Inches^4$
IZ	Area Moment of Inertia About the Vertical Axis, $Inches^4$
K	Panel Taper Ratio
L.S.	Stringer Length, Inches
MX	Moment About the Longitudinal Axis, Pound/Inches
MY	Moment About the Lateral Axis, Pound/Inches
MZ	Moment About the Vertical Axis , Pound/Inches
P	Stringer Load, Pounds
$P_{allow.}$	Allowable Stringer Load, Pounds
PY	Stringer Load Component Along the Lateral Axis, Pounds
PZ	Stringer Load Component Along the Vertical Axis, Pounds
Q	Shear Flow at Forward End of Bay, Pounds/Inch
Q/K	Average Shear Flow, Pounds/Inch
Q/KK	Shear Flow at Aft End of Bay, Pounds/Inch
S	Lateral Applied Load, Pounds
V	Vertical Applied Load, Pounds
Y	Lateral Coordinate, Inches
Z	Vertical Coordinate, Inches
σ	Stress, $Pounds/Inches^2$

List of Symbols (continued)

α	Coefficient of Thermal Expansion, Inches/Inch/Degree Fahrenheit

Subscripts

A	Aluminum
a	Adhesive
B	Boron/Epoxy
R	Reinforced
SK	Skin
STR	Aluminum Stringer

APPLICATION OF BORON/EPOXY REINFORCED ALUMINUM STRINGERS FOR THE CH-54B HELICOPTER TAIL CONE

PHASE I REPORT

DESIGN, ANALYSIS, FABRICATION AND TEST

by

R. T. Welge

SUMMARY

Phase I of this contract (NAS1-10459) was a preprototype study of the CH-54B tail cone in which component fabrication, testing, and analysis was done, and the strength adequacy of boron/epoxy reinforced members was verified.

The vertical stiffness of the CH-54B tail cone was maintained with an approximate 70 per cent saving in stiffening weight by the application of boron/epoxy reinforced stringers.

The boron/epoxy stringer reinforcement was configured such that the stiffness of the current production aluminum tail cone was achieved with minor changes. A boron/epoxy strip 0.750 x 0.250 inches was bonded to the vertical legs of the standard aluminum stringers. A joint analysis detailed the end taper of the boron/epoxy reinforcement necessary to reduce the peak shear stresses.

Conventional and boron reinforced panels were fabricated and comparative shear and compression panel tests conducted. Test results indicated that the shear capability of the panels was unchanged by the presence of the boron, while the compression test results showed the reinforced panels capable of withstanding higher loads. Of significance is the fact that an adequate bond and tapered boron/epoxy joint was achieved.

Comparative fatigue tests were conducted for both boron/epoxy reinforced stringers and conventional aluminum members. The tests were conducted at representative aircraft loads and cycles. Holes were drilled in the boron and aluminum fatigue specimens to simulate frame clip attachments. Both the boron reinforced and aluminum stringers satisfied the aircraft fatigue life requirements.

Load deflection values were obtained for the boron/epoxy reinforced stringers to determine the effective stiffness of the hybrid stringer. Tests verified the predicted stiffness for the tail cone using boron/epoxy reinforced stringers. Bolt holes in the boron/epoxy had no noticeable effect on the results.

An analysis of the tail cone was made with and without boron/epoxy reinforcements, and all positive margins of safety were achieved under all conditions. Induced thermal effects were predicted and confirmed by test. The thermal effects were accounted for in the analytical study.

Fabrication techniques, developed in this phase, were such that only two (2) out of thirty-five (35) test specimens were found to have areas of questionable bond. The Fokker bond tester was used to inspect all test specimens. Holes were drilled in the boron reinforcement with both diamond impregnated and high speed steel drills.

Tail cone fabrication drawings of the CH-54B incorporating boron reinforced stringers were made to facilitate construction in Phase II and to assess the required modifications. The basic geometry of the stringers and frames remain unchanged.

The Phase I study confirmed the fact that boron/epoxy reinforced stringers can be fabricated and that their static and fatigue strength is adequate to meet the requirements of the CH-54B.

1.0 INTRODUCTION

The original CH-54A helicopter airframe structure was designed for the applied static loads due to flight and ground conditions. During the flight development phase of the CH-54A, it became necessary to provide additional structure to increase the vertical bending stiffness of the tail cone and tail cone transition section in order to satisfy a dynamic fuselage requirement. Skin gages 0.040 inches in thickness on the top and the bottom of the tail cone and transition section were replaced with skins 0.080 - 0.140 inches in thickness. The weight increase due to stiffening was approximately 160 pounds.

Preliminary analysis of boron/epoxy reinforced stringers indicated that the required tail cone stiffness of the CH-54B could be achieved by using the original thin skins, and reinforcing the top and bottom stringers with approximately thirty (30) pounds of boron/epoxy and eighteen (18) pounds of aluminum skin stiffeners.

This study is Phase I of a two-phase program and was conducted to prove the feasibility of fabrication, analysis, structural strength and field maintenance using boron/epoxy reinforced stringers. Phase II includes fabrication of the tail cone and installation on an aircraft, flight testing, and in-service evaluation.

2.0 TAIL CONE ANALYSIS

Objective

The objective of this analysis was to substantiate the structural integrity of the tail cone structure and to assure that the vertical stiffness of the present CH-54B was not changed by the use of boron/epoxy reinforced stringers.

Approach

As Phase II of this contract is a flight test program and the use of boron/epoxy reinforced stringers is relatively new, a decision was made to retain the design static strength of the CH54B tail cone assuming no boron/epoxy reinforcement was present.

The analysis matrix incorporated eight sections of the tail cone, five critical flight conditions and three assumed tail cone reinforcement conditions. The assumed reinforcement conditions were: no boron reinforcement, complete boron reinforcement and partial boron reinforcement. The partial boron reinforcement condition assumed the boron completely debonded on various stringers in a tail cone section. This was done to assess the structural effect of a shift in the neutral axis on the section. A Sikorsky automated fuselage shear and bending analysis was used which utilizes the UNIVAC 1108 computer.

The analysis of the tail cone subjected to the loads of the above matrix of conditions is documented in Reference 1, "CH-54B Boron/Epoxy Reinforced Tail Cone Detailed Structural Substantiation".

Discussion

The tail cone of the CH-54B helicopter is of semi-monocoque construction with frames and stringers spaced at approximately 20 and 6 inches respectively. The tail cone is considered a cantilever beam having a required stiffness criteria to eliminate a tail resonance problem. The overall stiffness of the structure includes what is referred to as the tail cone, aft of Station 549, and the transition section, forward of Station 549. An overall view of the tail cone with respect to the aircraft is shown in Figure 2-1.

The addition of boron reinforced stringers permitted the removal of heavy aluminum top and bottom skins in both the transition and tail cone

section. Twelve stringers were reinforced with boron/epoxy, seven on the lower skin and five on the upper skin. The reinforcement permitted skin gage reductions from .140 inches to .040 inches in some sections of the tail cone.

The structural modifications made to the current structure due to the addition of boron/epoxy reinforced stringers were minimal. Analysis of the no boron condition necessitated the addition of short stringer sections to reduce skin buckling. These short stringer sections are referred to in this report as panel breakers. The partial boron condition had no effect on the structure. Some panel breaker locations necessitated removal of current frame lightening holes. The boron/epoxy stringer reinforcement was terminated at the tail cone manufacturing joint in order to retain the same fittings. The stringer reinforcement did not extend into the transition area. The present aircraft structural geometry and gages and the modifications required by the addition of the boron/epoxy reinforced stringers are shown in Figures 2-2, 2-3.

The stiffness of the overall reinforced structure meets that of the present tail cone, within computation accuracy, and is shown in Figure 2-4. Vertical bending stiffness, or deflection, of the boron reinforced and the current production tail cone was obtained by a double integration of the M/EI distribution where the moment of inertia was obtained from the computerized shear and bending analysis. The moment was based upon a unit vertical load applied at Station 749. The effective area modulus product for the reinforced stringer, which is an input into the computerized analysis program of the boron/epoxy stringer, was confirmed by the load strain tests as detailed in Section 5.0.

A Sikorsky automated fuselage shear and bending moment analysis utilizing the UNIVAC 1108 computer was used in the various structural analyses. The analysis of the no-boron case was further facilitated by a company automated program which determines the margins of safety in stiffened aluminum panels subjected to combined shear and compression loads. The critical geometry, assuming partial boron reinforcement, was found to be when the lower stringer reinforcements were assumed ineffective.

The analysis of the hybrid structure included the induced fabrication and environmental thermal effects. The stress-free condition of the boron reinforced stringer occurs at the curing temperature of 250° F. The critical condition for the structure is at -65° F. This temperature condition represents the maximum thermal gradient for the structure and is the minimum environmental temperature for the CH-54B. Thermal stress equations and test results are detailed in Section 6.0. The thermal effects of fabrication is to induce tension stresses in the aluminum stringers and compression stresses in the boron reinforcement at any temperature below that of the stress-free condition.

The aluminum stringer, boron reinforcement and aluminum skin loads for the externally applied loads and thermal induced loads were calculated by the formulas in Section 6.0. It is to be noted that the delta temperatures for the stringer and skin are different, as the skin is riveted to the aluminum stringer at room temperature while the stringer is only in a stress free condition at 250° F.

Individual component member and combined hybrid stringer element loads are presented in Figures 2-5 and 2-6. The critical flight design loads for the stringers used in the tail cone structure are also presented in the above figures. No tension flight design load is given in Figure 2-6, as this gage stringer does not experience this type of loading for the critical conditions analyzed.

The aluminum stringer is critical for an applied tension load, and the allowable load is based upon the allowable tensile stress minus the induced thermal stress. The boron/epoxy reinforcement is critical for an applied compression load. The allowable load was computed by a Sikorsky orthotropic plate stability program and includes the reduction for the induced thermal stresses.

The critical design conditions were as follows and are referenced in Tables 2-1, 2-2, and 2-3:

a. Yaw Left - G. W. 47000 lbs. fwd. c. g. (CH1F5)
b. Yaw Left - G. W. 47000 lbs. aft c. g. (CH2F5)
c. Yaw Left - G. W. 44620 lbs. neutral c. g. (CH7F5)
d. Yaw Kick Left - G. W. 30000 lbs. most fwd. c. g. (CH10F5)
e. Tail Down Landing, Main Gear Impact - G. W. 47000 lbs. fwd. c. g. (CH1G13)

A summary of the critical margins of safety for the tail cone is presented in Tables 2-1, 2-2, 2-3 and the corresponding stringer locations are shown in Figure 2-7. The margins of safety were obtained from the detailed analysis documented in Reference 1. The skin to stringer rivets were analized and found not to be critical.

Conclusion

The structural integrity of the tail cone is maintained for the critical flight conditions with and without boron/epoxy reinforced stringers. The modifications required to the aircraft structures by the addition of the reinforced stringers are small.

FIGURE 2-1. CH-54B HELICOPTER.

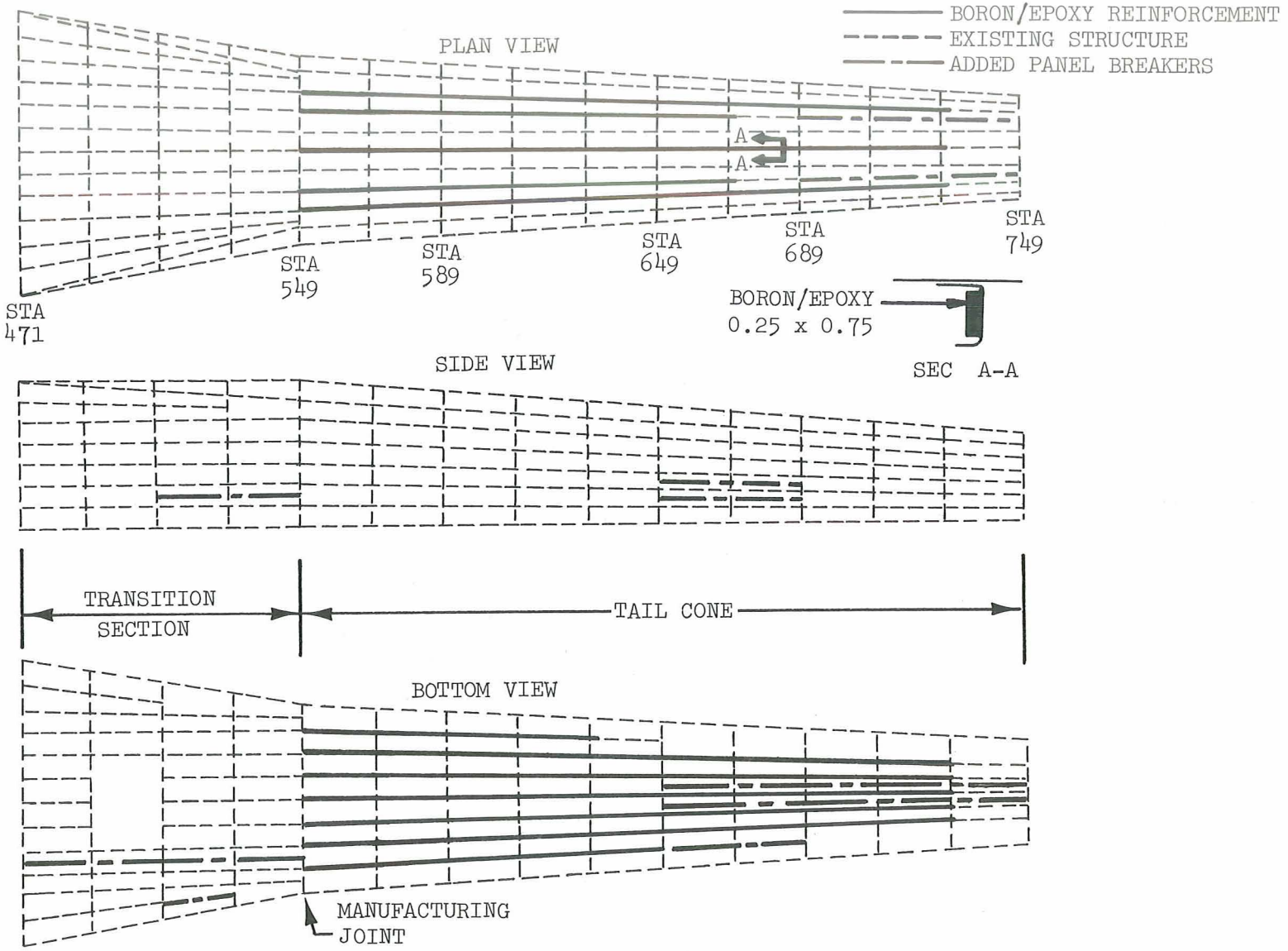

FIGURE 2-2. CH-54B TAIL CONE STRINGER MODIFICATIONS.

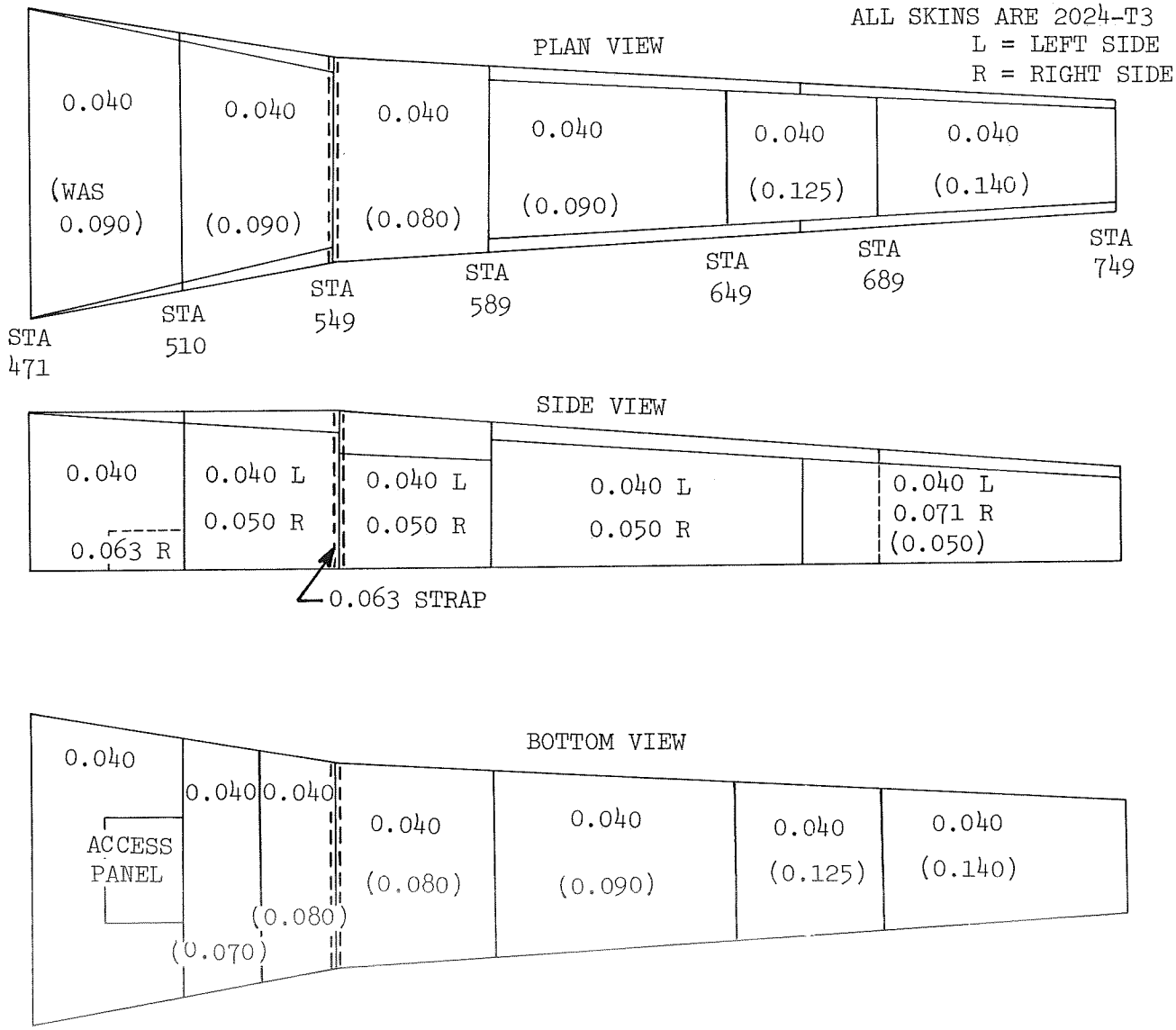

FIGURE 2-3. CH-54B TAIL CONE SKIN GAGE MODIFICATIONS.

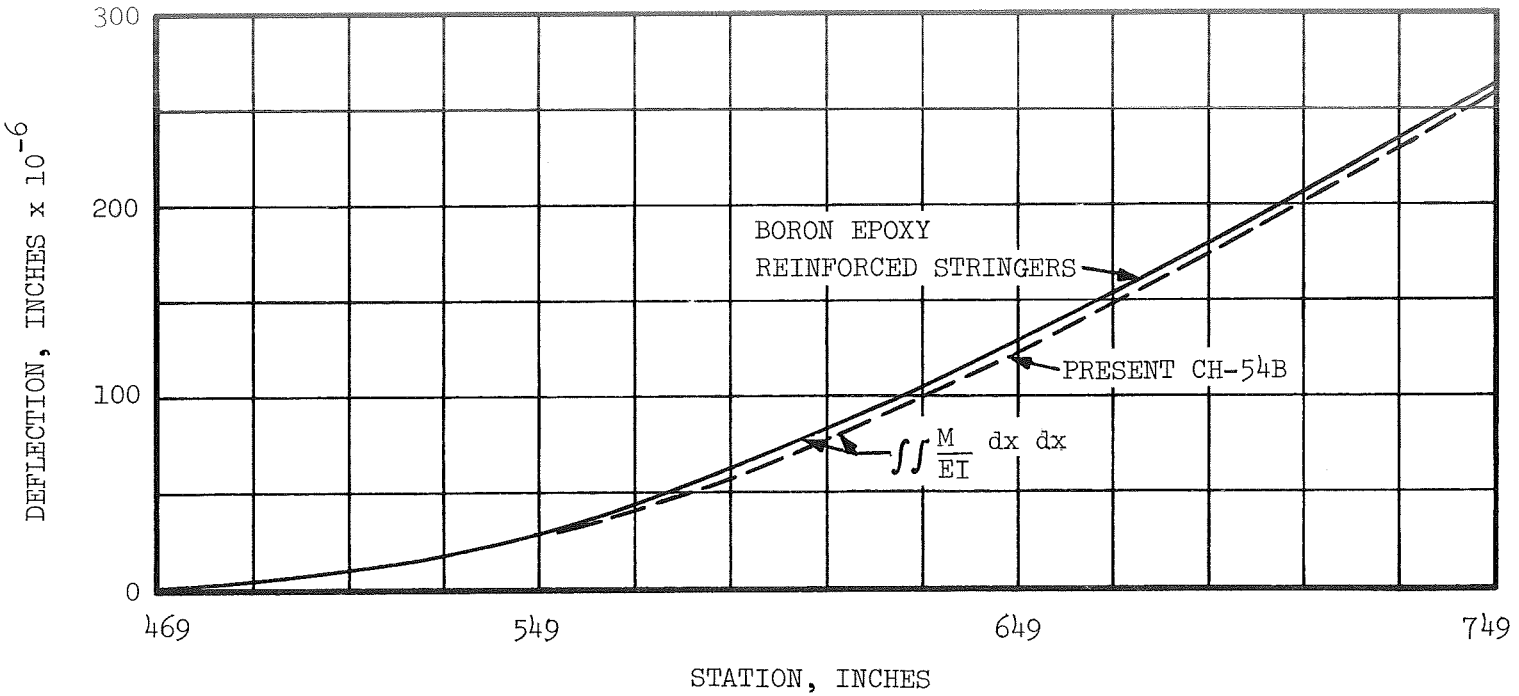

FIGURE 2-4. CH-54B FUSELAGE VERTICAL DEFLECTION.

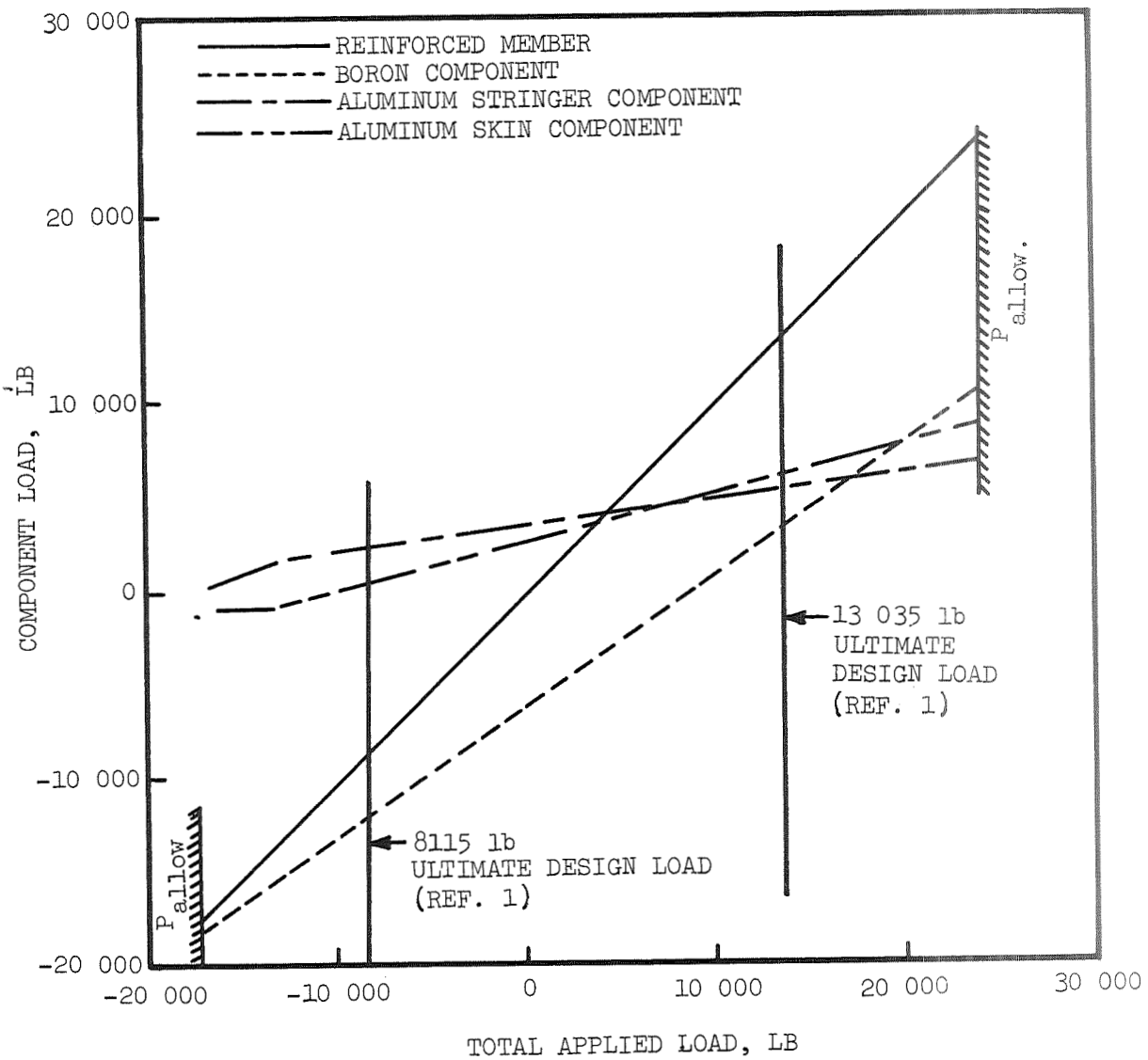

FIGURE 2-5. BORON/EPOXY REINFORCED STRINGER LOAD VERSUS TOTAL APPLIED LOAD FOR A 0.050-INCH ALUMINUM STRINGER AT -65° F.

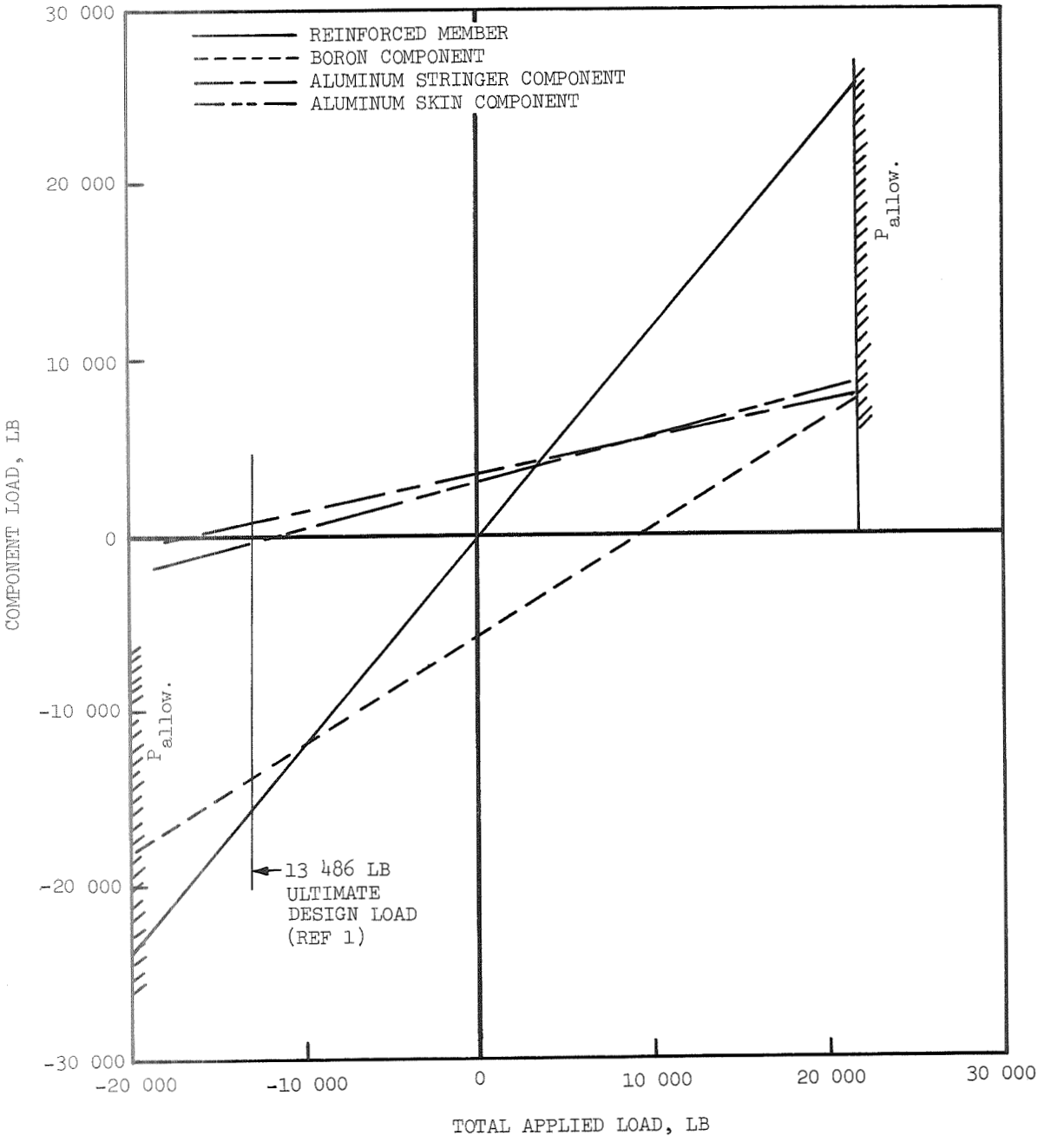

FIGURE 2-6. BORON/EPOXY REINFORCED STRINGER LOAD VERSUS TOTAL APPLIED LOAD FOR A 0.063-INCH ALUMINUM STRINGER AT -65° F.

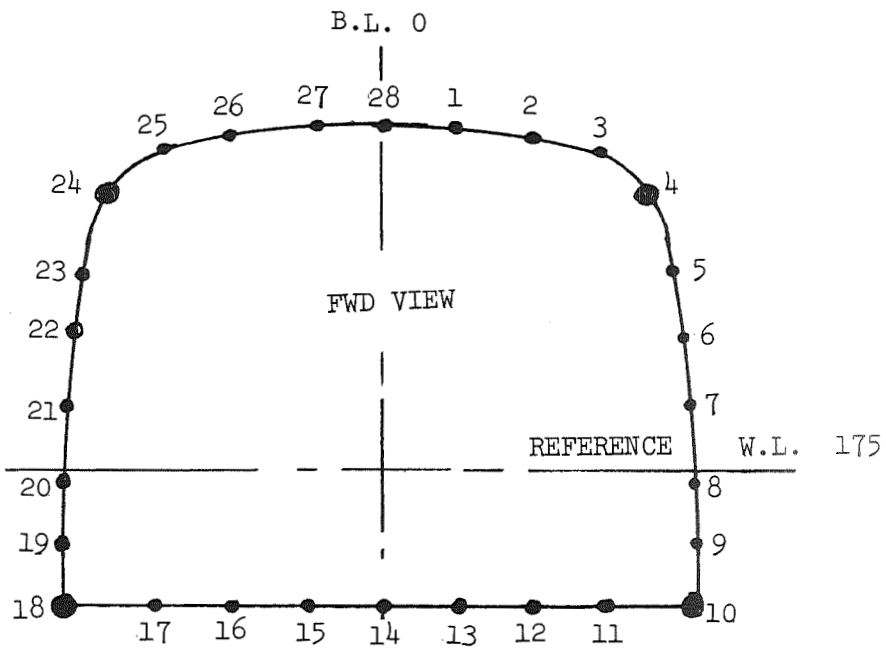

FIGURE 2-7. TAIL CONE STRINGER NUMBERING SYSTEM.

TABLE 2-1.

MINIMUM MARGINS OF SAFETY
TRANSITION SECTION STATION 471 to 549
(NONREINFORCED)

STA. 471

STRINGER NUMBER	CONDITION	MARGIN OF SAFETY
11	c	.04
15	c	.05
16	c	.05

STA. 490.5

16	c	.03

STA. 510

12	c	.03
16	c	.01

STA. 529.5

10	c	.05
12	c	.02
16	c	.03

TABLE 2-2

MINIMUM MARGINS OF SAFETY
TAIL CONE STATIONS 549 to 749
(NONREINFORCED)

STA. 549

STRINGER NUMBER	CONDITION	MARGIN OF SAFETY
9	d	.01
9	c	.01
11	d	.01
19	e	.01
23 STRINGER TO FITTING	d	.04

STA. 589

7	d	.05
7	b	.04
7	c	.03
9	d	.00
9	c	.00

STA. 649

5	b	.03
5	c	.03
6	d	.04
6	b	.01
6	c	.01
7	b	.05
7	c	.04
8	c	.05
9	d	.01
9	c	.01
13	d	.03

STA. 689

6	d	.01
6	b	.01
12	d	.01
13	d	.04
16	d	.05

TABLE 2-3.

MINIMUM MARGINS OF SAFETY
TAIL CONE STATION 549 to 749
REINFORCED WITH BORON/EPOXY

STA. 549

STRINGER NUMBER	CONDITION (see Ref. 1)	MARGIN OF SAFETY
5 (1)	b	.05

STA. 549

7 (1)	c Partial Bond Failure	.05

(1) These are side stringers and are not reinforced with boron/epoxy

3.0 BORON/EPOXY REINFORCED TAPER GEOMETRY

Objective

This investigation was made to determine the boron/epoxy taper geometry such that the induced shear stress peaks in the adhesive were reduced to an acceptable stress level.

Approach

In designing the boron/epoxy taper joint, various criteria had to be met. The taper had to be short enough to maintain the required tail cone stiffness yet be long enough to achieve low values of adhesive shear stress and basic stringer stresses. A computerized Sikorsky-developed program for the analysis and optimum design of bonded tapered joints was used to define the joint geometry. The data input included the design allowable adhesive shear stress and adherend direct stresses such that the geometry of the taper would result in a satisfactory stress field.

Discussion

A Sikorsky joint analysis program was used to analyze the tapered joints. The shear modulus of AF-126-2 adhesive in the linear range (up to 2,500 psi) used in the analysis was 80,000 psi for an average bond thickness of 0.005 inches.

The test specimens used in this study were fabricated with a 4-inch taper; however, a 12.5-inch taper was found necessary for acceptable tail cone load redistribution. An analysis was made and resulting stresses compared for both tapers. The analysis also included the effects of a fiberglass insert fabricated into the tapered ends.

To reduce the high peak shear stresses still remaining at the end of the joint, two layers of 0^{o} fiberglass/epoxy (1002-S) were introduced over the first two inches of the joint bewteen the boron and aluminum as illustrated in Figure 3-1. This had the effect of introducing a "soft" insert at the joint end, thereby reducing the sudden discontinuity in stiffness. The taper designs include practical constraints such as the minimum taper thickness and step size being integer multiples of ply thickness.

The reinforced stringer test specimens were subjected to a concentrated load, whereas in the actual aircraft loads are also induced into the stringer by variable skin shear loads. An analysis was made of the 4-inch taper under the test specimen loading conditions with and without the fiberglass insert. An analysis was also made of the 4-inch and 12.5-inch tapered joint under the aircraft loading conditions with the fiberglass insert.

In all joint analyses the loads were applied uniformly to the aluminum stringer skin combination. This uniform load distribution was redistributed by means of shear lag due to the presence of boron/epoxy reinforcement bonded to the aluminum stringer. Figure 3-2 illustrates the expected direct stress distribution at various stations along the reinforced stringer. In order to compute the shear lag characteristics of load redistribution, the aluminum stringer was considered unwrapped and made integral with the skin. The boron/epoxy reinforcement was converted into its equivalent aluminum area and divided into a series of equivalent concentrated areas.

In figures (3-3) through (3-27), the plots of adhesive shear stress versus distance from the joint end, are illustrated by a solid line representing the analytical output from the bonded joint design computer program and a discontinuous line labled "expected practical distribution."

The analysis assumes a constant shear strain across the adherend thickness. This is an approximation to simplify the analysis in order to reduce computer time during optimization. In reality the shear strain is a maximum at the inner surface of the adherend next to the adhesive and zero on the free outer surface. The discontinuous line is an attempt to estimate and correct the adherend shear lag error through the adherend thickness produced by this analytical assumption.

As the adherend becomes thicker so the influence of any discontinuity on the outer free surface is felt less abruptly by the adhesive layer on the inner surface.

The results on the analysis for the 4-inch tapered joint under applied test loads are shown in Figures 3-3 through 3-14. The fiberglass insert had the effect of reducing the initial adhesive peak shear stress at the joint end in the tension case from 2,130 psi to 980 psi. (See Figures 3-3 and 3-4). The initial adhesive peak stress was reduced from 5,930 psi to 2,850 psi for the compression case (See Figures 3-9 and 3-10). Analytically, the glass insert is shown to reduce the initial peak adhesive shear stress by 53 per cent for the tension condition and 52 per cent for the compression condition.

The computed shear stress distribution from analysis, indicates a series of rapid stress gradient changes due to the geometry discontinuities produced by the introduction of each additional layer of composite. Although the glass insert significantly reduced the primary shear stress peak, a second shear stress peak is produced, at a distance of 0.25 inches from the joint end coincident with the first layer of boron/epoxy. If this

peak is realistic, the reduction in maximum adhesive shear stress is reduced to 37 per cent for the tensile case and 40 per cent for the compressive case.

In Figure 3-4, the expected practical distribution illustrates a region of near constant shear stress over approximately 2.5 inches. This is the general region in which apparent bond deviations were found in the fatigue tests.

The design of the bonded joint for the actual aircraft reinforced stringer loads followed a similar procedure to that utilized for the test specimens.

From the fuselage analysis (see Reference 1), significant loads are introduced to the boron/epoxy reinforced stringers from the longerons in the tail cone/transition or manufacturing joint area. This load transfer is made through shear in the skins. The load redistribution in this region is due to the termination of the boron/epoxy stringer reinforcement and the resulting decrease in stringer loads and increase in longeron loads. To prevent overstressing the aluminum stringer, the taper length was increased from 4 inches to 12.5 inches, thus spreading the length over which the load is transferred from or to the boron/epoxy reinforcement. The respective tapers are shown in Figure 3-15.

Figures 3-16 through 3-27 show the resulting shear and direct stress distributions in the adhesive and adherends for the 4- and 12.5-inch tapers. The critical tension and compression flight loads were applied to both tapered joints. The fiberglass insert was assumed in both tapers.

The computed shear stress distribution in the 12.5-inch joint shown in Figure 3-16 indicates an initial shear stress of 1,000 psi at the joint end. This value reduces rapidly to approximately 450 psi and peaks again to 1,460 psi at the beginning of the first layer of boron/epoxy. A secondary major peak of 1,100 psi occurs two inches from the joint end where the glass insert ends and the reinforcement becomes all boron/epoxy. This secondary peak compares to approximately 1,400 psi for the corresponding 4-inch taper. (See Figure 3-17).

It is expected that the practical adhesive shear stress distribution will not follow such rapid stress gradients as discussed previously but will follow a smoothed distribution curve as illustrated in Figures 3-16, 3-17. Therefore, in the 12.5-inch taper, maximum shear stress of 1,120 psi and 2,900 psi in the tension and compression respectively are expected as compared with 1,320 psi and 2,900 psi for the corresponding 4-inch tapered joint.

The correlation of the joint analysis with test data was beyond the scope of this program; however, the joint design for the test specimens did withstand the application of the design static and dynamic loadings.

Conclusions and Recommendations

The insertion of two layers of unidirectional glass/epoxy, approximately two inches in length, between the boron/epoxy reinforcement and the aluminum stringer at the ends of the tapered joints reduces the peak adhesive shear stresses by approximately 53 per cent.

The resulting adhesive shear stress distribution for the 4-inch tapered boron/epoxy reinforcement test specimens shows that the maximum shear stress is one-half inch away from the joint end. It is questionable whether the rapid shear stress gradient changes in the adhesive, as analytically predicted, are practically possible. A smoothing procedure was attempted, resulting in an adhesive shear stress distribution which indicates a general region of high shear stress approximately 2.5 inches away from the joint end.

The maximum adhesive shear stresses in the 12.5-inch taper are equal to or less than those in the 4-inch taper. It is therefore recommended that the longer taper be installed on the flight test article in Phase II of this contract.

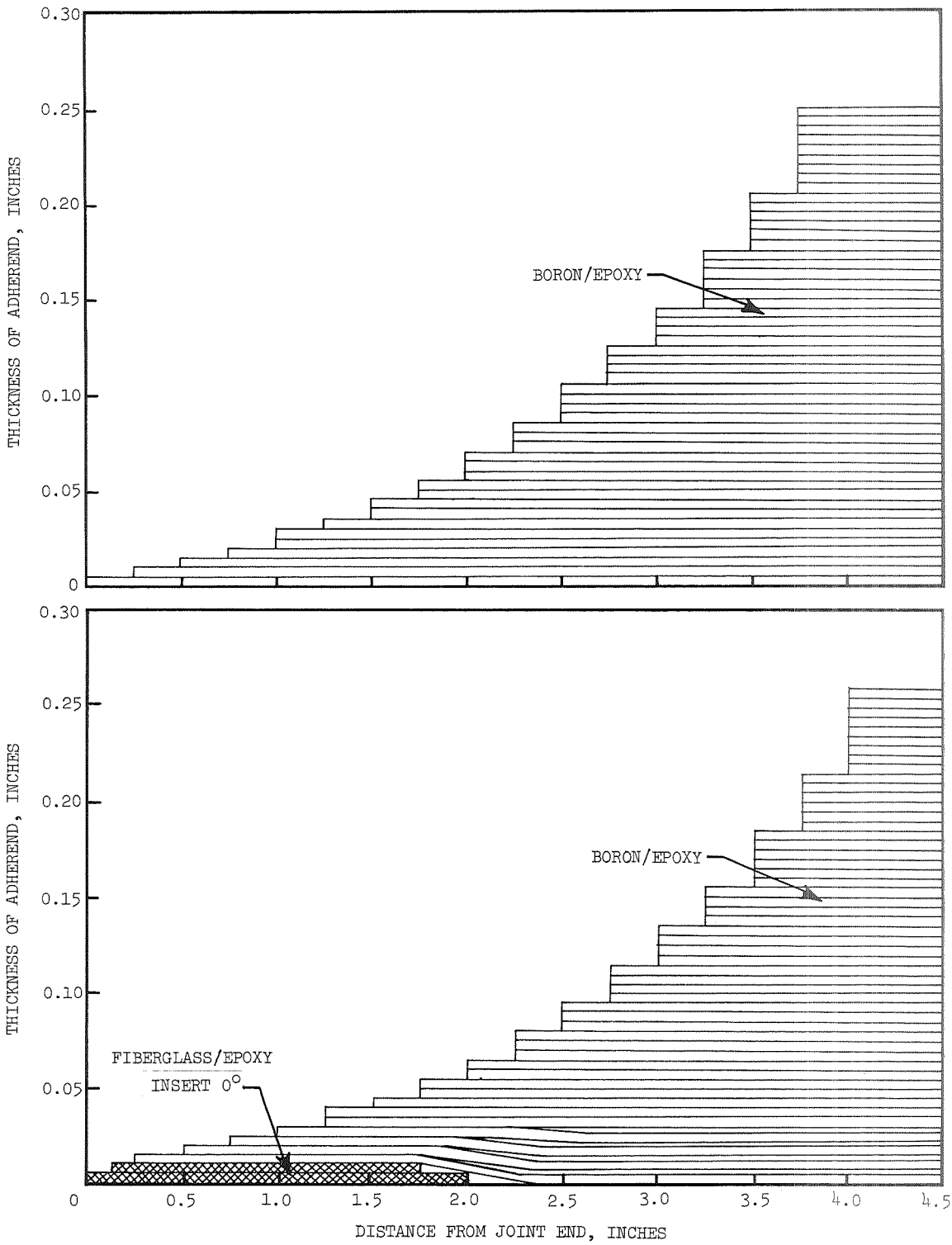

FIGURE 3-1. 4-INCH TAPERED JOINT GEOMETRY.

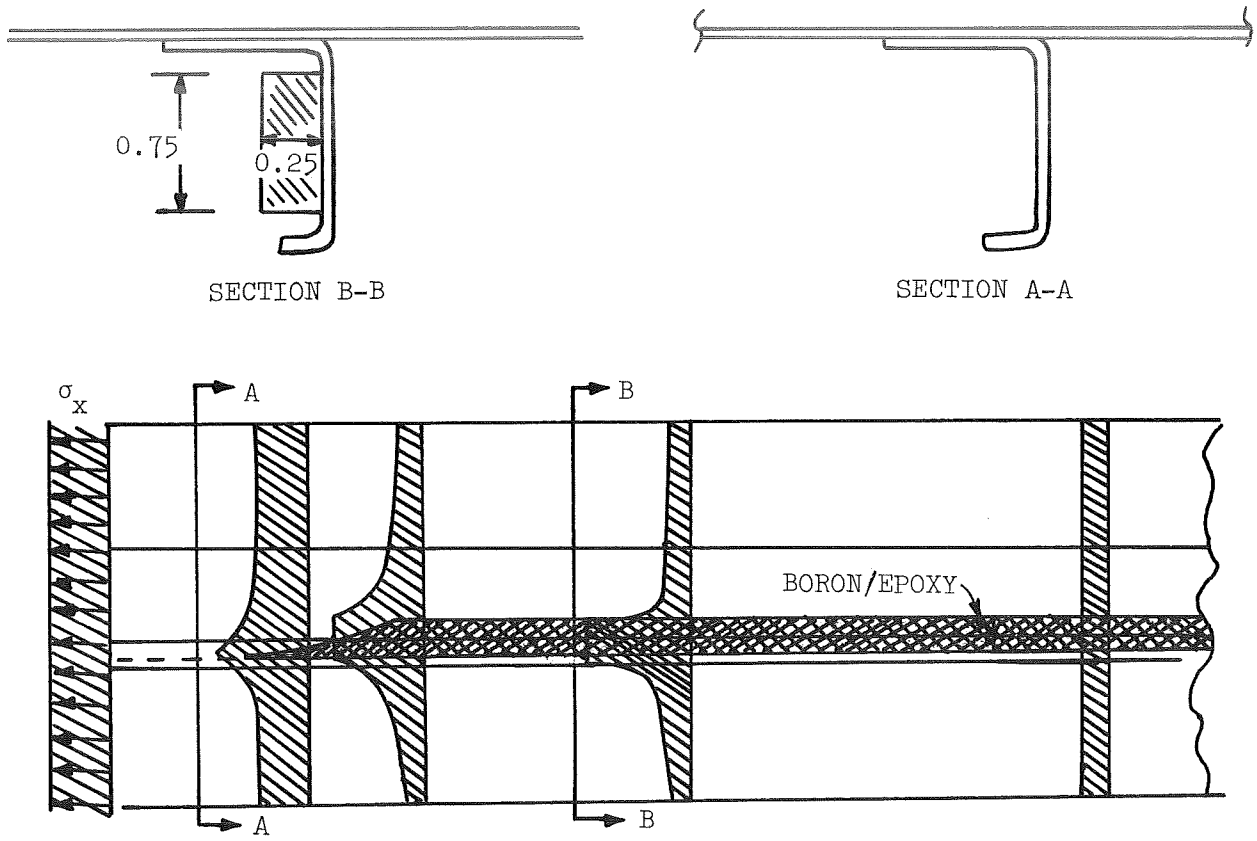

FIGURE 3-2. σ_x STRESS DISTRIBUTION ALONG LENGTH OF REINFORCED STRINGER.

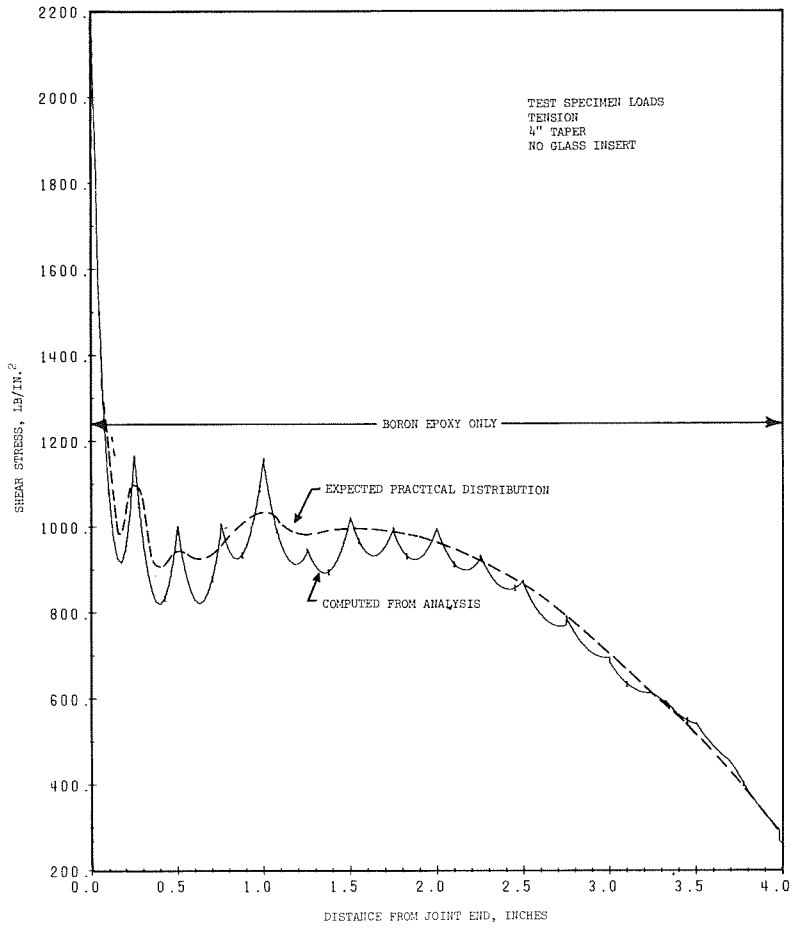

FIGURE 3-3. ADHESIVE SHEAR STRESS DISTRIBUTION IN 4-INCH TAPERED TENSILE JOINT - NO GLASS INSERT - TEST LOADS.

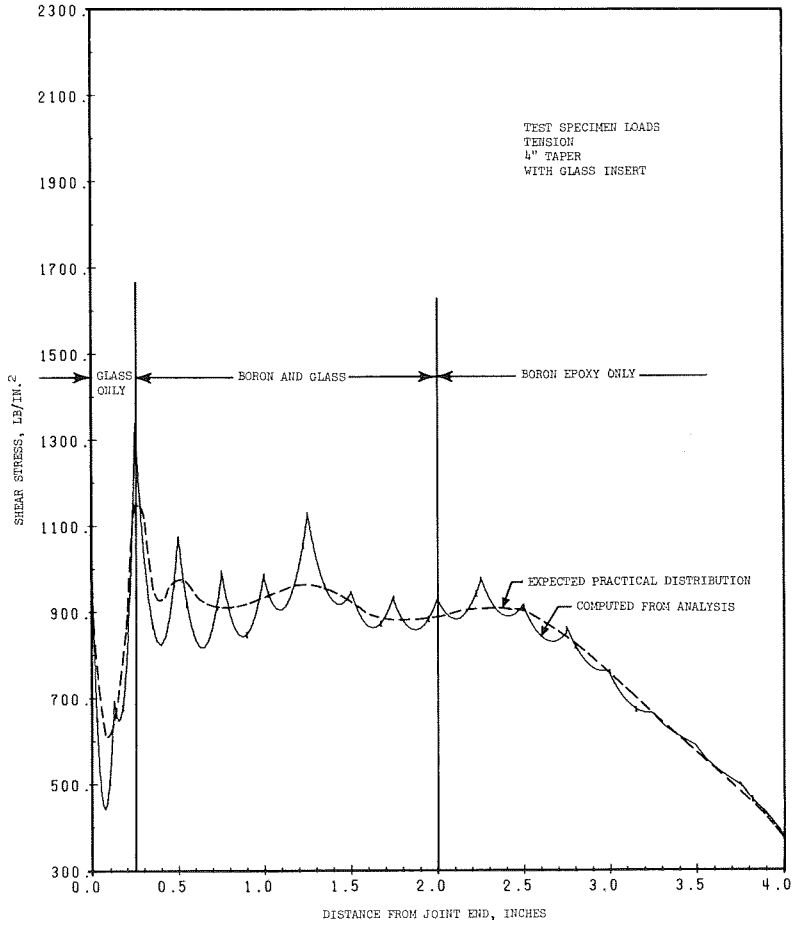

FIGURE 3-4. ADHESIVE SHEAR STRESS DISTRIBUTION IN 4-INCH TAPERED TENSILE JOINT - WITH GLASS INSERT - TEST LOADS.

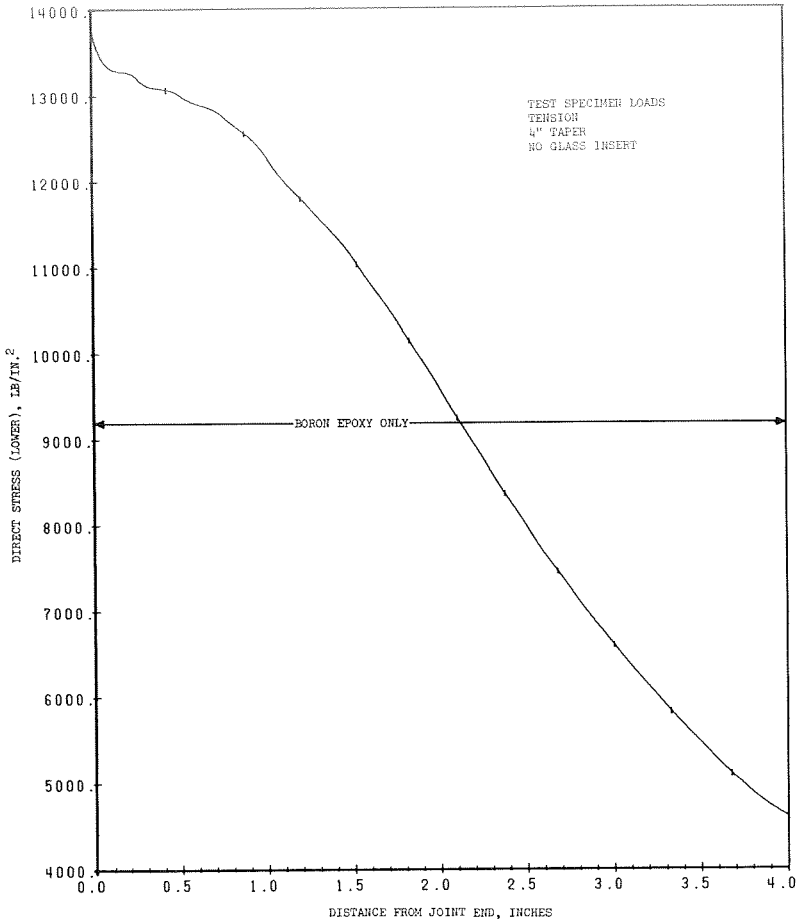

FIGURE 3-5. ALUMINUM STRESS DISTRIBUTION IN 4-INCH TAPERED TENSILE JOINT - NO GLASS INSERT - TEST LOADS.

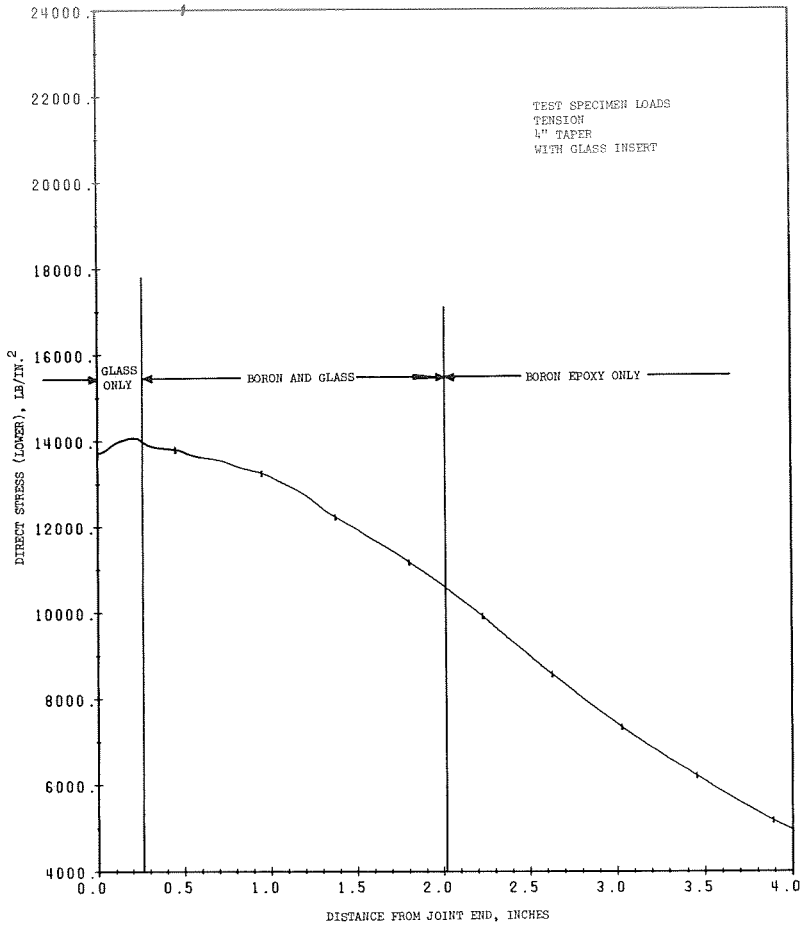

FIGURE 3-6. ALUMINUM STRESS DISTRIBUTION IN 4-INCH TAPERED TENSILE JOINT - WITH GLASS INSERT - TEST LOADS.

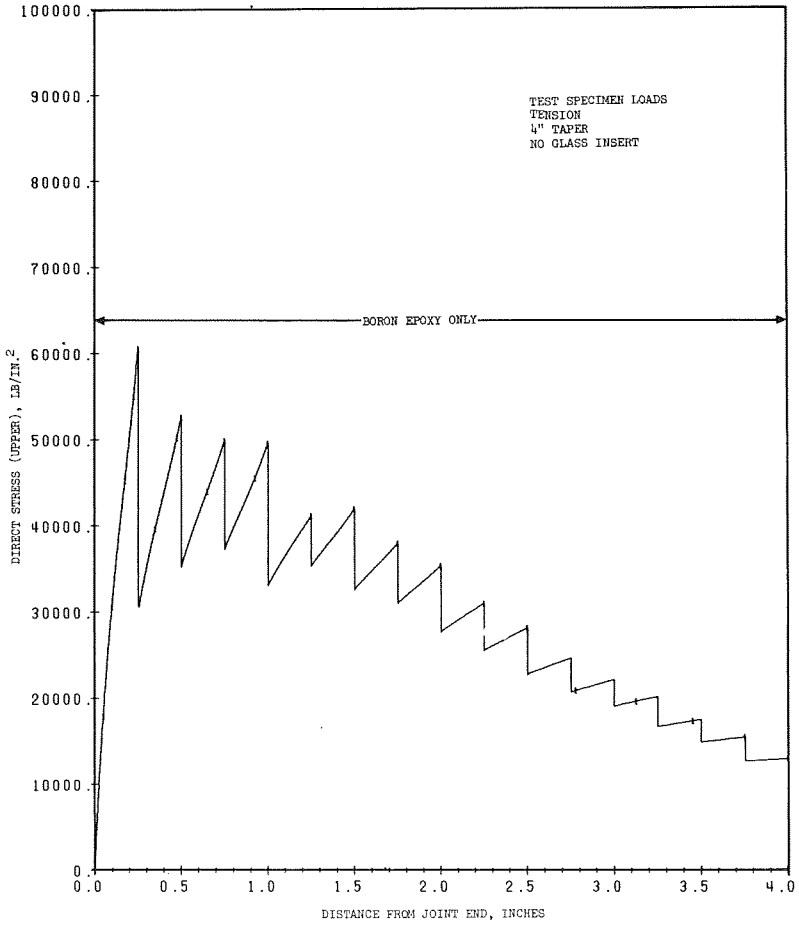

FIGURE 3-7. BORON/EPOXY STRESS DISTRIBUTION IN 4-INCH TAPERED TENSILE JOINT - NO GLASS INSERT - TEST LOADS.

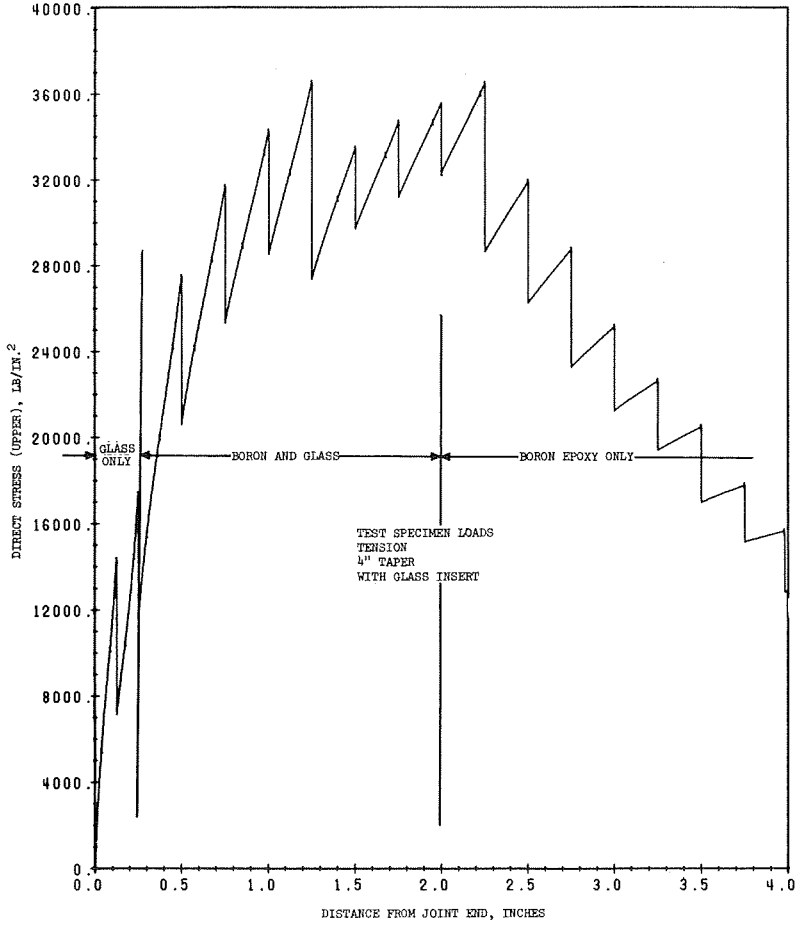

FIGURE 3-8. BORON/EPOXY STRESS DISTRIBUTION IN 4-INCH TAPERED TENSILE JOINT - WITH GLASS INSERT - TEST LOADS.

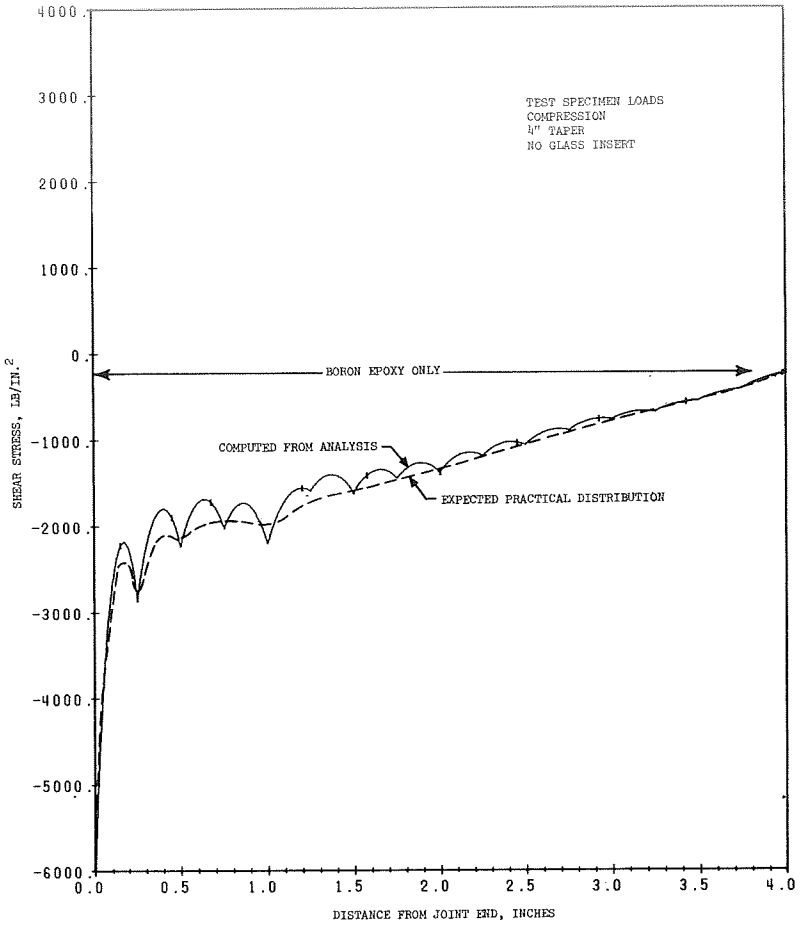

FIGURE 3-9. ADHESIVE SHEAR STRESS DISTRIBUTION IN 4-INCH TAPERED COMPRESSION JOINT - NO GLASS INSERT - TEST LOADS.

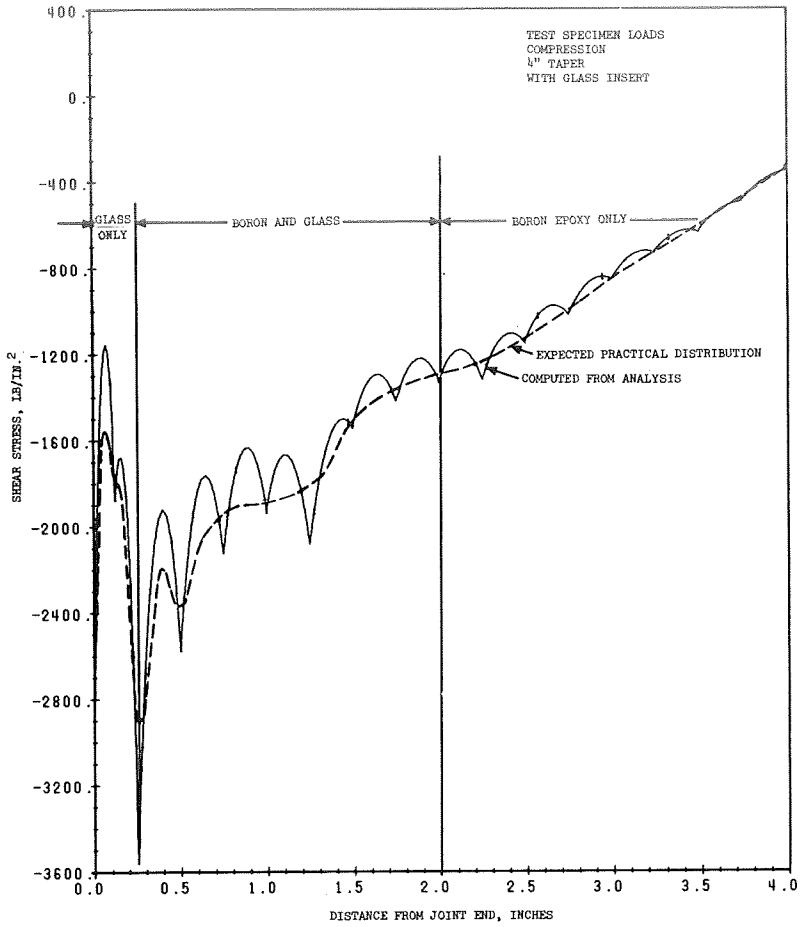

FIGURE 3-10. ADHESIVE SHEAR STRESS DISTRIBUTION IN 4-INCH TAPERED COMPRESSION JOINT - WITH GLASS INSERT - TEST LOADS.

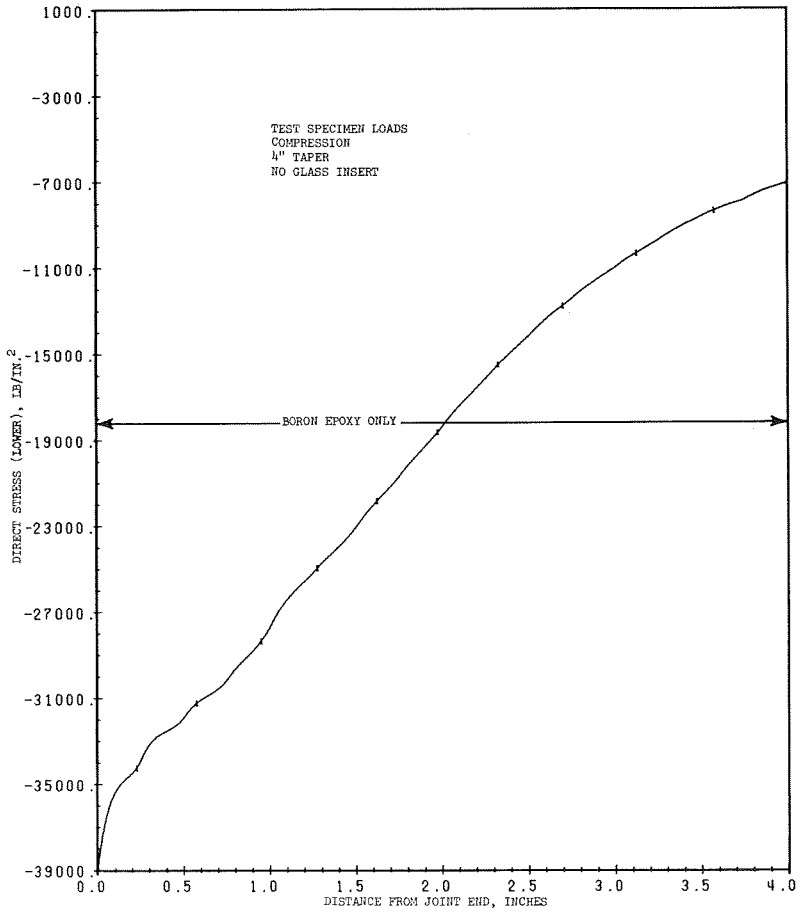

FIGURE 3-11. ALUMINUM STRESS DISTRIBUTION IN 4-INCH TAPERED COMPRESSION JOINT - NO GLASS INSERT - TEST LOADS.

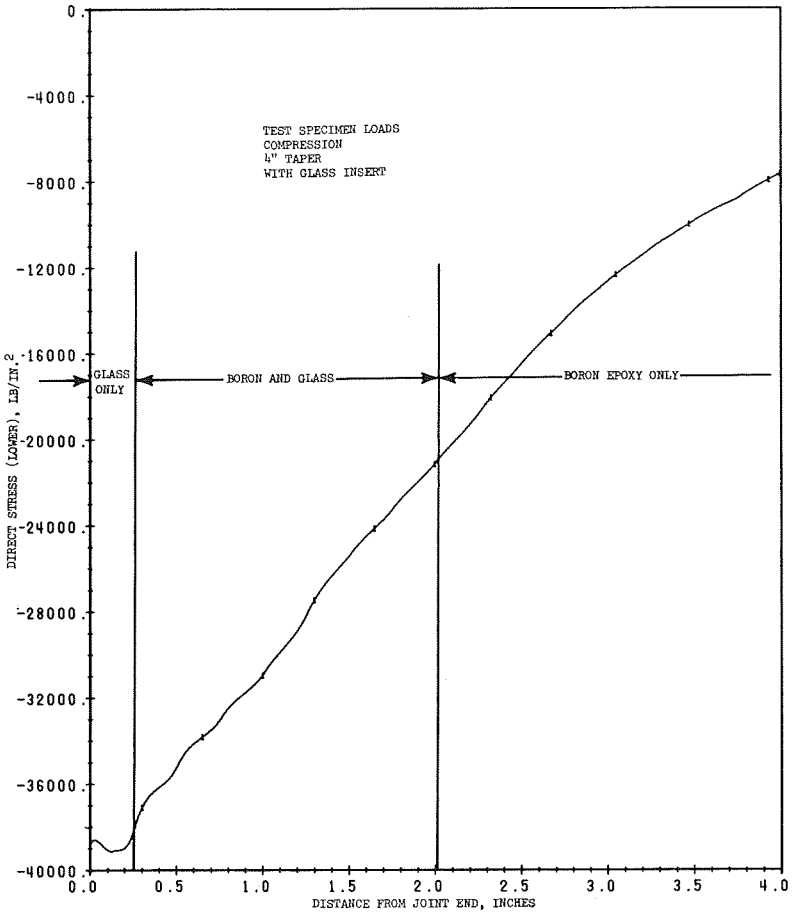

FIGURE 3-12. ALUMINUM STRESS DISTRIBUTION IN 4-INCH TAPERED COMPRESSION JOINT - WITH GLASS INSERT - TEST LOADS.

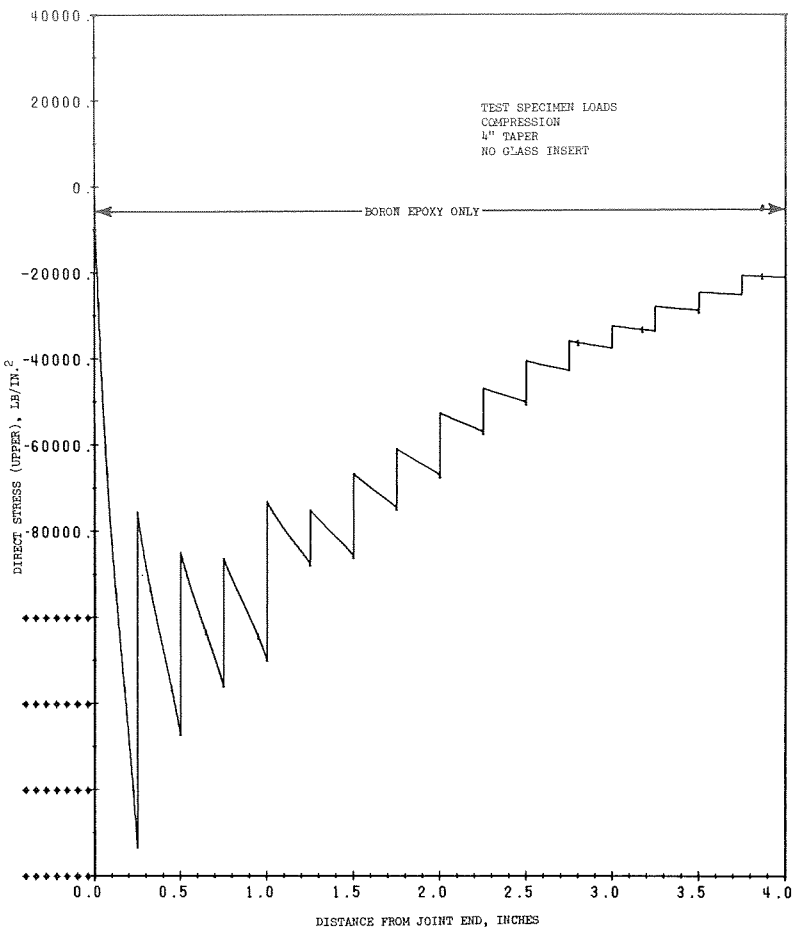

FIGURE 3-13. BORON/EPOXY STRESS DISTRIBUTION IN 4-INCH TAPERED COMPRESSION JOINT - NO GLASS INSERT - TEST LOADS.

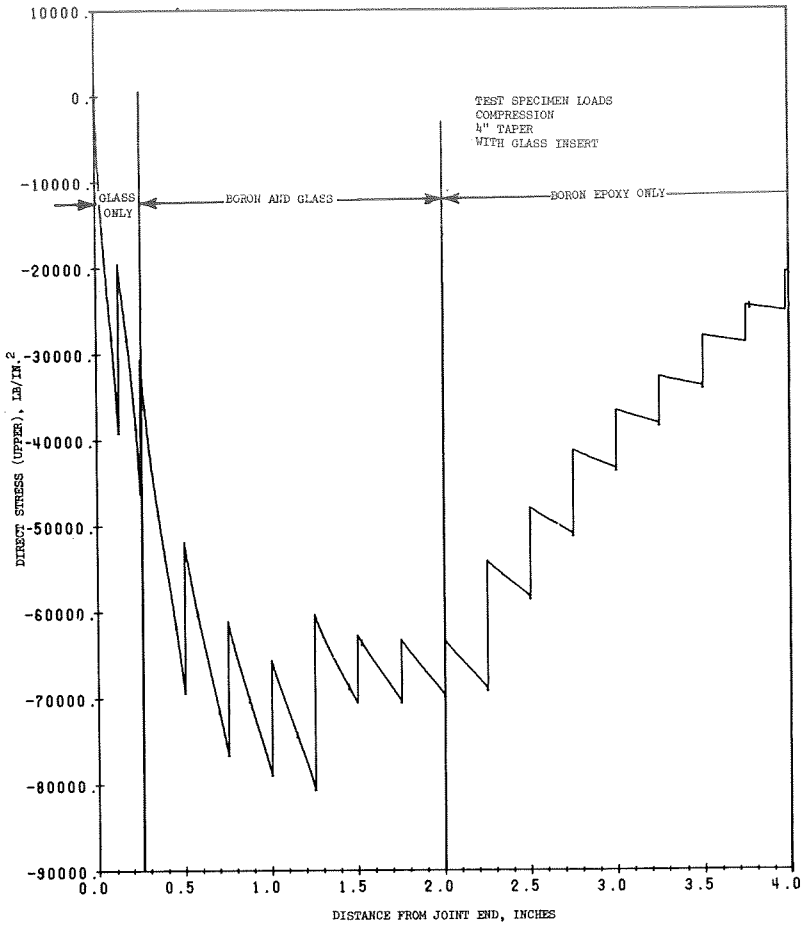

FIGURE 3-14. BORON/EPOXY STRESS DISTRIBUTION IN 4-INCH TAPERED COMPRESSION JOINT - WITH GLASS INSERT - TEST LOADS.

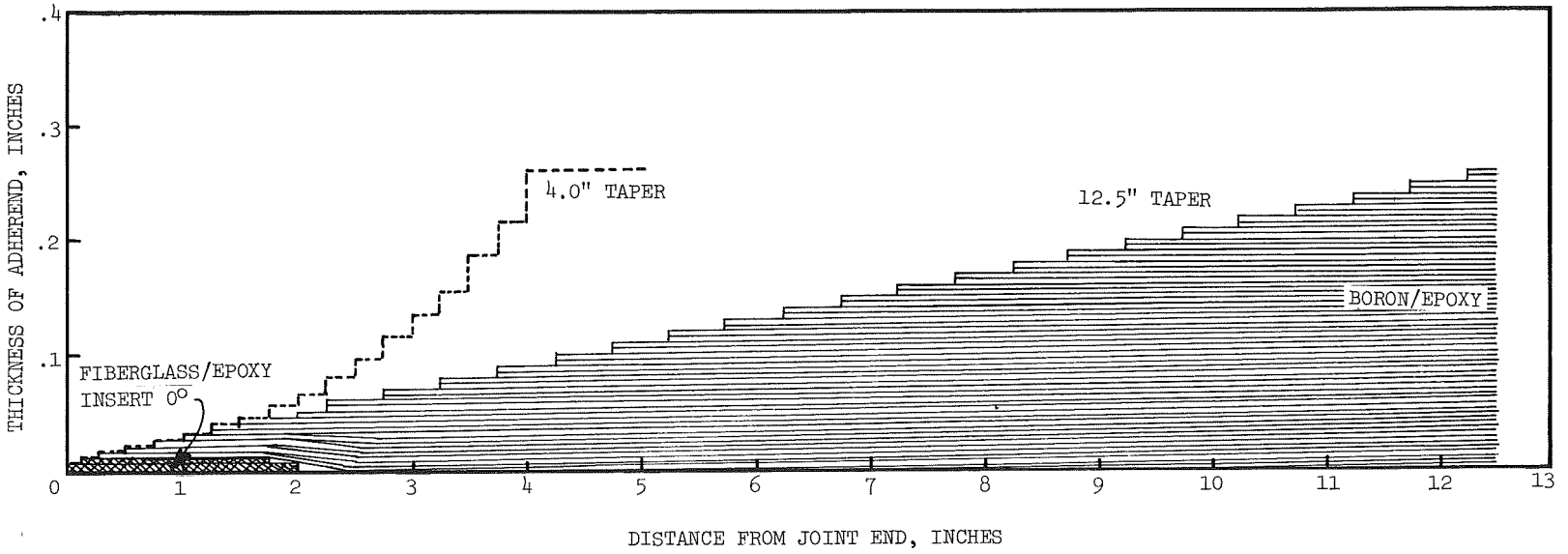

FIGURE 3-15. 12.5-INCH TAPERED JOINT GEOMETRY.

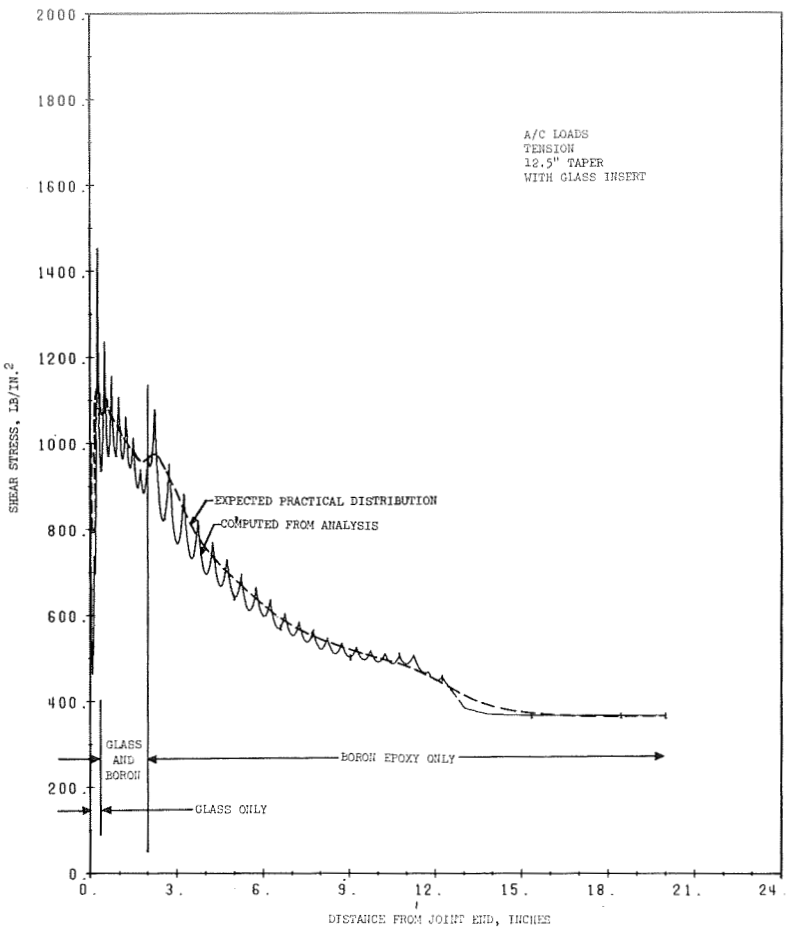

FIGURE 3-16. ADHESIVE SHEAR STRESS DISTRIBUTION IN 12.5-INCH TAPERED TENSION JOINT - WITH GLASS INSERT - FLIGHT LOADS.

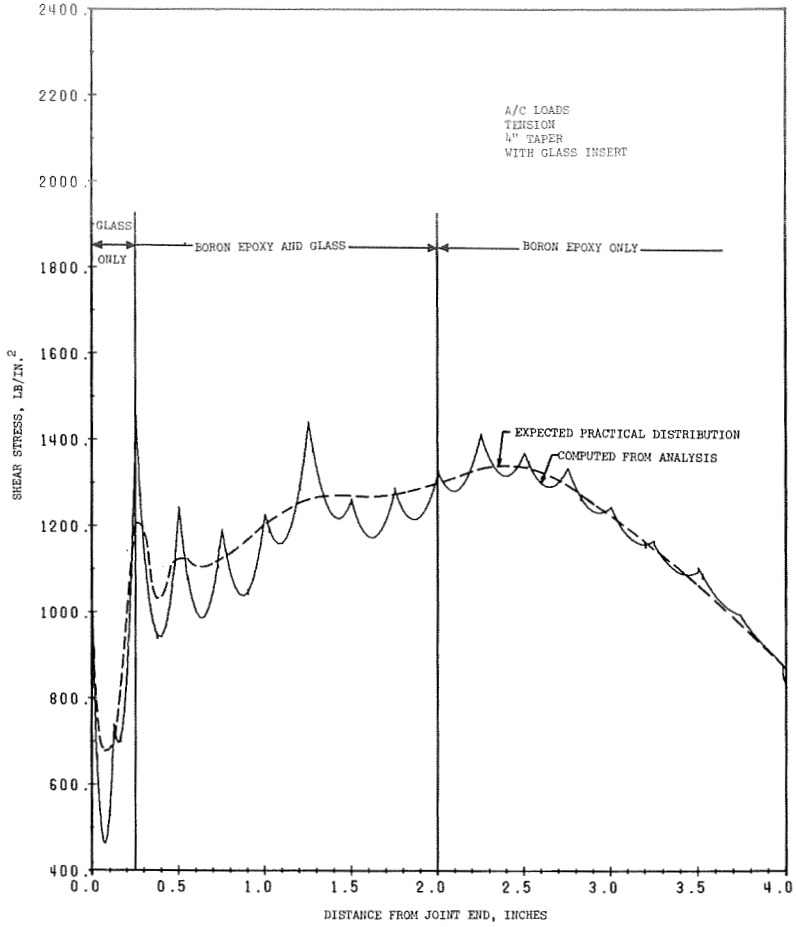

FIGURE 3-17. ADHESIVE SHEAR STRESS DISTRIBUTION IN 4-INCH TAPERED TENSION JOINT - WITH GLASS INSERT - FLIGHT LOADS.

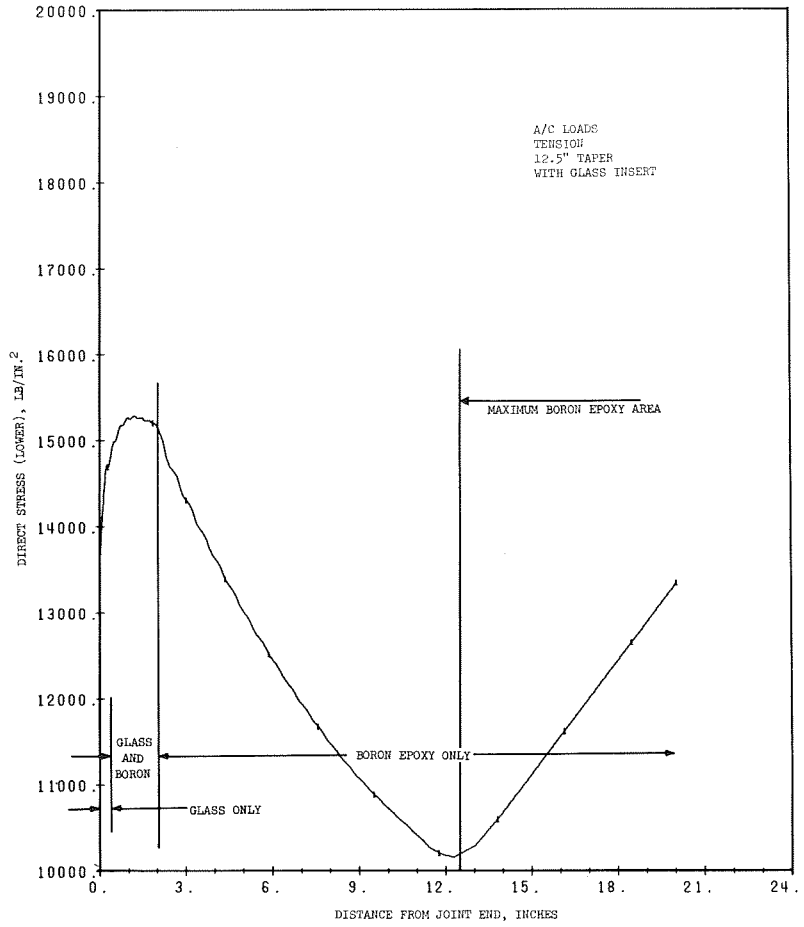

FIGURE 3-18. ALUMINUM STRESS DISTRIBUTION IN 12.5-INCH TAPERED TENSION JOINT - WITH GLASS INSERT - FLIGHT LOADS.

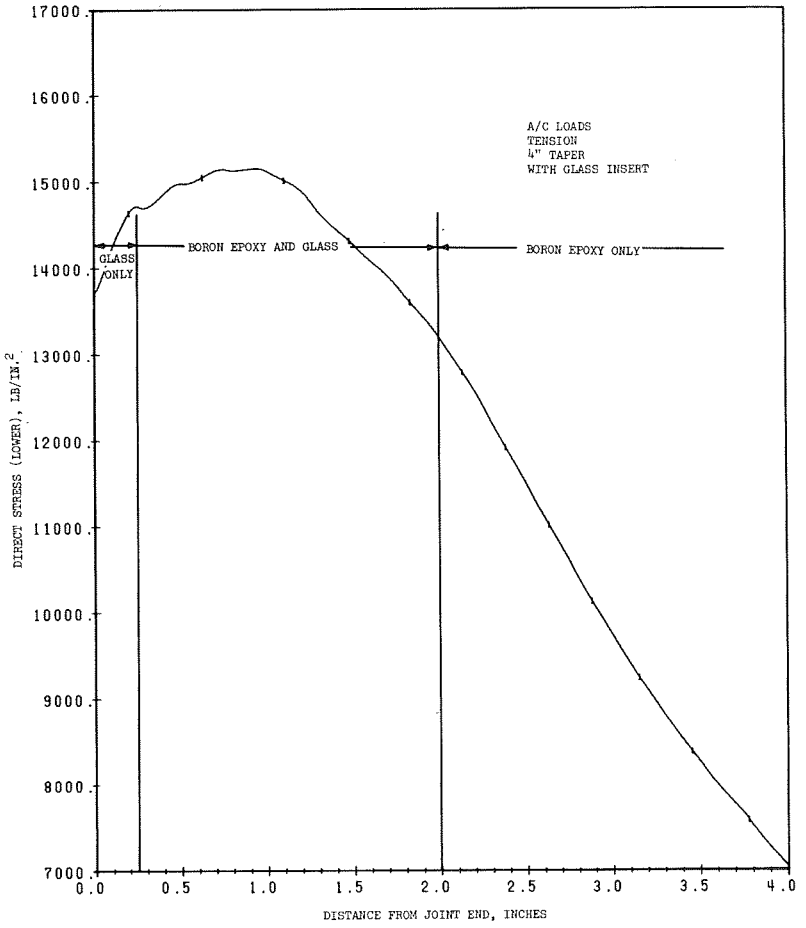

FIGURE 3-19. ALUMINUM STRESS DISTRIBUTION IN 4-INCH TAPERED TENSION JOINT - WITH GLASS INSERT - FLIGHT LOADS.

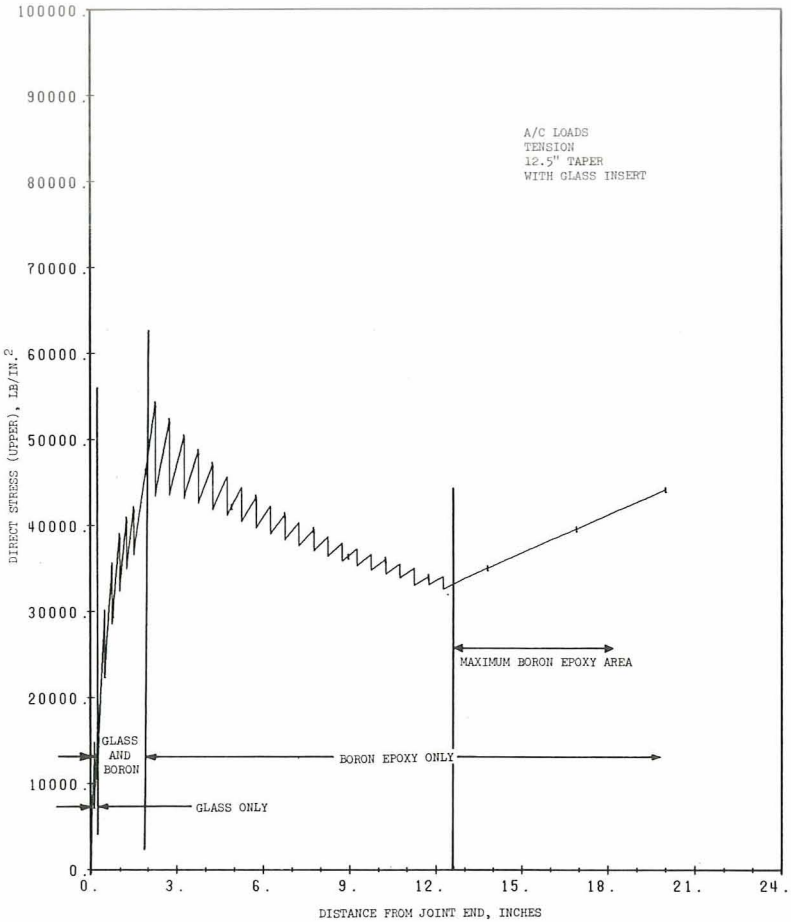

FIGURE 3-20. BORON/EPOXY STRESS DISTRIBUTION IN 12.5-INCH TAPERED TENSILE JOINT - WITH GLASS INSERT - FLIGHT LOADS.

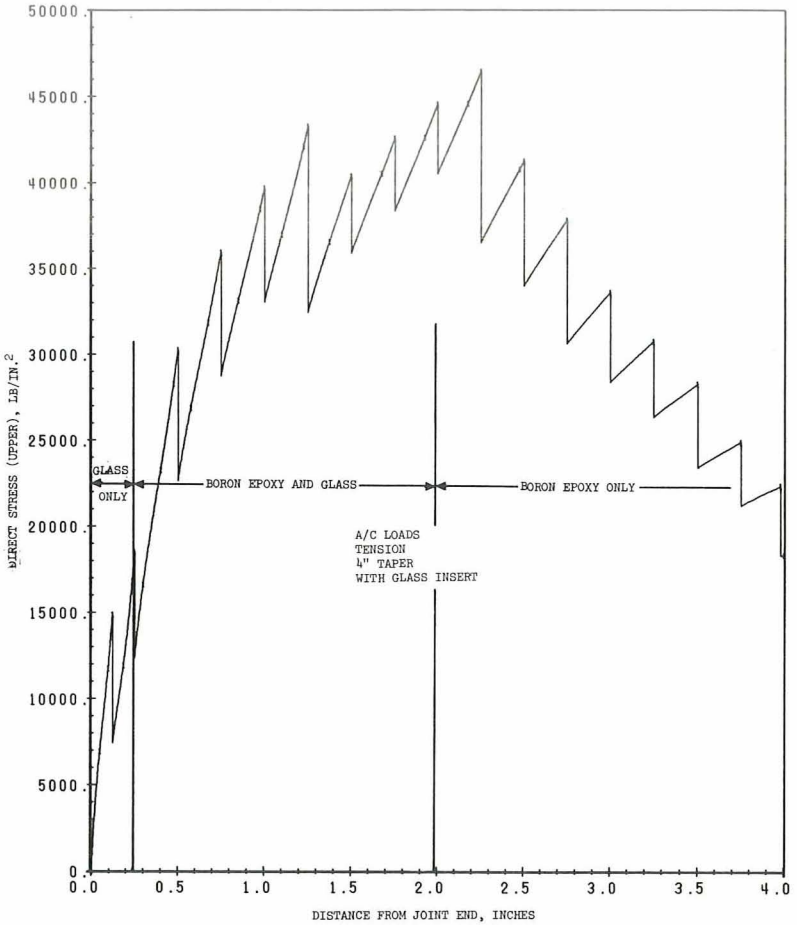

FIGURE 3-21. BORON/EPOXY STRESS DISTRIBUTION IN 4-INCH TAPERED TENSILE JOINT - WITH GLASS INSERT - FLIGHT LOADS.

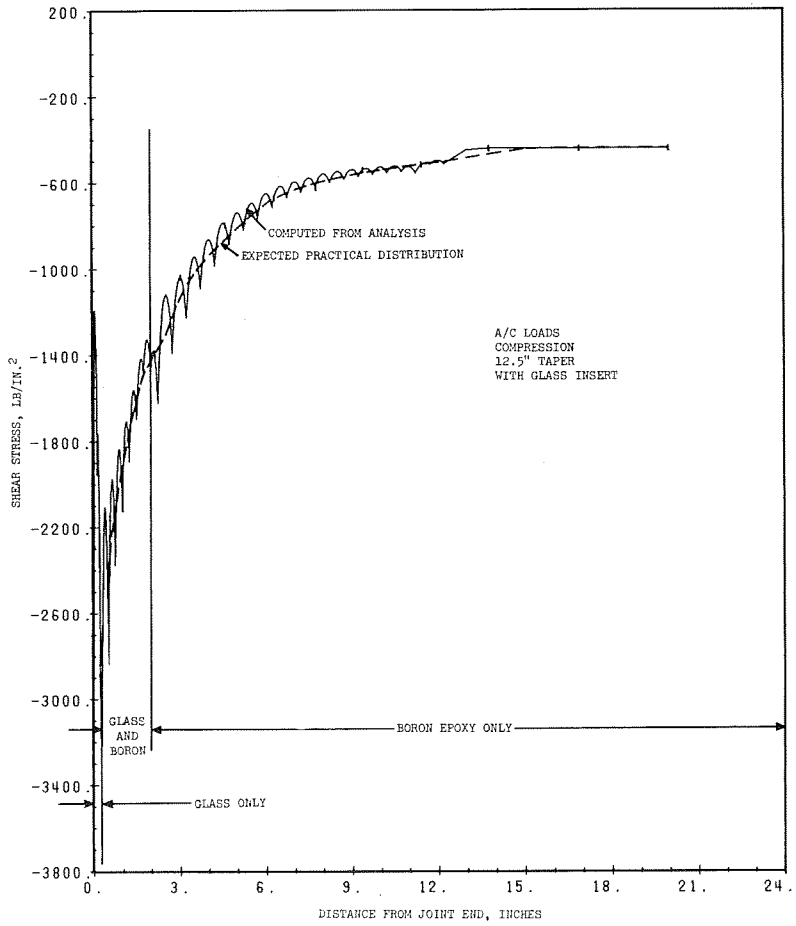

FIGURE 3-22. ADHESIVE SHEAR STRESS DISTRIBUTION IN 12.5-INCH TAPERED COMPRESSION JOINT - WITH GLASS INSERT - FLIGHT LOADS.

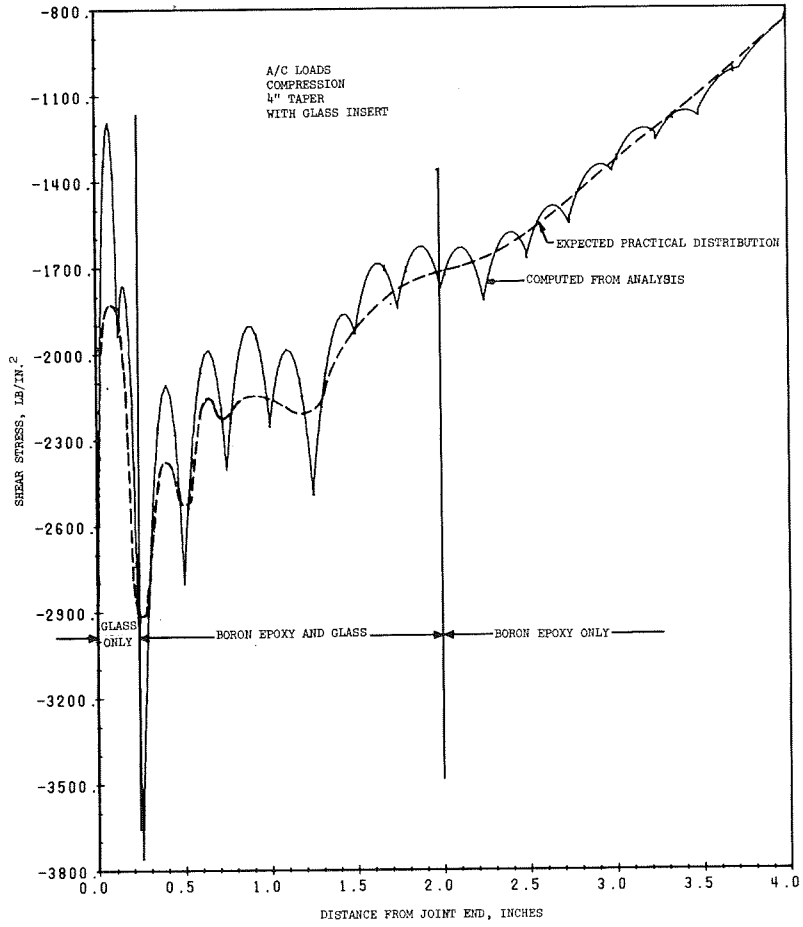

FIGURE 3-23. ADHESIVE SHEAR STRESS DISTRIBUTION IN 4-INCH TAPERED COMPRESSION JOINT - WITH GLASS INSERT - FLIGHT LOADS.

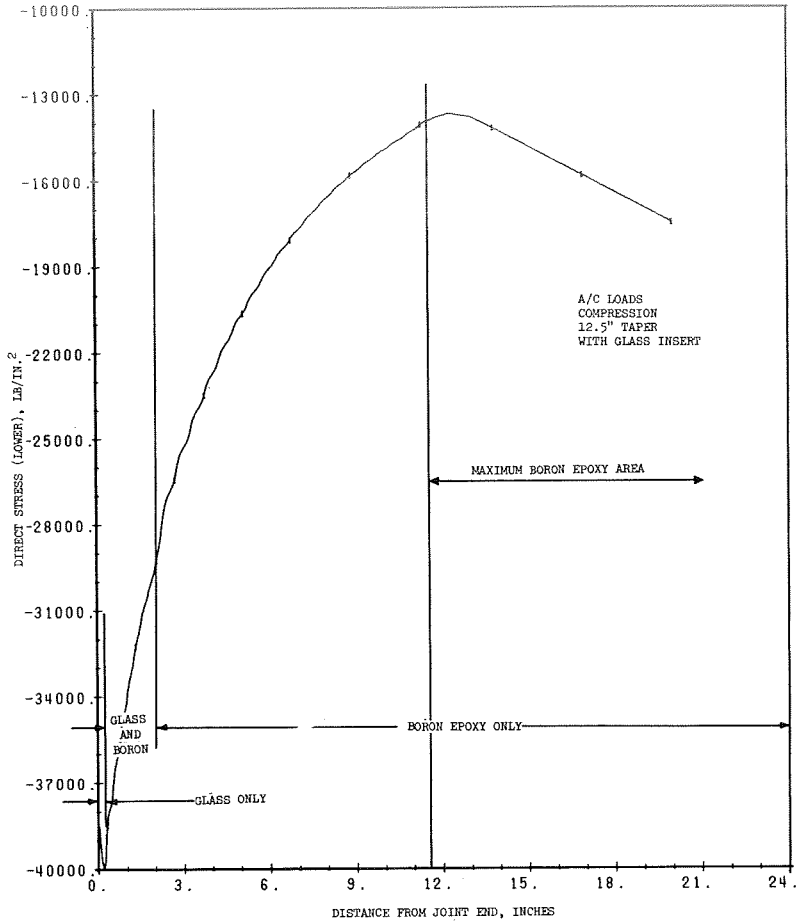

FIGURE 3-24. ALUMINUM STRESS DISTRIBUTION IN 12.5-INCH TAPERED COMPRESSION JOINT - WITH GLASS INSERT - FLIGHT LOADS.

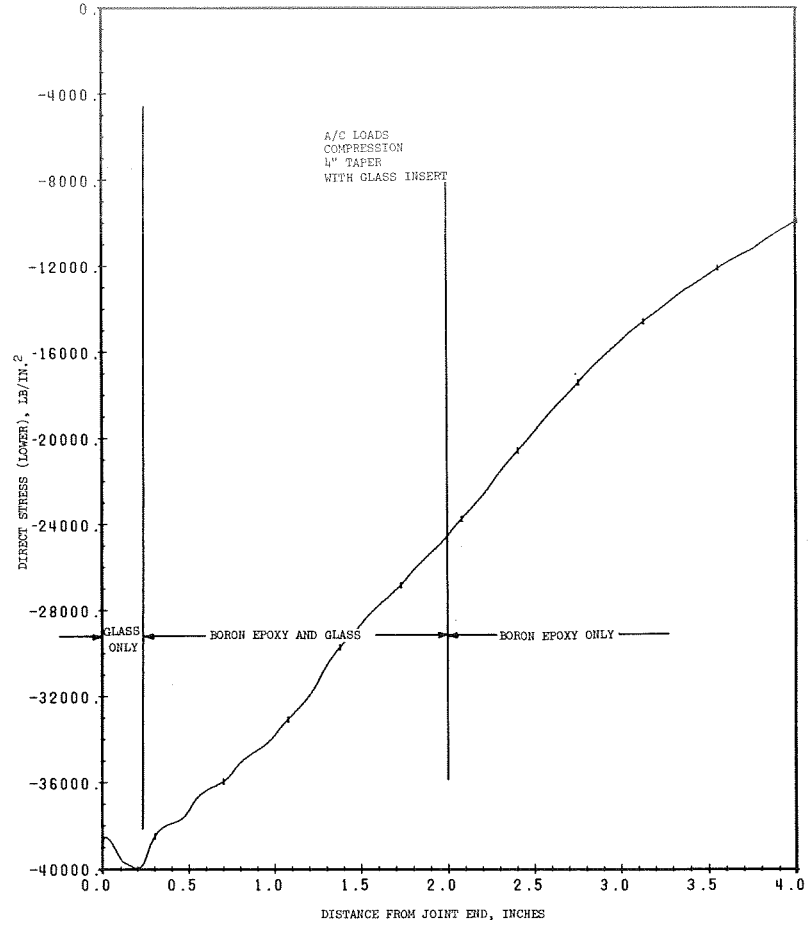

FIGURE 3-25. ALUMINUM STRESS DISTRIBUTION IN 4-INCH TAPERED COMPRESSION JOINT - WITH GLASS INSERT - FLIGHT LOADS.

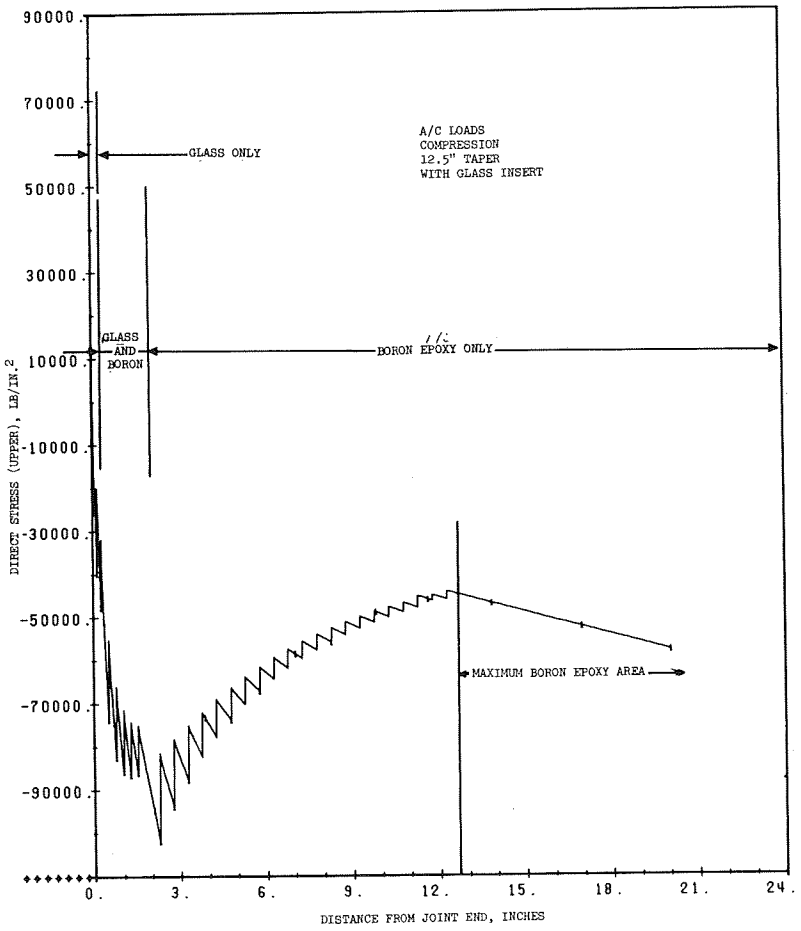

FIGURE 3-26. BORON/EPOXY STRESS DISTRIBUTION IN 12.5-INCH TAPERED COMPRESSION JOINT - WITH GLASS INSERT - FLIGHT LOADS.

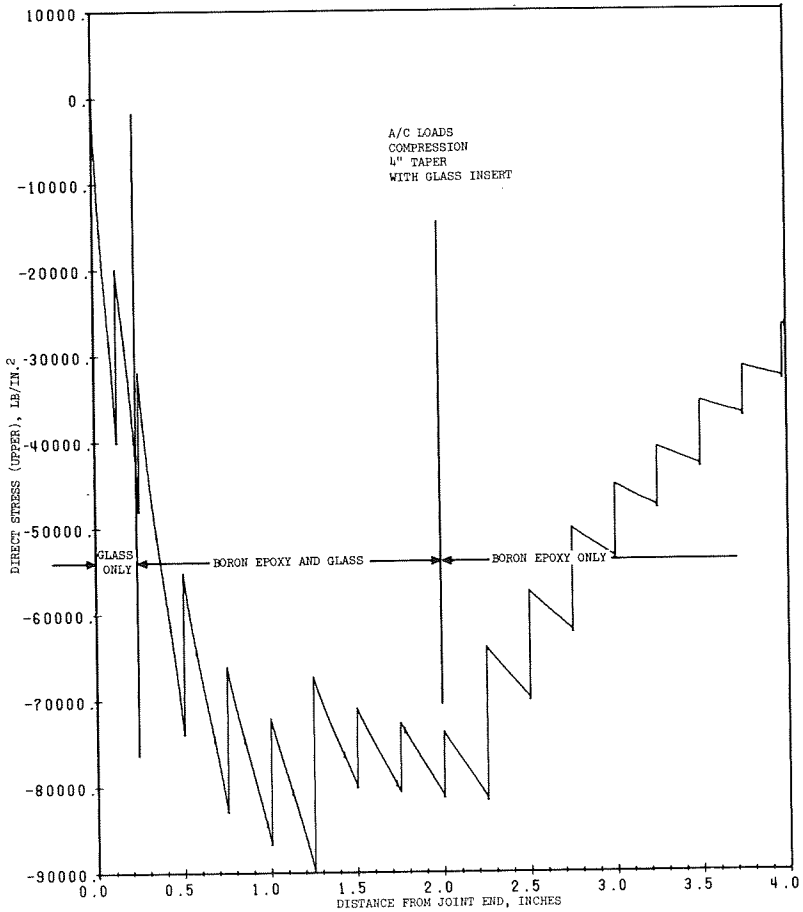

FIGURE 3-27. BORON/EPOXY STRESS DISTRIBUTION IN 4-INCH TAPERED COMPRESSION JOINT - WITH GLASS INSERT - FLIGHT LOADS.

4.0 FABRICATION

Objective

The objective of the fabrication portion of this program was to develop techniques suitable for the fabrication, assembling and inspecting of bonded and riveted boron/epoxy reinforced aluminum stringers for the CH-54B helicopter.

Approach

The feasibility of fabricating and assembling boron/epoxy reinforced stringers under normal factory conditions was determined by the fabrication of thirty-five short test specimens and three twenty-foot, full-sized specimens. Normal manufacturing procedures such as drilling and fastening were also perfected. Nondestructive inspection (NDI) was made on all the test specimens before and after testing. Most of the fatigue specimens were also inspected during the tests. Fabrication fixtures were made such that they could be used in the production phase of this contract.

Tooling Fixture

To facilitate fabrication of the test specimens, two steel fixtures were made, one six-channel, 84-inch-long laminating fixture and the other a six-channel, 20-foot-long laminating fixture. The shorter tool was used to fabricate the test specimens under 48 inches long, while the longer fixture was used to fabricate full-sized aircraft stringers. These laminating fixtures were converted into bonding fixtures with slight modifications. A simple trolley, as shown in Figure 4-1, was provided to apply the 0.75-inch boron/epoxy tape to the channels in the laminating tool. A roller, also shown in Figure 4-1, was fabricated to compact the layup in the channels during the layup process.

The 0.75-inch-wide boron/epoxy tape was not received in time for the fabrication schedule; therefore, a simple stripping tool, Figure 5-2, consisting of a series of knife blades accurately spaced to the required widths was made. This tool performed extremely well with no severing of filaments on the tape being slit. As the tape was slit, it was rewound on a segmented spool for application to the layup tool.

No major problems were encountered during the laminating process of the short specimens for testing. After cure it was found that the tool had to be disassembled before removing the cured reinforcements. When it was attempted to remove the first cured reinforcement from the tool, the ply adjacent to the tool surface became delaminated. Upon closer examination it was revealed that a slight radius existed on the corner of the tool channel bars and allowed the first ply to extrude into the void area provided by the radius, and when the cured part was lifted from the tool, the undercut restrained the part and caused the delamination.

To allow for thermal expansion, the aluminum caul plate was cut approximately 0.010-inch narrower than the tool channel. Under curing pressure this gap produced a ridge of one or two filaments on the upper edge of each cured reinforcement. When handled, the first test specimens were extremely dangerous due to the ridges produced by the filaments. To overcome this on all subsequent specimens and the full length stringer reinforcements, one ply of Style 7781 preimpregnated glass fabric was applied to the surface of the reinforcement before cure. This step eliminated any further handling problems.

In the fabrication of the full-size demonstration stringer reinforcements, two specific problems were encountered. Segmented aluminum caul plates were used, and on two stringer reinforcements, where they butted, the thermal expansion of the caul plates during the cure cycle caused them to lift at their ends. A pressure void was created, and the laminate cross-section was measurably thicker in these areas. On one of the reinforcements, the caul plates were not properly seated prior to bagging, causing the cured reinforcement to have a nonuniform thickness. Both problems are readily remedied by using a continuous caul plate and allowing the laminated reinforcements to compact under vacuum for a minimum of eight hours and reinspecting before cure.

Specimen Fabrication

All specimens fabricated for test and installation evaluation consisted of boron/epoxy laminates fifty-ply thick or 0.25-inch thick and 0.75-inch wide. Specimen lengths, as determined by test requirements, were 18.0 inches long for all compression and shear specimens, 23.5 inches long for all static tension and fatigue specimens, and 17 feet 8 inches for the representative aircraft reinforcement members. All specimens were fabricated with tapered ends, utilizing the 4-inch taper as analytically developed in Section 3. The boron/epoxy reinforcement was cured in the autoclave at 85 psi plus vacuum for 210 minutes at temperatures of 350° F. Foam inserts were used at the tapered ends to prevent bridging of the vacuum bagging film between the tool channel bars and the boron/epoxy.

After completion of the laminating operations, the tool was converted to a bonding fixture (see Figure 4-3). Channel bars 1, 3, 5, and 7 were removed and placed upon the remaining bars 2, 4, and 6, providing support for the vertical legs of the stringers to be bonded. The aluminum stringers

and the boron/epoxy reinforcement strips were prepared in accordance with Sikorsky Aircraft applicable production process specifications. The boron/epoxy reinforcement was bonded to the aluminum stringer in the autoclave at 50 psi, plus vacuum, and 250° F. for sixty-five minutes at temperature.

The three completed twenty-foot stringer/reinforcement assemblies were visually inspected for bond continuity. At this time it was discovered that the single-ply laminates at the tapered ends were disbonded on two of the three stringers. Adhesive was placed under the unbonded areas, the stringers mechanically clamped to provide pressure in the areas of disbond and placed in an autoclave with production parts which were to be cured at 320° F. This high cure temperature (70° F. above the original cure cycle) and the lack of clamping pressure between parts caused a complete disbond between the reinforcement and the aluminum stringer. Stringers and reinforcements were stripped, prepared, and rebonded. Visual and nondestructive inspection, utilizing a Fokker bond test instrument, showed two or three areas of bond deviation on each specimen.

Bond Inspection Techniques

Nondestructive inspection techniques to determine bondline deviations were used to verify adhesive bonding techniques utilized in the assembly of the boron/epoxy reinforcements to the aluminum stringers.

Each demonstration stringer and/or test spec men was examined by Quality Assurance personnel utilizing production nondestructive inspection techniques developed for determining bond integrity on all bonded main and tail rotor blade assemblies. An audible frequency deviation technique, more commonly referred to as coin tapping, was used to determine whether gross unbonded areas existed. Indications of bond line deviations were marked on the aluminum stringer side of the bonded assembly. A Fokker bond tester utilizing the principle of transducer resonance was then used to verify the indicated bond line deviations. Bond line deviations were discovered on three of the short test specimens and three of the demonstration stringers. Two new short test specimens were fabricated and tested. The third test specimen which indicated a bond deviation was used in a fatigue test and is reported in Section 8.0. The bond deviations in two of thre three demonstration stringers is shown in Figure 4-4. The Fokker bond tester was used to monitor possible bond deviations during the fatigue tests.

Drilling and Riveting

Drilling of the reinforced stringer to provide holes for attachment of the frame to stringer clips was accomplished on a delta floor model drill press equipped with a Hyprez electrogrip coolant transfer jacket attachment supplied with water coolant by a pressurized spray-mist unit. This machine

is shown in Figure 4.5. A diamond grit 5/32-inch core drill was used to drill the initial hole through the boron/epoxy reinforcement to the point of contact with the aluminum stringer (see Figure 4-6). Conventional high speed steel (HSS) drills were used to drill through the aluminum stringer.

It was found that upon riveting assemblies, the laminate split or cracked between the rivets parallel to the filament orientation of the reinforcement laminate as shown in Figure 4-7. The splitting of the boron/epoxy strip is due to the expansion and/or bending of the rivet in the hole. As an alternate method for fastening, Hi-Lok fasteners were evaluated. The diamond grit 3/32-inch core drill was used to drill the initial hole through the boron/epoxy, and several high speed steel drills were used as reamers. The hole diameter for the Hi-Lok fasteners was 0.163 inches. The Hi-Lok fasteners, although slightly heavier than corresponding rivets, produced no splitting or cracking in the laminate (see Figure 4-8).

For field repair evaluation, fastener holes were drilled in several samples of boron/epoxy reinforcements with conventional high speed steel drills. Water was used as a lubricant, and a pilot hole was initially made. The life of a drill in this application is extremely short. An average of four drills were used to make one hole. The effect of boron/epoxy on drills is shown in Figure 4-9.

Assembly of boron/epoxy reinforced stringers to aluminum skin panels presented no problems. Squeeze riveting techniques similar to those used for all aluminum structures were employed. The 20-foot reinforced stringers are shown riveted to a representative skin panel in Figure 4-10.

Conclusions and Recommendations

Fabrication and assembly techniques developed in this program have provided the information necessary to produce, in limited production, hybrid structures similar to those described and have reduced the fabrication of those components to a state-of-the-art manufacturing process.

It is recommended that further studies be made on the meaning of indicated bond deviations.

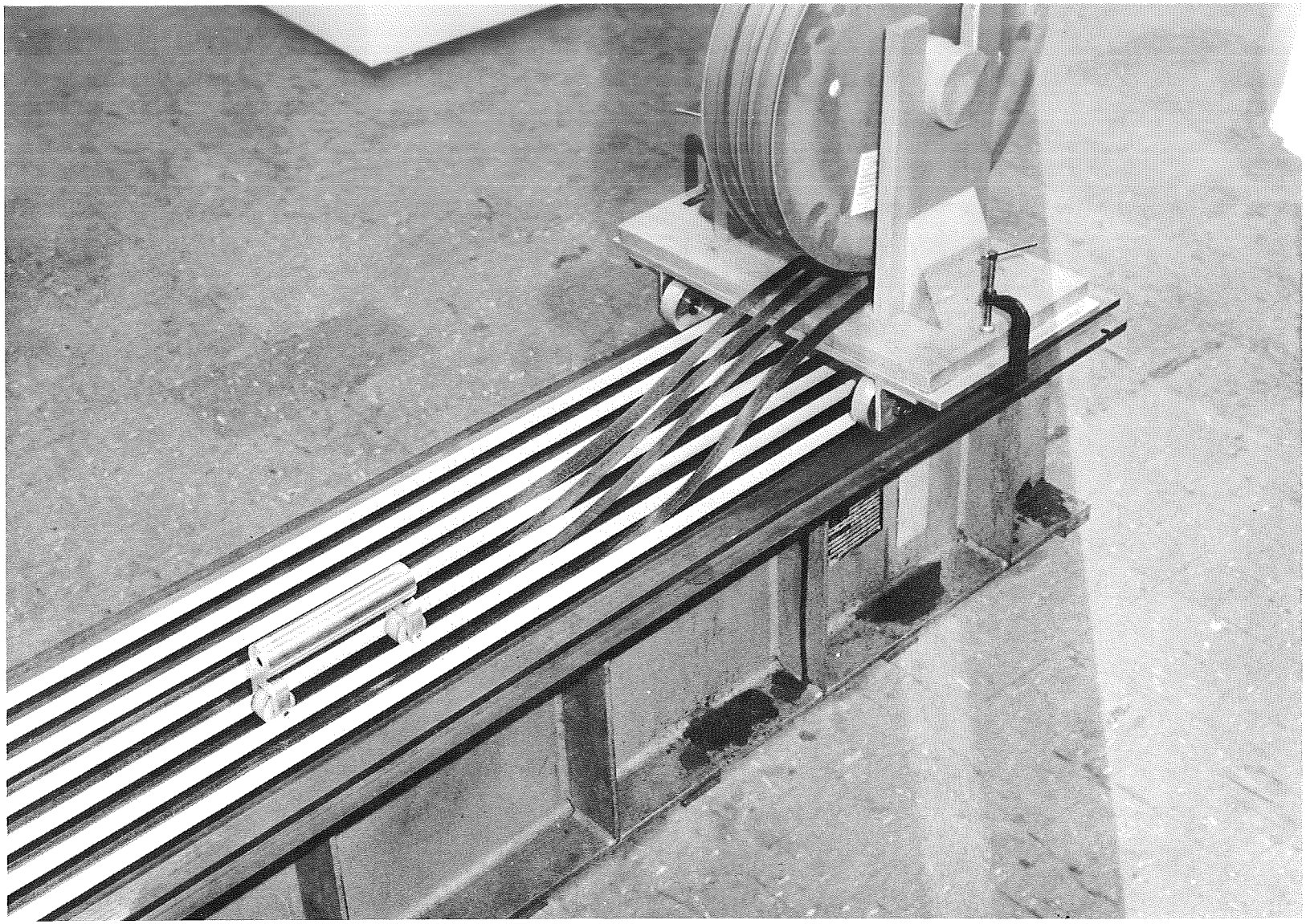

FIGURE 4-1. LAMINATING AND BOND FIXTURE.

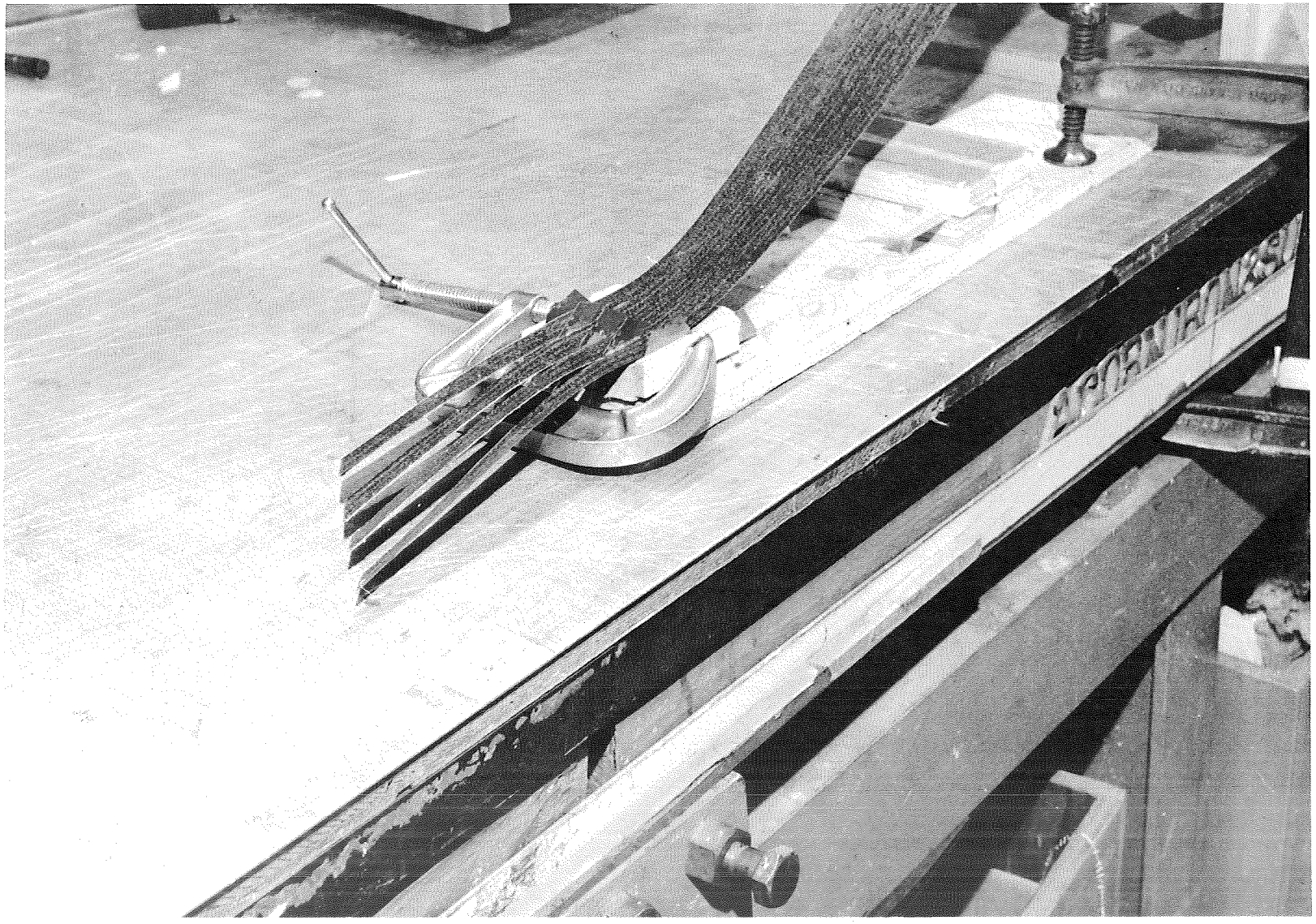

FIGURE 4-2. STRIPPING TOOL.

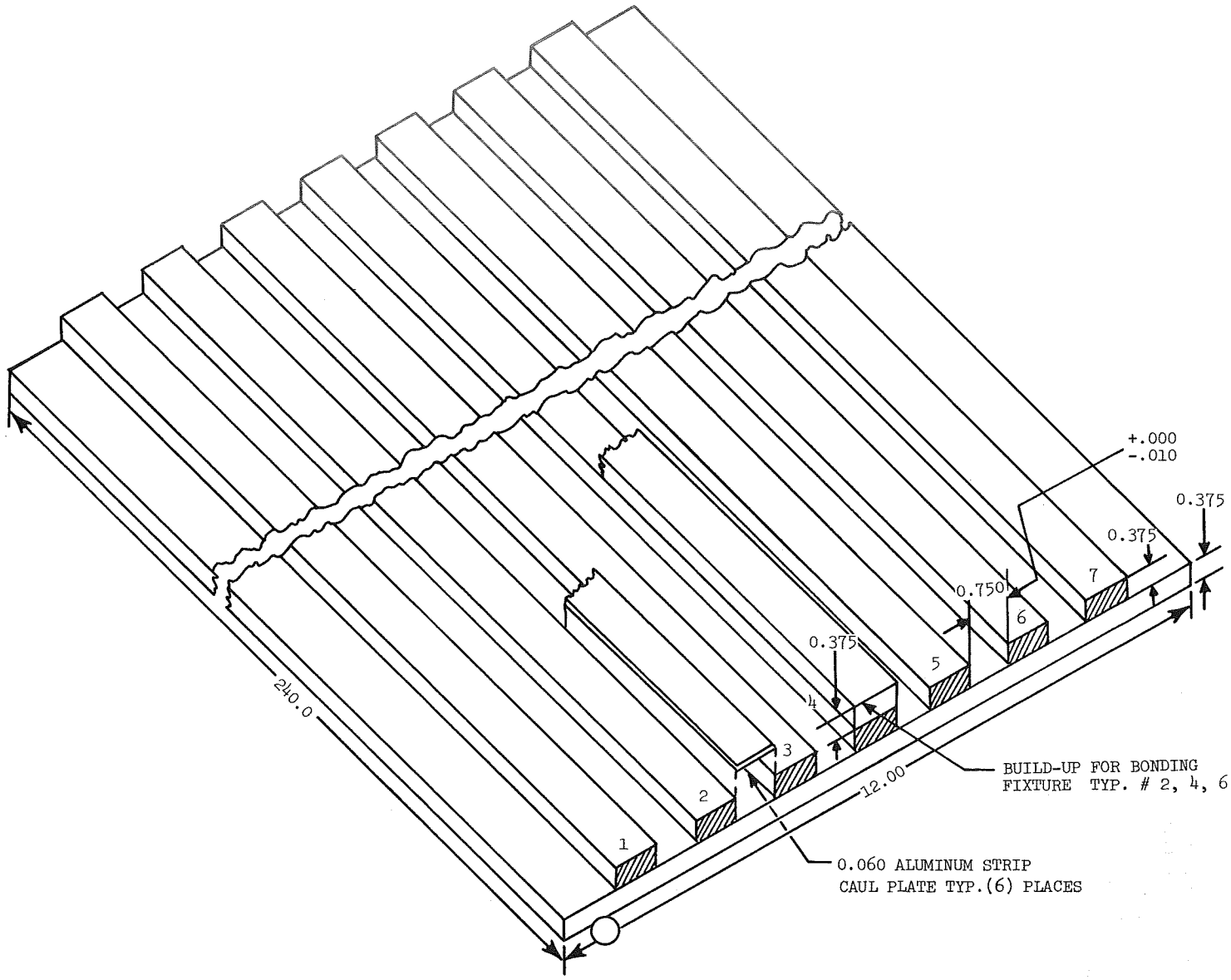

FIGURE 4-3. LAMINATING/BONDING FIXTURE CONVERSION.

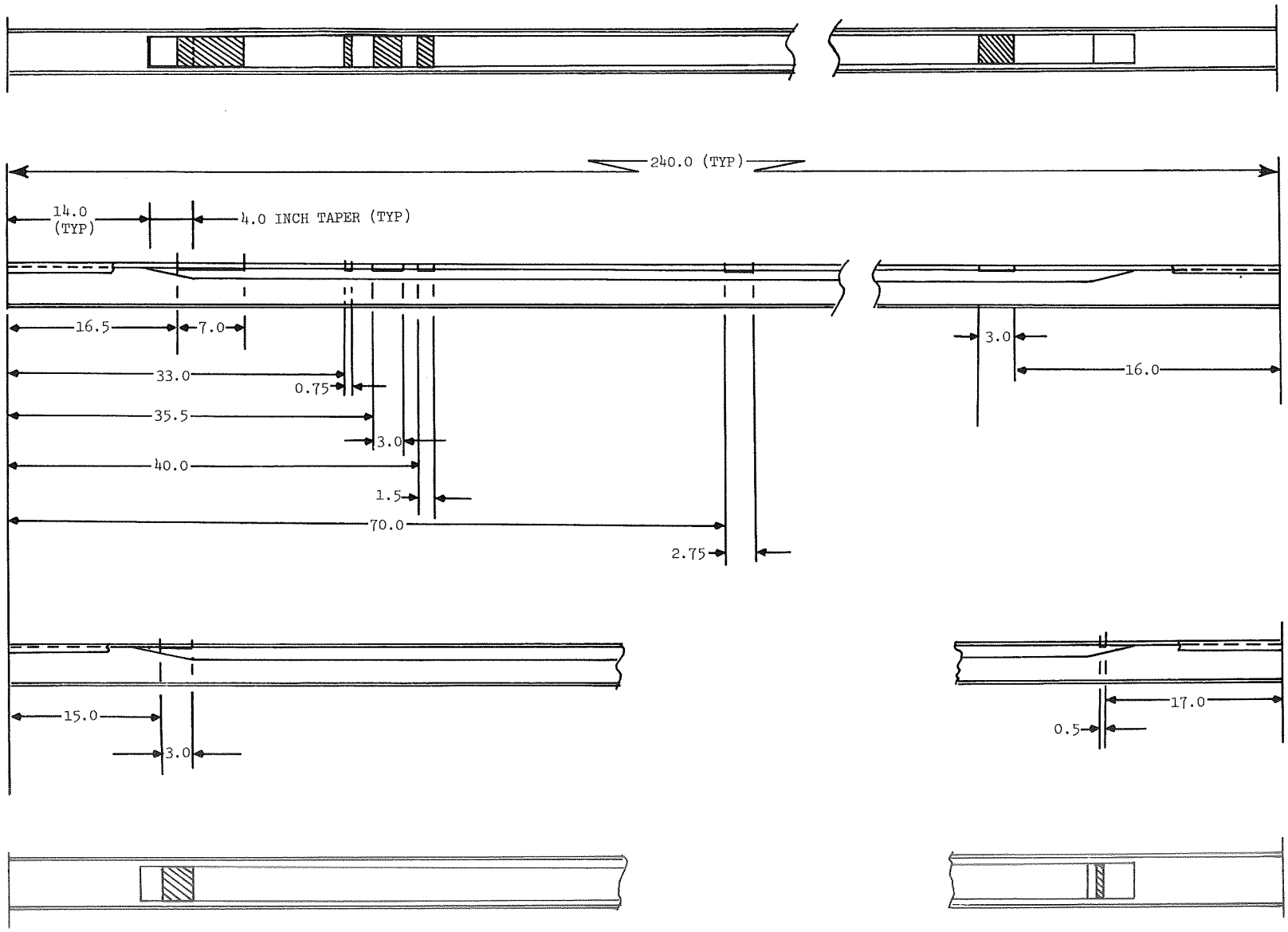

FIGURE 4-4. AREAS OF BOND DEVIATIONS IN 20-FOOT DEMONSTRATION REINFORCED STRINGERS

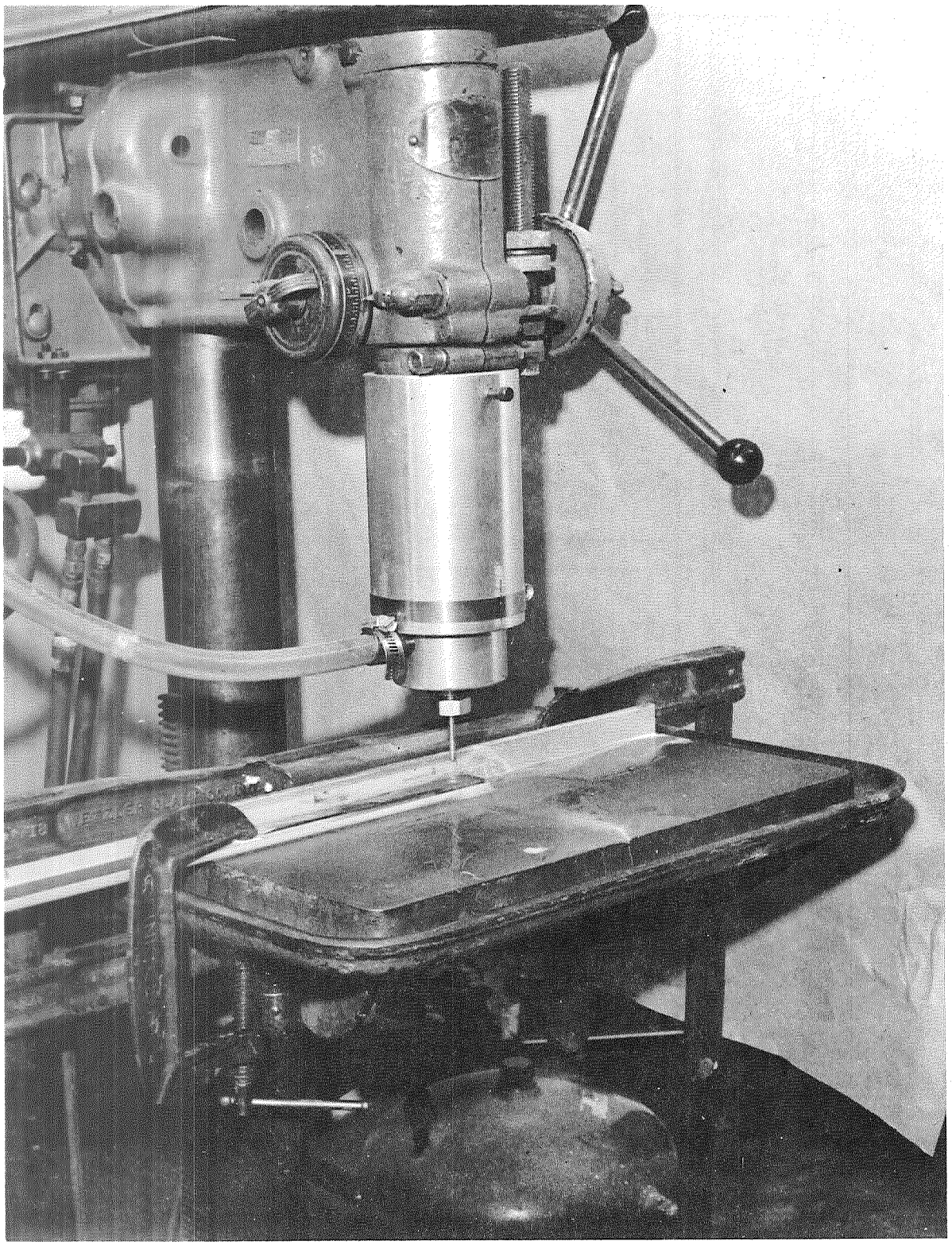

FIGURE 4-5. BORON/EPOXY DRILLING FIXTURE.

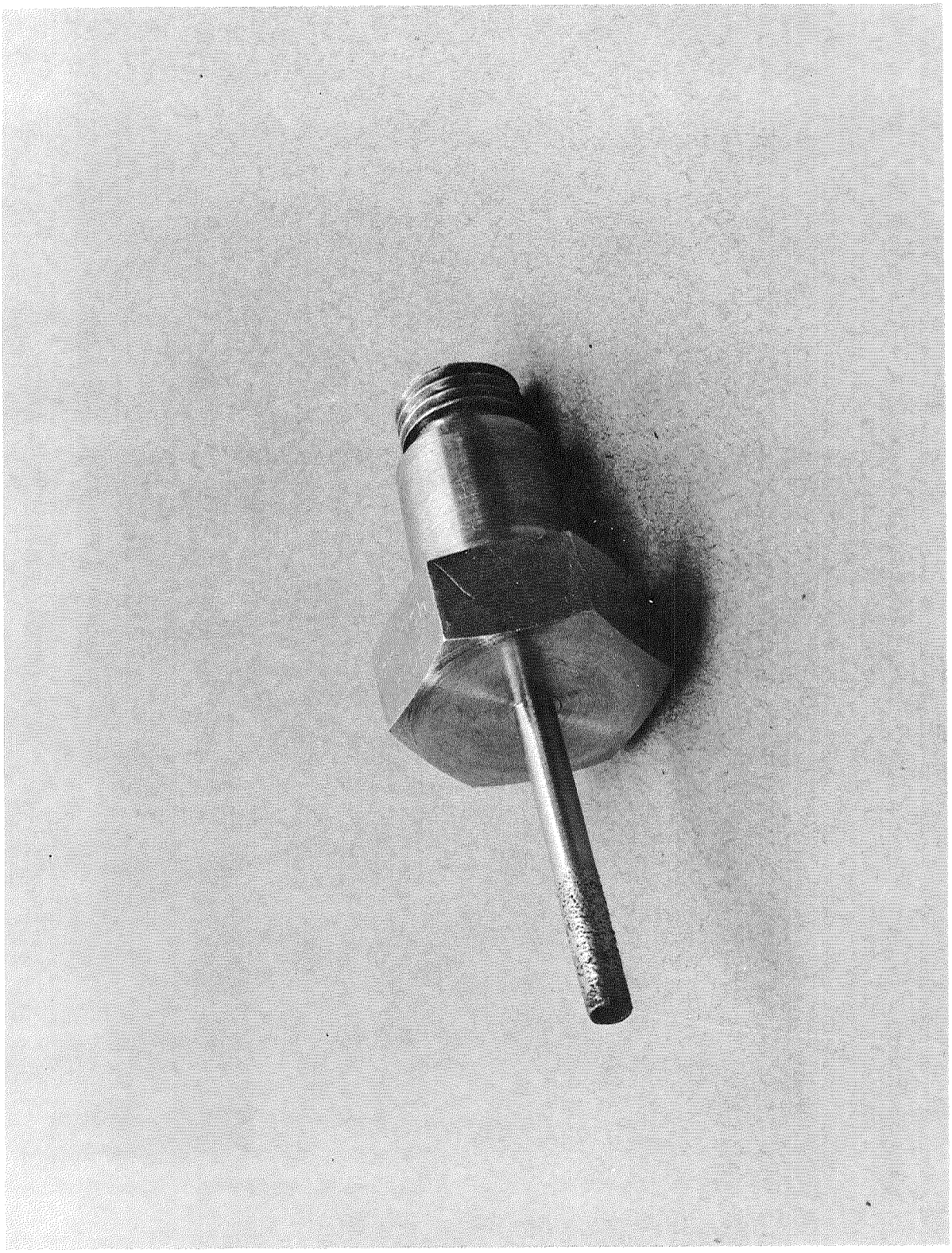

FIGURE 4-6. DIAMOND CORE DRILL.

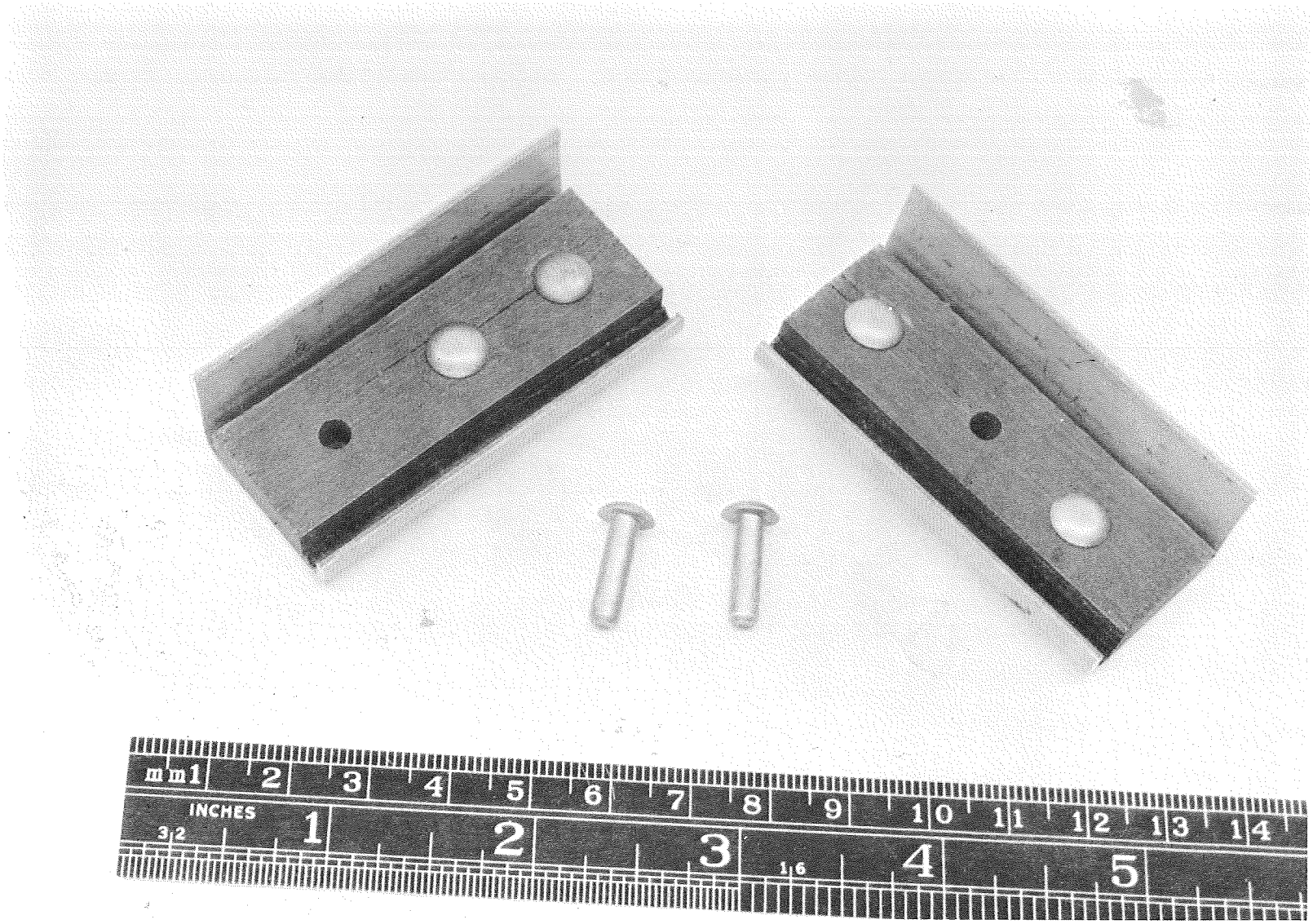

FIGURE 4-7. BORON/EPOXY RIVETED SPECIMENS.

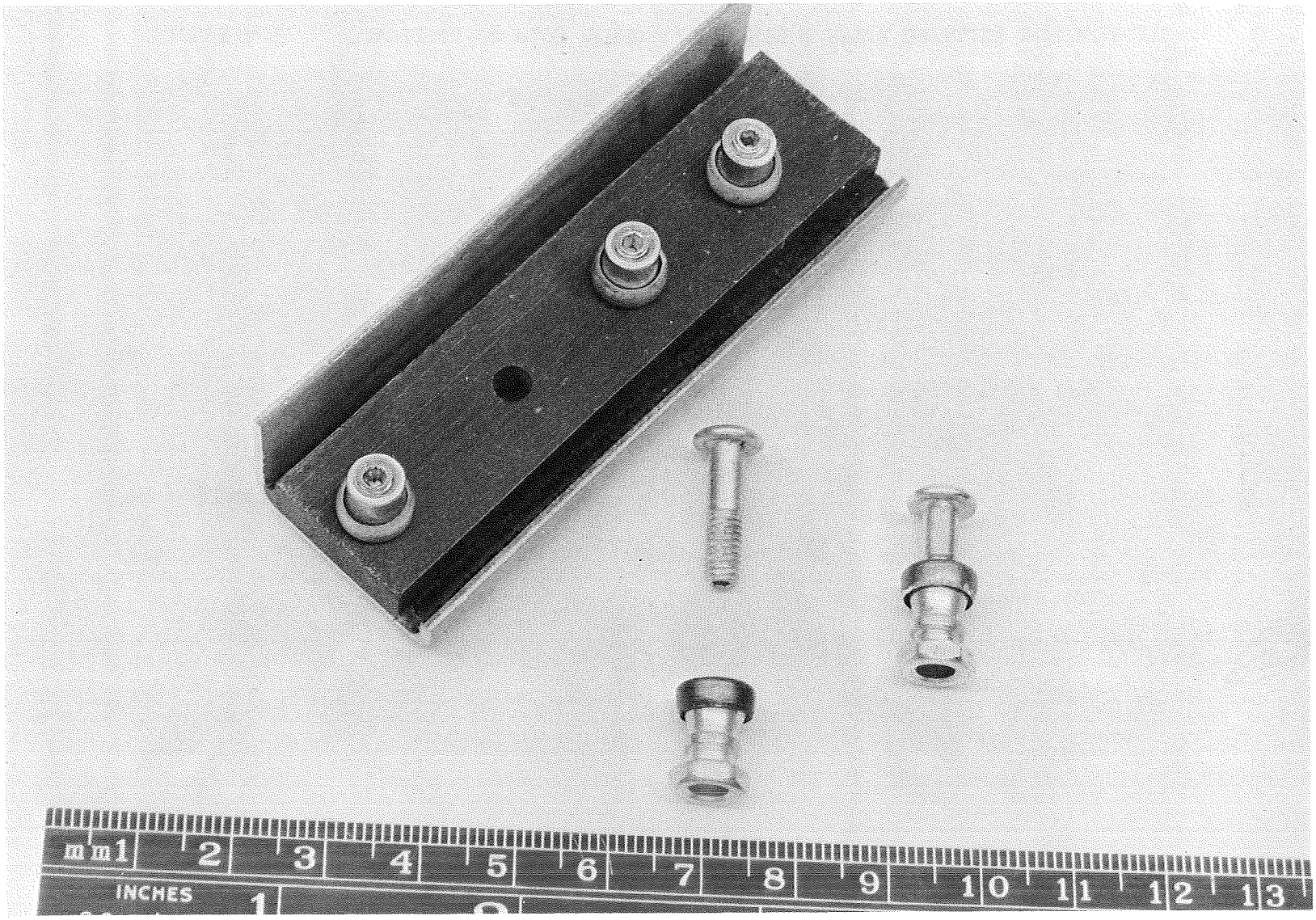

FIGURE 4-8. HI-LOK FASTENERS IN BORON/EPOXY.

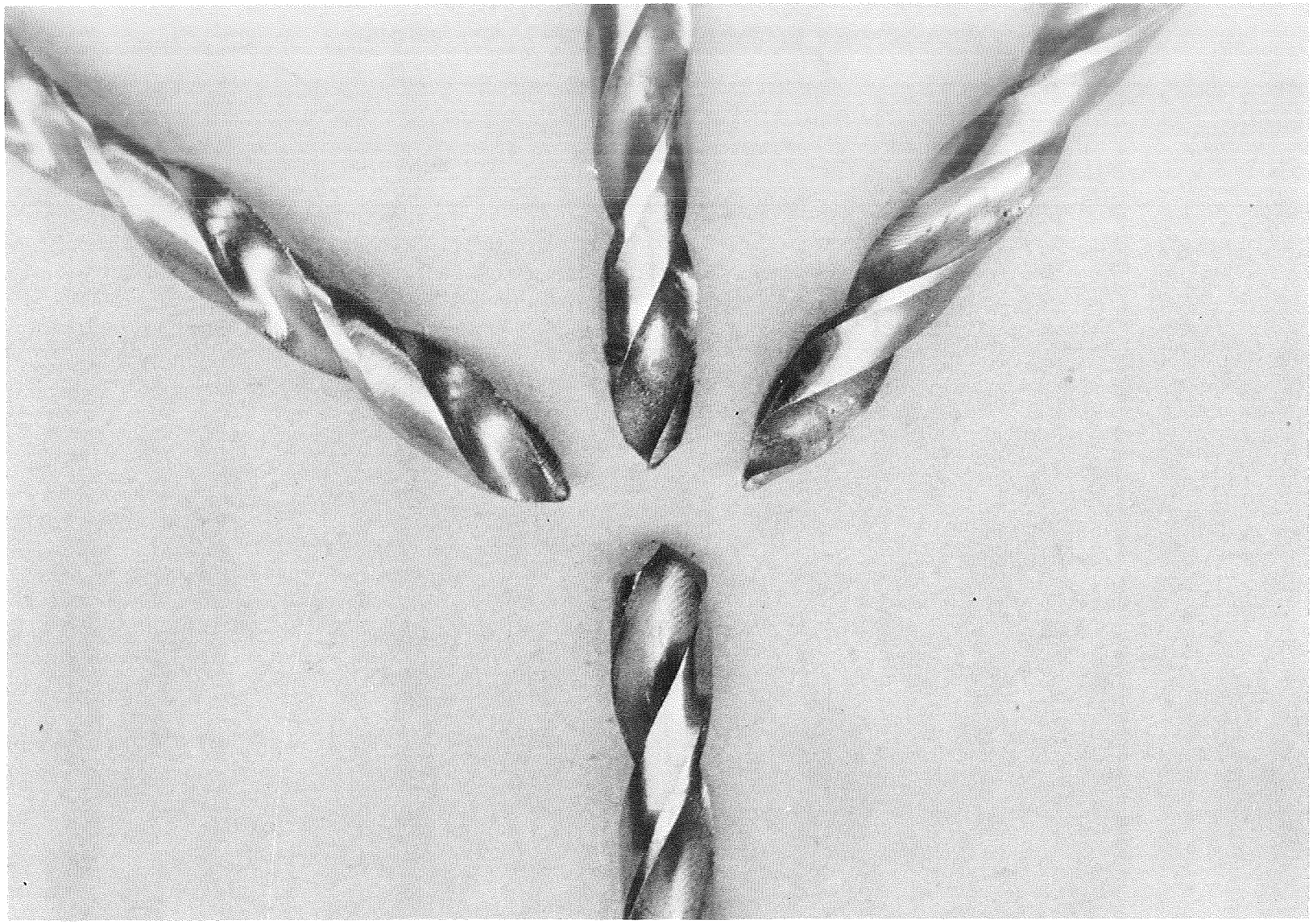

FIGURE 4-9. CONDITION OF HIGH SPEED STEEL DRILLS AFTER DRILLING BORON/EPOXY.

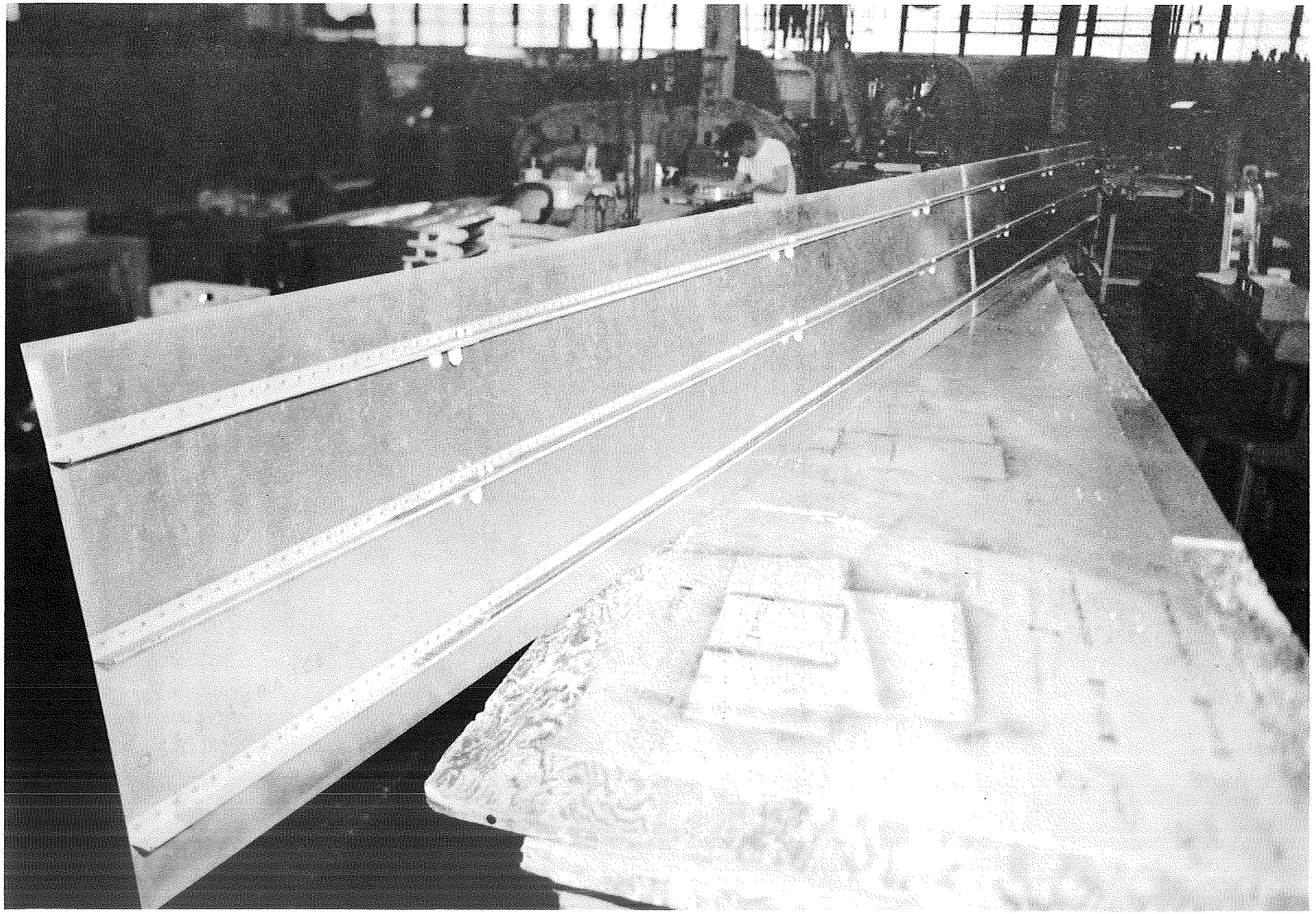

FIGURE 4-10. 20-FOOT REINFORCED STRINGERS RIVETED TO SKINS.

5.0 TENSILE LOAD/STRAIN TEST

Objective

The objectives of these tests were: (1) to obtain comparative tensile test data on production aluminum stringers and on stringers reinforced with a boron/epoxy composite, and (2) to determine the load strain curves and the effective area modulus (AE) product for each type stringer.

Approach

Test specimens were strain gaged and subjected to tensile loading to failure. Three boron/epoxy specimens were tested: two with representative frame to stringer clips and one without clips. Three aluminum specimens, all with clips, were tested. Measured strains were used to develop load/strain curves and the area-modulus (AE product). Verification of the effective area modulus of the boron/epoxy stringer is necessary to assure the required tail cone stiffness.

Test Specimens

The 24-inch x 6-inch skin stringer test panels shown in Figures 5-1 and 5-2 consisted of both nonreinforced stringers with clips attached to the stringer midpoint and boron/epoxy reinforced stringers both with and without clips at the midpoints.

The boron reinforced specimens were fabricated with fiberglass inserts on one tapered end and all boron on the other.

Tests and Results

Strain gaged production and boron/epoxy reinforced stringer specimens were mounted in a specially designed test fixture shown in Figure 5-3 and were tested to failure as shown in Figure 5-4. For the nonreinforced stringers, the test fixture was aligned to remove all bending from the specimen; however, for the boron/epoxy reinforced specimens it was not possible to eliminate all bending in the specimen due to a shift of the neutral axis resulting from the bonding of the boron/epoxy reinforcement to the stringer. For these specimens the fixture was aligned to eliminate bending in the aluminum, and bending in the boron reinforcement was accepted.

Tensile loads were applied in increments, to failure, and strain measurements were recorded for each load increment. The test results are tabulated in Table 5-1, and the strains are plotted in Figures 5-5 and 5-6. A load strain curve is presented in Figure 5-7.

Tests of tension loads resulted in the specimens failing at either tapered end. Therefore, no conclusions could be made as to the relative merits of the glass tapered end or of the all boron tapered end.

Discussion

All the nonreinforced stringer specimens experienced tensile failure initiating in the stringer at the clip rivet hole and progressing through the stringer and skin.

The boron/epoxy stringer specimens experienced two types of failures: failure of the bond, and tension failure of the aluminum stringer. The reinforced stringer, without clips, experienced failure of the boron/epoxy composite-to-stringer bond without subsequent failure of the aluminum stringer or skin. One reinforced stringer, with clips at the midpoint, experienced tensile failure in the stringer at the clip rivet hole, followed by a simultaneous failure of both the boron/epoxy bond and the aluminum skin. The second reinforced stringer, with clips at the midpoint, experienced a partial failure of the boron/epoxy-to-stringer bond. Increasing load resulted in complete bond failure and fracture of the aluminum skin and stringer at the clip rivet hole.

The load/strain curve for the reinforced stringers shown in Figure 5-7 is presented in terms of load versus strain at the neutral axis of the reinforced section. Strain at the neutral axis was plotted to compensate for the bending experienced in the boron/epoxy reinforcement discussed previously. Strain at the neutral axis was obtained from plots of the measured bending strain distribution across the reinforced section for each loading increment shown in Figures 5-5 and 5-6.

Analysis

The tension modulus of the aluminum/skin panel was substantiated by tests and analysis:

Net area of aluminum skin/stringer is 0.310 in.^{2}

The calculated tension modulus in the test panel at a load of 5,000 pounds and a strain of 1,500 x 10^{-6} in./in. (see Figure 5-7) is:

$$\sigma_A = \frac{P}{A} = \frac{5,000}{0.310} = 16,100 \text{ lb./in.}^2$$

$$E_A = \frac{\sigma_A}{\varepsilon} = \frac{16{,}100}{1{,}500 \times 10^{-6}} = 10.75 \times 10^6 \text{ lb./in.}^2$$

Net area of boron/epoxy reinforced panel is 0.457 in.^{2}.

The tension modulus and area modulus product $(AE)_R$ of the boron/epoxy reinforced test panel at a load of 5,000 pounds and a strain of 500×10^{-6} in./in. (see Figure 5-7) is:

$$\sigma_R = \frac{P}{A} = \frac{5{,}000}{0.457} = 10{,}900 \text{ lb./in.}^2$$

$$E_R = \frac{\sigma_R}{\varepsilon} = \frac{10{,}900}{500 \times 10^{-6}} = 21.9 \times 10^6 \text{ lb./in.}^2$$

$$(AE)_R = .457(21.9 \times 10^6) = 10.0 \times 10^6$$

The maximum skin/stringer area of the current aircraft is 0.931 in.^{2}.

Therefore, the maximum area modulus produce $(AE)_A$ is equal to:

$$(AE)_A = 0.931(10.5 \times 10^6) = 9.80 \times 10^6$$

An effective area, based on AE, is an input into the computer shear and bending analysis program (see Reference 1). The area moment of inertia and consequently the stiffness is an output of this program.

The boron/epoxy was converted into an equivalent aluminum area for the computer program as follows:

$$A_{equiv.} = \frac{E_B}{E_A}(A_B) = \frac{33.1 \times 10^6}{10.5 \times 10^6}(0.187)$$

$$= 0.592 \text{ in.}^2$$

Area of boron/epoxy plus stringer and skin is 0.923 in.^{2}.

The area modulus product for the hybrid stringer is therefore:

$$(AE)_R = 0.923(10.5 \times 10^6) = 9.75 \times 10^6$$

From the above analysis and test results, it was determined that the area modulus product for the boron/epoxy reinforcement is essentially equal to the maximum current aircraft area modulus product.

The conversion of the reinforcement into an equivalent aluminum area yields essentially the same area modulus product as that substantiated by test.

Conclusions and Recommendations

Based on the results of the tests presented in this section, it is concluded that:

(1) The tensile strength of the boron/epoxy reinforced stringers is equivalent to that of the nonreinforced stringers.

(2) The limiting factor in the load-carrying ability of the reinforced stringer is the bond strength.

(3) The experimentally determined area-modulus product for both the reinforced and the nonreinforced stringers agreed with the theoretical values.

(4) The area modulus product of the reinforced stringer is equivalent to that of the current production aluminum skin-stringer.

(5) No conclusion can be found from these tests concerning the advantage or disadvantage of the glass insert in the tapered ends.

TABLE 5-1. TENSILE TEST RESULTS

Test No.	Specimen Number	Boron/Epoxy Reinforced	Clips at Midpoint	Failure Load (lb.)	Remarks
1	Al-T1	no	yes	17,000	Figure 5-8
2	Al-T2	no	yes	16,800	Figure 5-8
3	Al-T3	no	yes	16,700	Figure 5-8
4	B-T1	yes	no	17,000	Figure 5-9
5	BC-T2	yes	yes	17,800	Figure 5-10
6	BC-T3	yes	yes	16,300* 17,500	Partial bond failure, stringer, skin and bond failure - Figure 5-11

T - tension

Al - aluminum specimen

B - boron reinforced specimen

C - clip

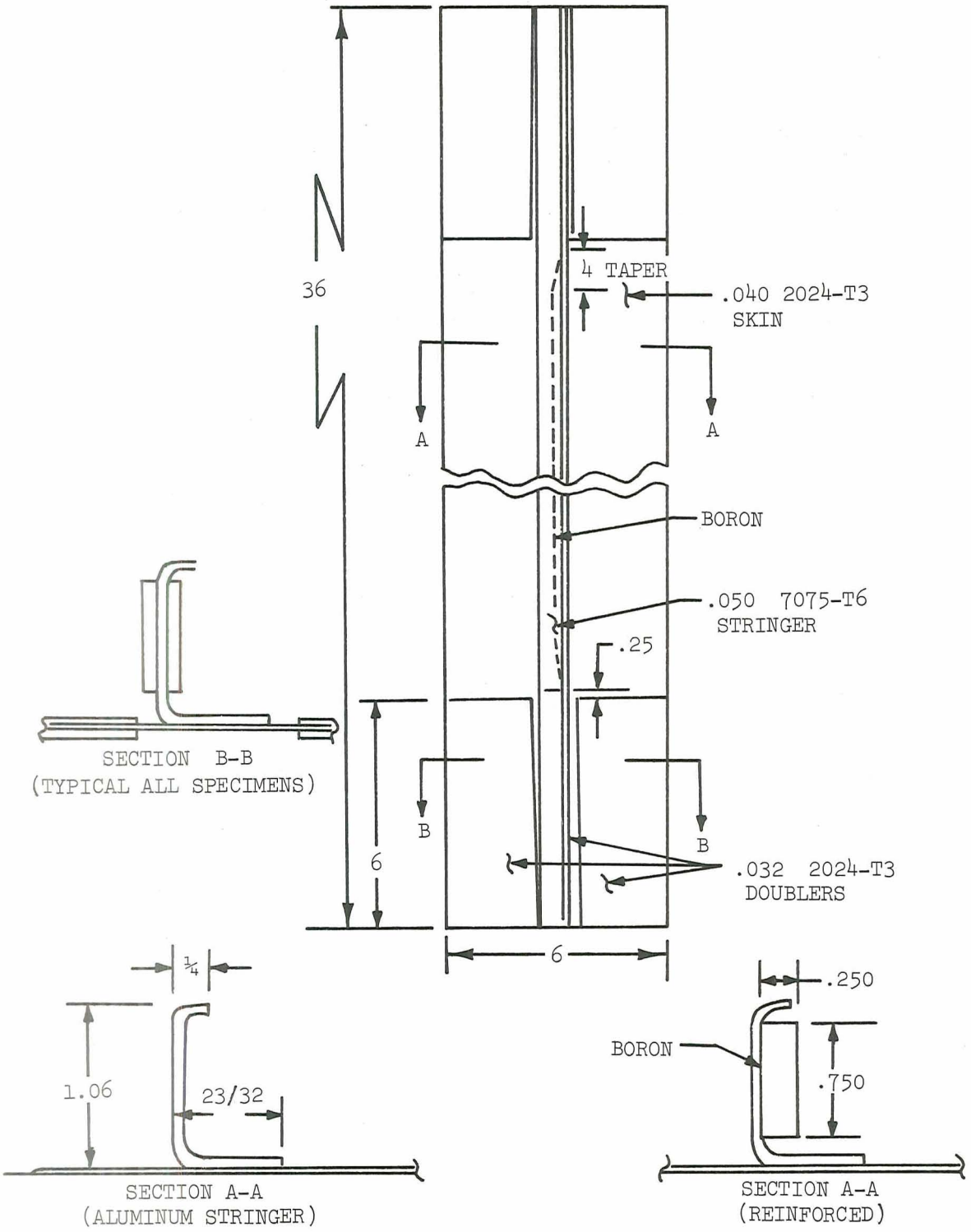

FIGURE 5-1. TENSION AND FATIGUE TEST SPECIMEN GEOMETRY.

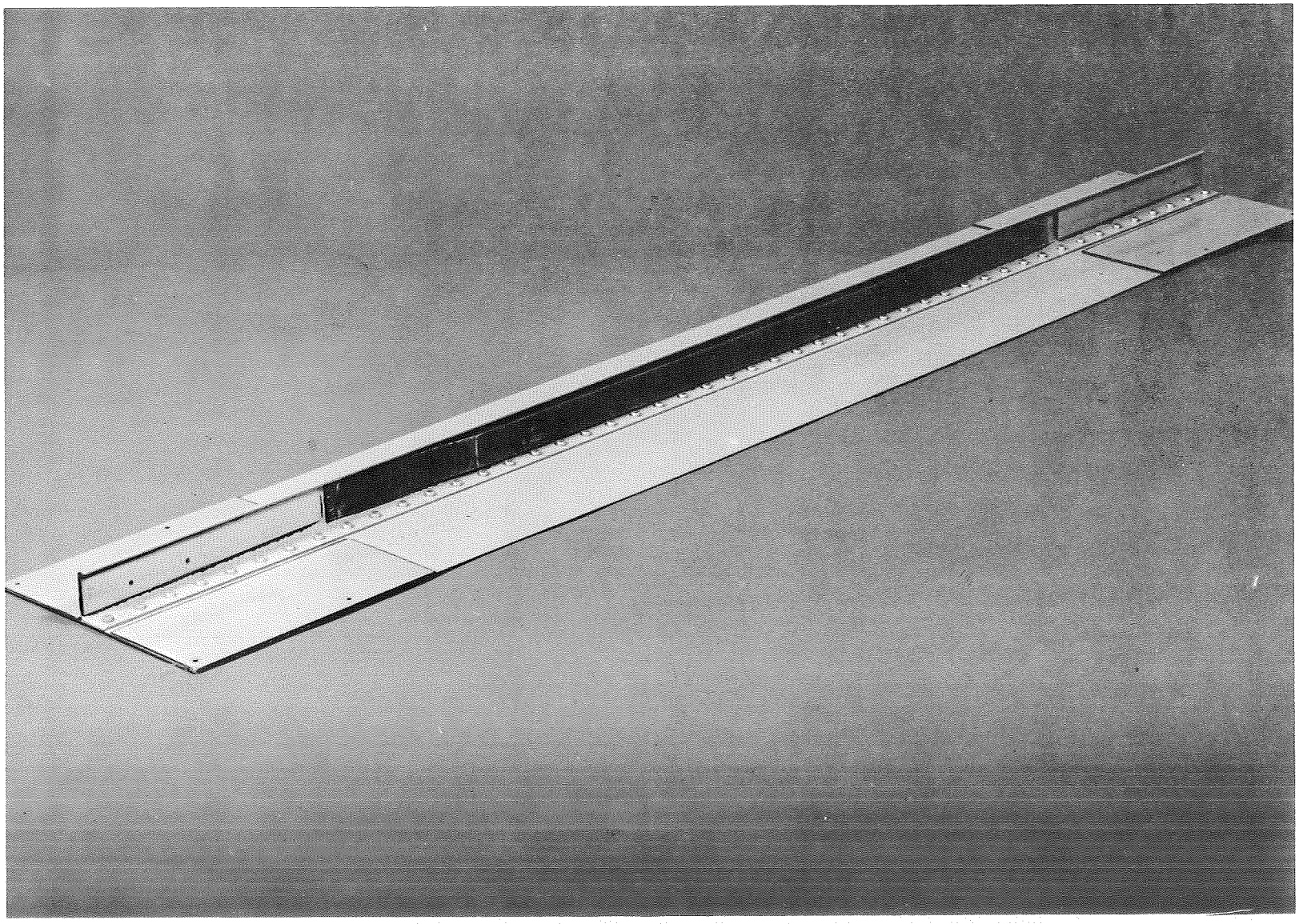

FIGURE 5-2. TENSION TEST BORON/EPOXY REINFORCES STRINGER SPECIMEN.

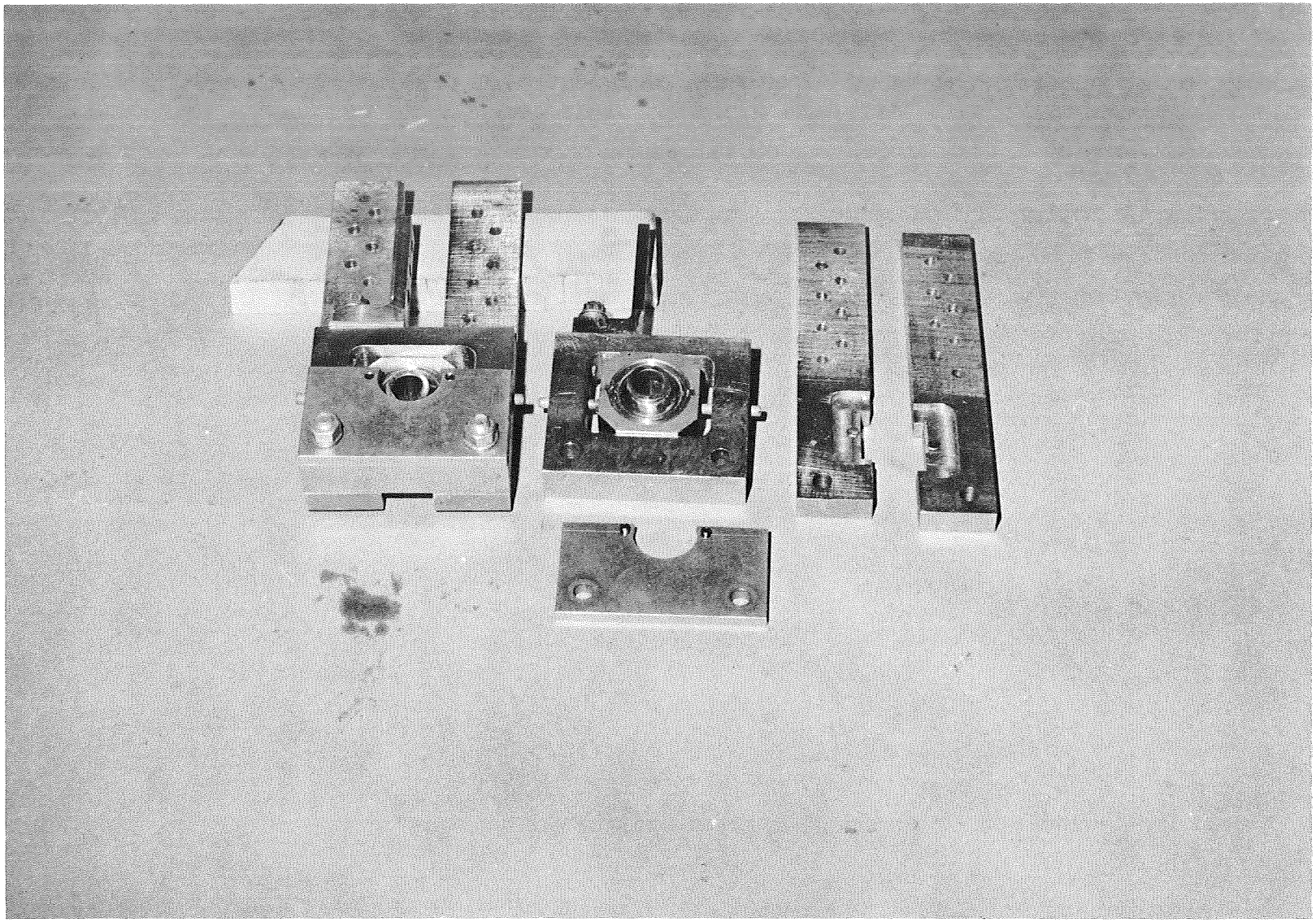

FIGURE 5-3. TENSIÓN AND FATIGUE TEST FIXTURE.

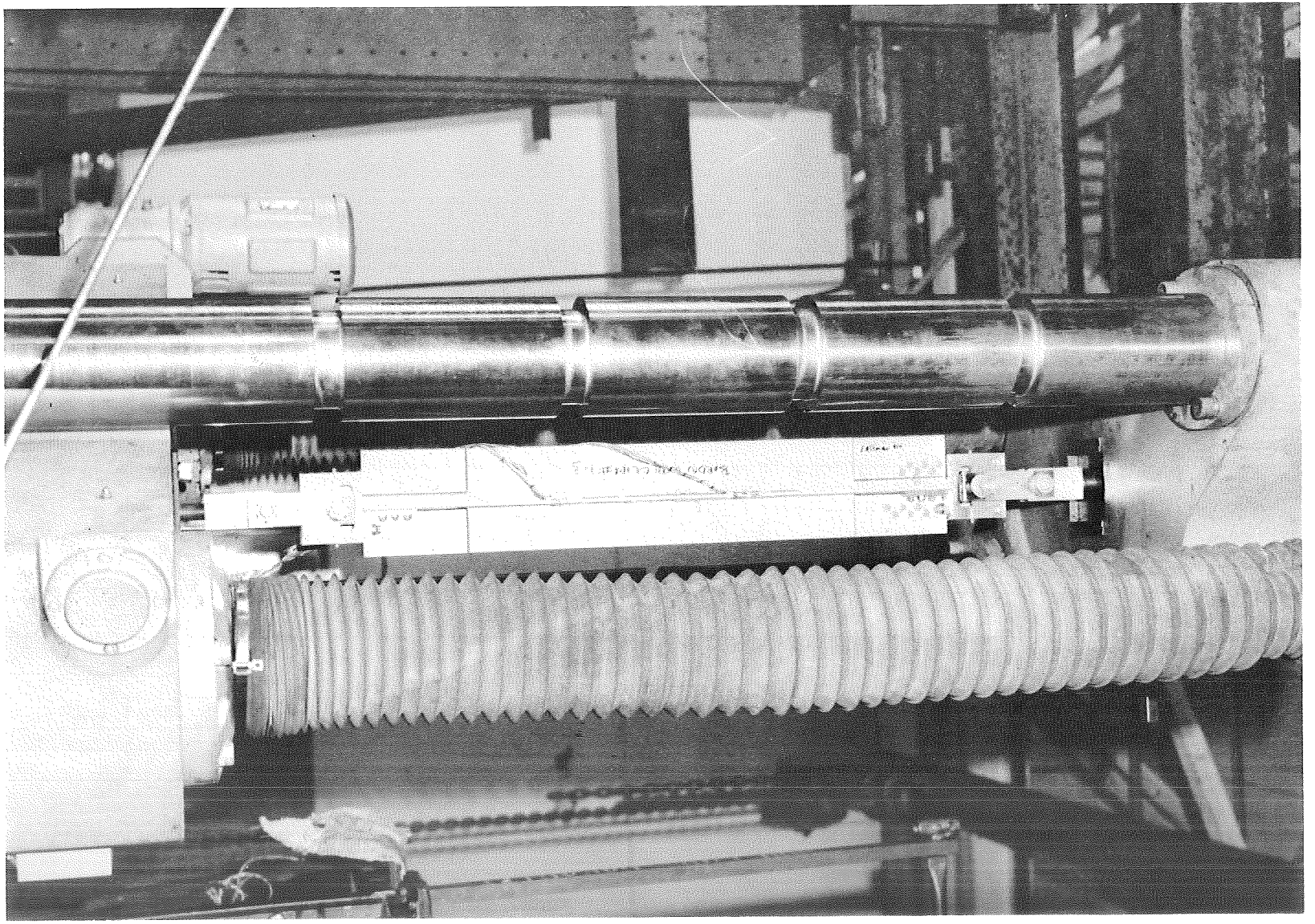

FIGURE 5-4. TENSILE LOAD/STRAIN TEST SET-UP.

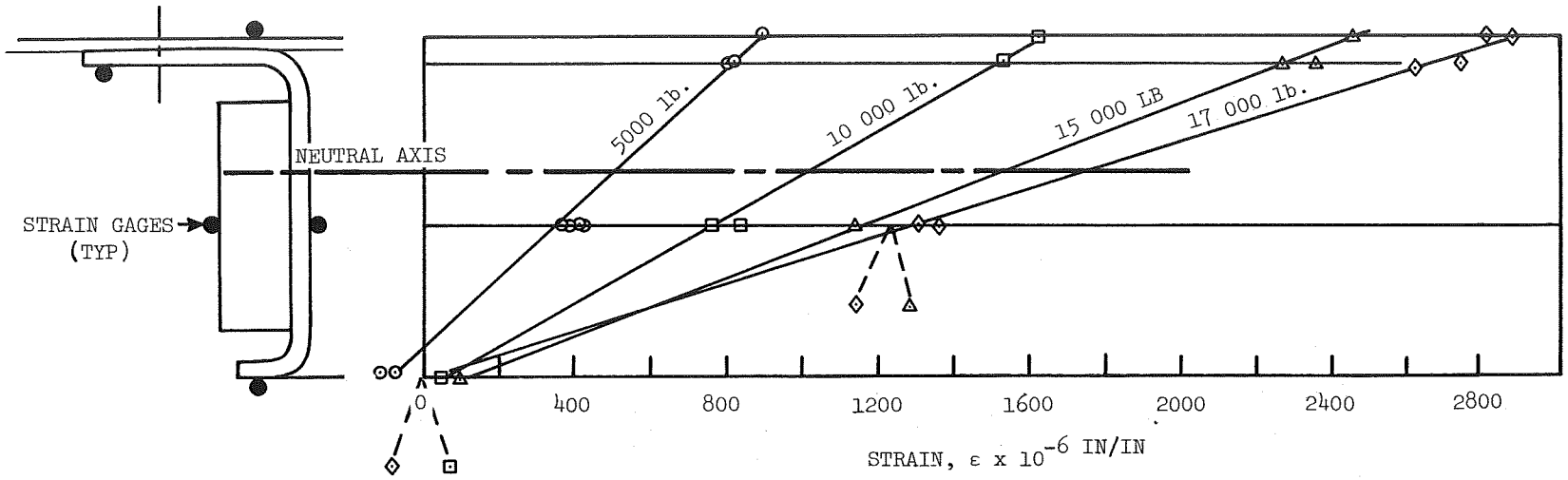

FIGURE 5-5. TENSILE STRAINS MEASURED IN BORON/EPOXY REINFORCED STRINGERS - NO CLIPS.

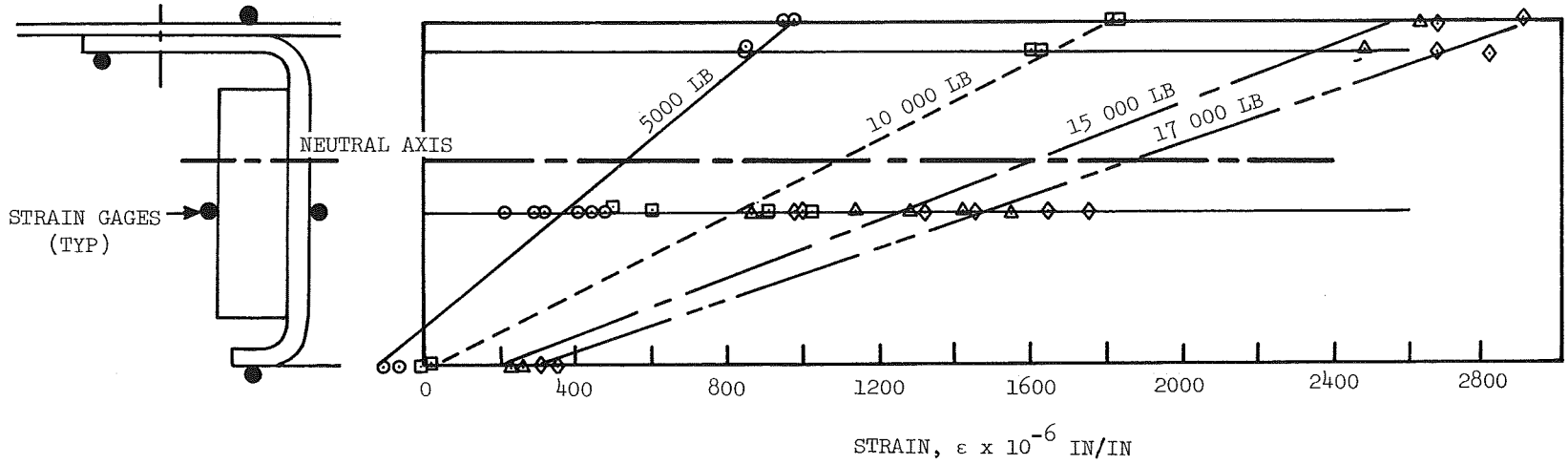

FIGURE 5-6. TENSILE STRAINS MEASURED IN BORON/EPOXY REINFORCED STRINGERS - WITH CLIPS.

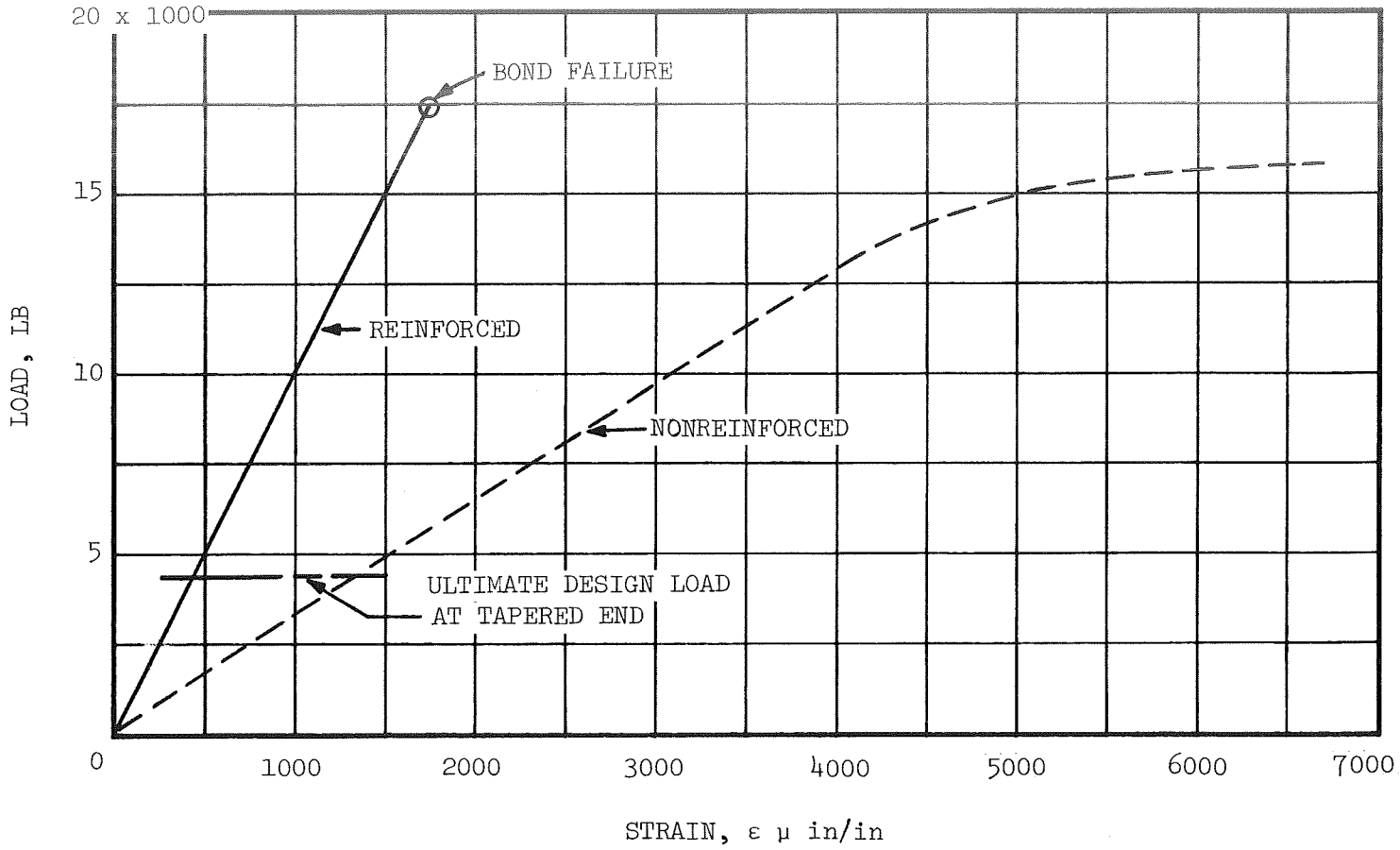

FIGURE 5-7. TENSILE LOAD VERSUS STRAIN FOR REINFORCED AND NONREINFORCED STRINGERS.

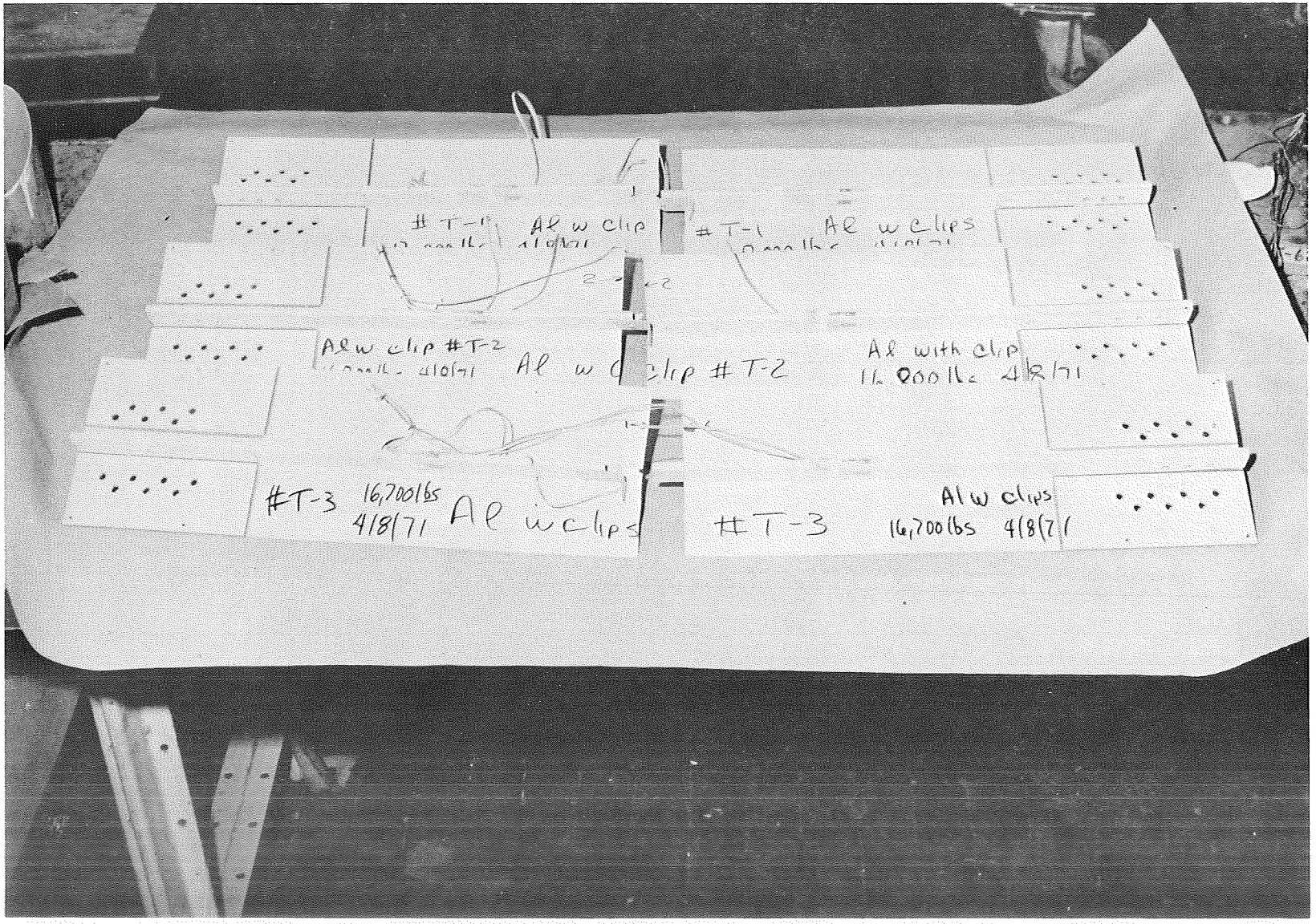

FIGURE 5-8. TENSILE FAILURES IN NONREINFORCED STRINGER SPECIMENS.

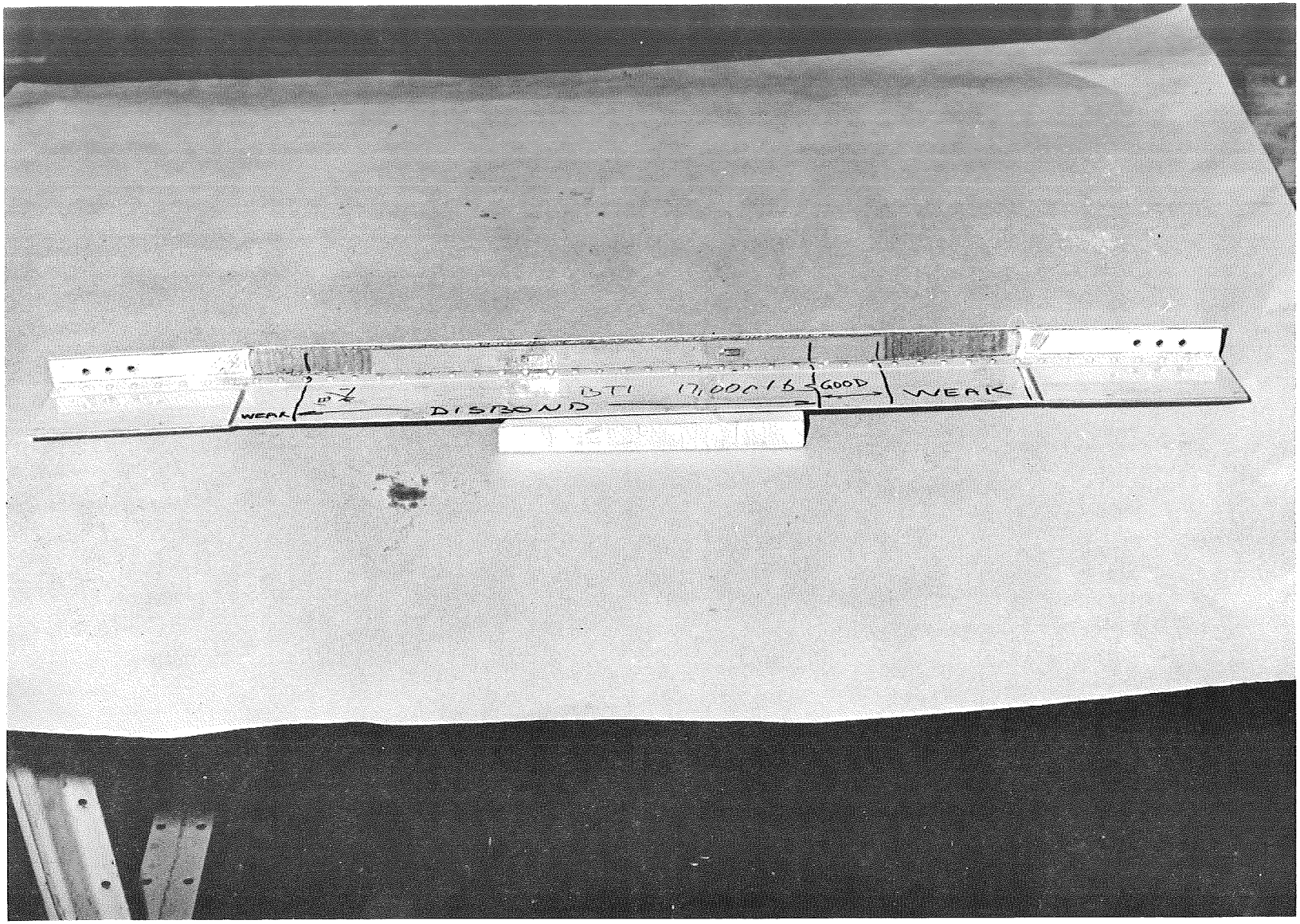

FIGURE 5-9. BOND FAILURE IN REINFORCED STRINGER TENSILE SPECIMEN.

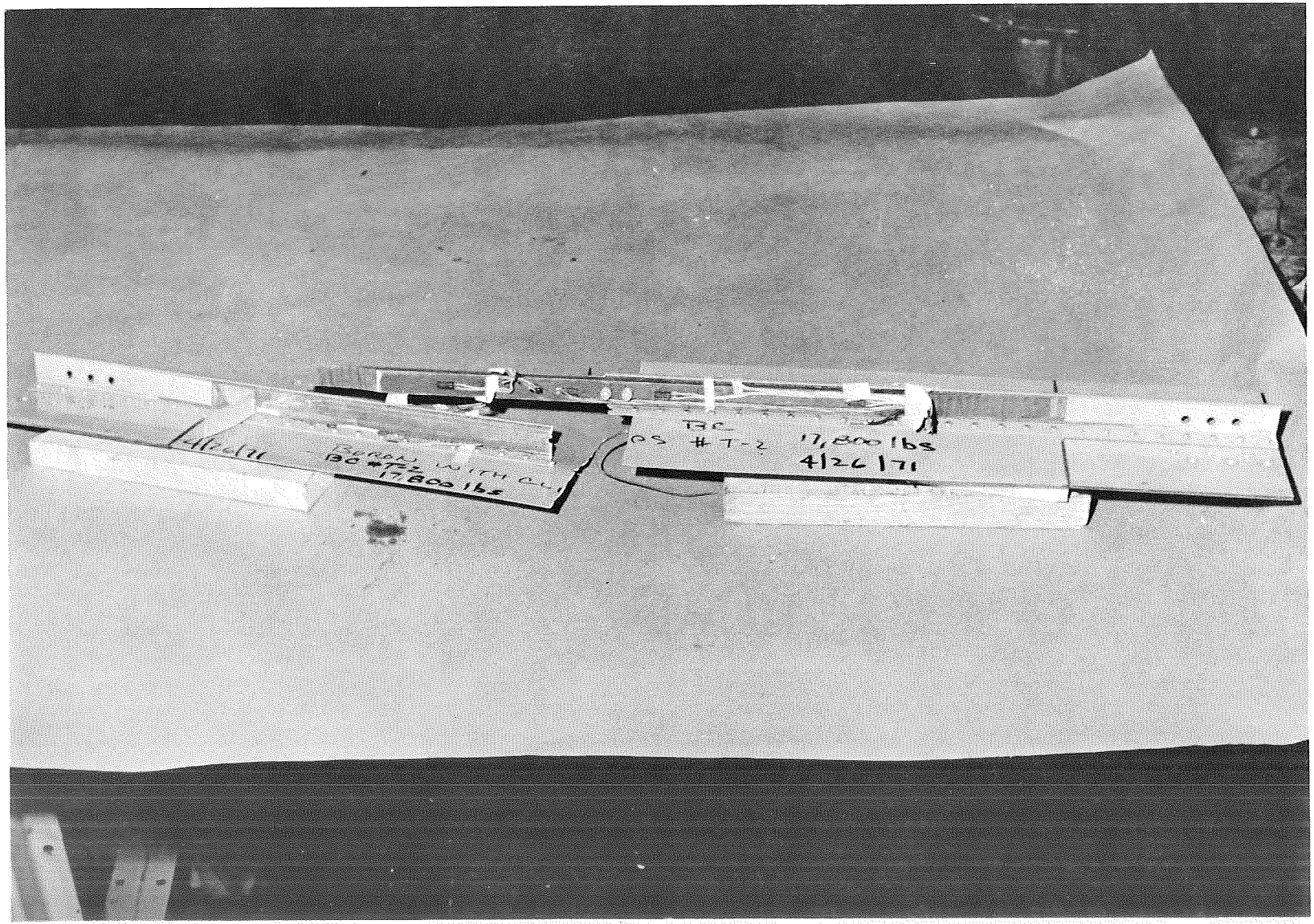

FIGURE 5-10. TENSILE FAILURE IN REINFORCED STRINGER SPECIMEN.

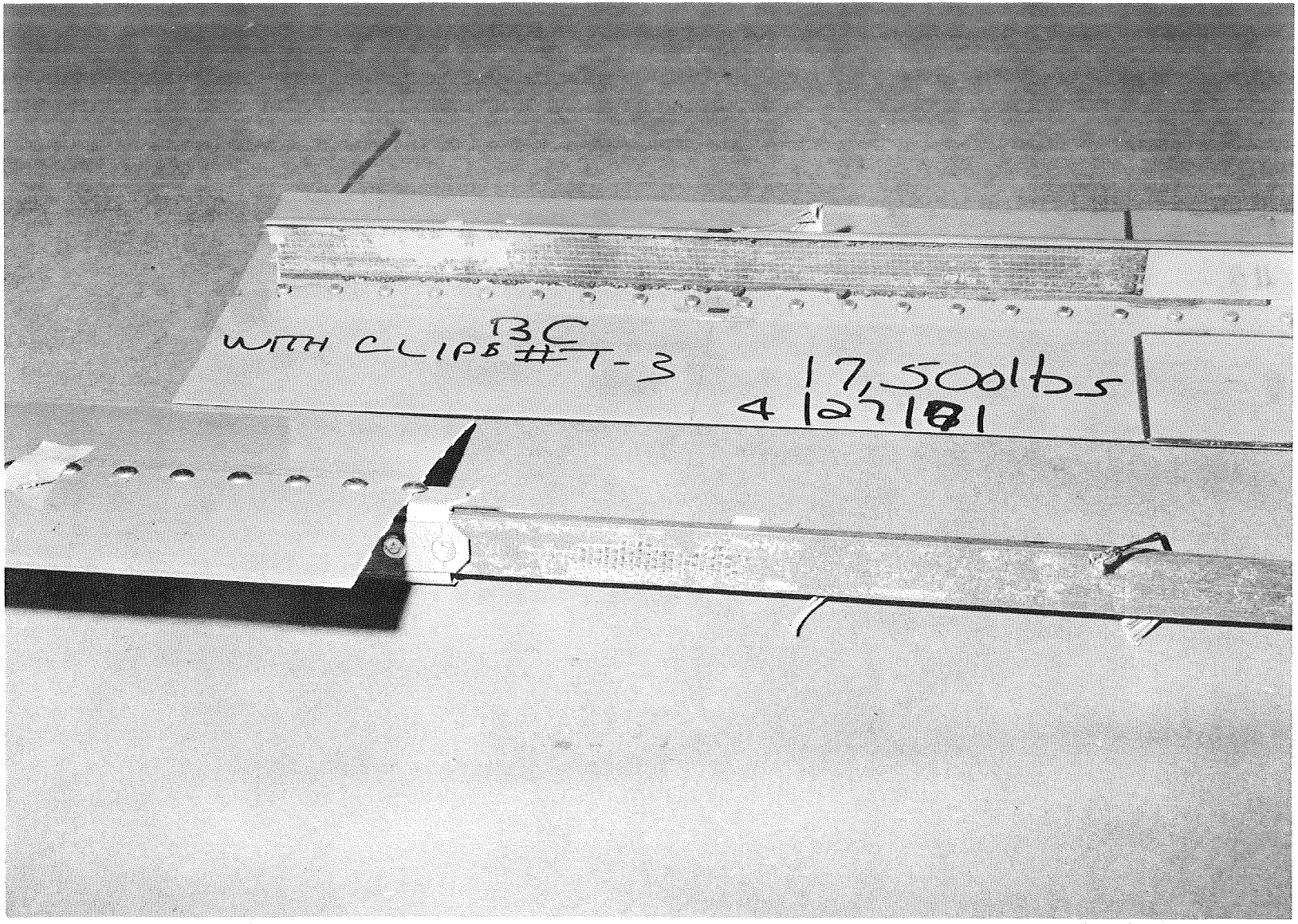

FIGURE 5-11. TENSILE FAILURE IN REINFORCED STRINGER SPECIMEN.

6.0 RESIDUAL THERMAL STRESSES

Objective

Objectives of this test were: (1) to determine the thermal stresses induced in the boron/epoxy reinforced stringer; (2) to establish the design coefficients of thermal expansion for aluminum and boron/epoxy composite; (3) to verify the analysis for the prediction of thermal stresses.

Approach

An aluminum stringer and a boron/epoxy strip were instrumented and bonded together. The instrumentation was then monitored as the bonded piece was cooled from the bonding temperature of +250° F. to -65° F. An additional "dummy" aluminum stringer and boron/epoxy block were instrumented and monitored over the same temperature range. The "dummy" instrumentation was used to determine both the thermal coefficients of expansion for the aluminum and the boron and the temperature-induced apparent strain corrections for the strain gages used. The instrumentation on the bonded piece was used to determine the thermal stresses induced in the bonded piece.

Test Specimens

The test specimens shown in Figure 6-1 consisted of a 48-inch aluminum stringer and a 48-inch by 0.25-inch by 0.75-inch boron/epoxy reinforcing strip for measurement of residual strains. A "dummy" aluminum stringer and boron/epoxy block for measurement of the coefficient of thermal expansion are also shown in Figure 6-1.

Testing and Results

The aluminum stringer and the boron/epoxy reinforcing strip were strain gaged prior to bonding and were placed in a curing oven and bonded together. The strain-gaged "dummy" strips were placed in the oven at the same time. After a one-hour curing period at +250° F., the specimens were cooled to room temperature with oven temperature and specimen strain measurements periodically recorded.

The reinforced stringer was inspected by the Fokker bond test, and no bond deviations were found. The reinforced and "dummy" strips were then placed in an environmental chamber shown in Figure 6-2 and were cooled to -65° F. The temperatures were held until the specimen and chamber were in equilibrium, and strain and temperature measurements were periodically recorded.

The resulting thermal strains, corrected for temperature-induced apparent strains, are shown in Figure 6-3. The analytically predicted induced thermal strains are also shown in Figure 6-3. Test deviations from predicted values in the region of cure to room temperature may be attributed to the fact that the temperature read was that of the oven upon cooling and not necessarily that of the specimen.

Discussion

The strain gages used in these tests were self-temperature-compensating gages. These gages, when bonded to a material having the same coefficient of thermal expansion as the gage, will compensate for strains resulting from thermal expansion or contraction of the material. Limits are defined by a temperature-induced apparent strain curve supplied with each type of gage.

The strain gages bonded on the "dummy" aluminum stringer had a compensating temperature coefficient of 13×10^{-6} in./in./$^{\circ}$F. The output from these gages was examined over the entire temperature range of $+250^{\circ}$ F. to -65° F. and was found to be well within the limits defined by the temperature-induced apparent strain curve for this type gage. From these results it was concluded that the thermal coefficient of thermal expansion for the aluminum stringer was 13×10^{-6} in./in./$^{\circ}$ F.

The strain gages bonded on the boron/epoxy "dummy" block had a compensating temperature coefficient of 5×10^{-6} in./in./$^{\circ}$ F. This value was somewhat higher than the design value for boron of $2.0 - 3.0 \times 10^{-6}$ in./in./$^{\circ}$ F. and resulted in the measured strain output being outside the limits defined by the temperature-induced apparent strain curve. The thermal coefficient of expansion for the boron was then determined in the following manner. The theoretical temperature strain output for the unbonded strain gage was calculated for the temperature range. The measured strain output was then subtracted from the theoretical strain gage output. The differential in strain was attributed to strain in the "dummy" boron block. This difference in strain was divided by the change in temperature to obtain a coefficient of thermal expansion of 2.14×10^{-6} in./in./$^{\circ}$ F.

The "dummy" aluminum and boron gages were also used to determine the corrections for the temperature-induced apparent strain in the bonded aluminum/boron composite stringer. Since the "dummy" gages were self-temperature compensating, there should have been no measured output from the "dummy" over the entire temperature range. Both the aluminum and the

boron "dummy" gage outputs were examined separately, and the corrections required to null the gage output at each temperature were also applied to the same type gage on the bonded specimen at that temperature.

The bonded specimen was inspected by the Fokker Bond Tester and no bond deviations were found.

Analysis

The predicted induced thermal strains in the components of the hybrid stringers are shown in Figure 6-3. The thermal adhesive shear stress peaks to a maximum at the ends of an untapered joint as shown in Figure 6-4 and diminishes to zero over the majority of the reinforcement length. At the same time, the direct stresses in the adherends are zero at the ends of the joint and reach a constant maximum value over the majority of the reinforcement length.

The analysis of the model shown in Figure 6-4 results in a second order linear differential equation from which the following equations for the three component stresses are formed:

$$\sigma_B = k\left[\frac{\sinh(\mu L) - \sinh(\mu X) - \sinh(\mu(L - X))}{\sinh(\mu L)}\right]$$

$$\sigma_A = -(\sigma_B) \cdot \left(\frac{A_B}{A_A}\right)$$

$$\tau = \frac{A_B k \mu}{b}\left[\frac{\cosh(\mu(L - X)) - \cosh(\mu X)}{\sinh(\mu L)}\right]$$

where $$k = \frac{E_B A_A E_A \Delta T(\alpha_B - \alpha_A)}{(A_B E_B + A_A E_A)}$$

$$\mu^2 = \left(\frac{G_a b}{t_a}\right)\frac{(A_B E_B + A_A E_A)}{A_B E_B A_A E_A}\left[\frac{1}{\left(\frac{G_a}{t_a}\left[\frac{t_a}{G_a} + \frac{A_B}{2G_B b} + \frac{A_A}{2G_A b}\right]\right)}\right]$$

where

G_a = adhesive shear modulus

b = joint width

t_a = adhesive thickness

A_A = cross-sectional area of adherend A

A_B = cross-sectional area of adherend B

E_A = tensile modulus of adherend A

E_B = tensile modulus of adherend B

G_A = shear modulus of adherend A

G_B = shear modulus of adherend B

α_A = thermal coefficient of expansion of adherend A

α_B = thermal coefficient of expansion of adherend B

ΔT = change in temperature

The maximum values of thermal stress are:

when $X = (\frac{L}{2})$ $\quad \sigma_B = (\sigma_B)$ max.

$\sigma_A = (\sigma_A)$ max.

$$(\sigma_B)_{max} = k\left[\frac{\sinh(\mu L) - \sinh(\frac{\mu L}{2}) - \sinh(\frac{\mu L}{2})}{\sinh(\mu L)}\right]$$

$$= k\left[1 - \frac{2\sinh(\frac{\mu L}{2})}{\sinh(\mu L)}\right]$$

if $(\mu L) > 5$, then $\left[1 - \frac{2\sinh(\frac{\mu L}{2})}{\sinh(\mu L)}\right] \simeq 1$

then

$$(\sigma_B)_{max} = k$$

$$(\sigma_A)_{max} = -\frac{kA_B}{A_A}$$

when $X = 0$, $\tau = (\tau)_{max}$

$$(\tau)_{max} = \frac{A_B k\mu}{b} \frac{\cosh(\mu L) - \cosh(0)}{\sinh(\mu L)}$$

if $(\mu L) > 5$ then, $\frac{\cosh(\mu L) - 1}{\sinh(\mu L)} \simeq 1$

$$(\tau)_{max} \simeq \frac{A_B k\mu}{b}$$

Figure 6-5 illustrates the sequence, in chronological order, of the fabrication versus temperature history to which the reinforced stringer/skin assembly is most likely to be subjected. The internal loads of this assembly are computed for each of the three components. These component loads P_{STR}, P_B, and P_{SK} for aluminum stringers, boron/epoxy reinforcement and aluminum skin respectively are given by the following equations.

$$P_{STR} = \frac{A_{STR}E_A}{(A_{STR} + A_{SK})E_A + A_BE_B}\left[P + A_BE_B(\alpha_A - \alpha_B)\Delta T^*\right]$$

$$+ \frac{A_{STR}E_A}{A_{STR}E_A + A_BE_B}\left[A_BE_B(\alpha_A - \alpha_B)\Delta T\right]$$

$$P_B = -\frac{A_BE_B}{(A_{STR} + A_{SK})E_A + A_BE_B}\left[P - (A_{STR} + A_{SK})E_A(\alpha_A - \alpha_B)\Delta T^*\right]$$

$$+ \frac{A_BE_B}{(A_{STR}E_A + A_BE_B)}\left[A_{STR}E_A(\alpha_A - \alpha_B)\Delta T\right]$$

$$P_{SK} = \frac{A_{SK}E_A}{(A_{STR} + A_{SK})E_A + A_BE_B}\left[P + A_BE_B(\alpha_A - \alpha_B)\Delta T^*\right]$$

where

P_{STR} = load in the aluminum stringer

P_B = load in the boron/epoxy

P_{SK} = load in the aluminum skin

ΔT is the temperature change from curing the bond between the boron/epoxy and the aluminum stringer at 250° F. and cooling the assembly to room temperature 70° F.

ΔT^* is the temperature change from 70° F. when the skin is riveted to the reinforced stringer to the minimum environmental temperature of the CH-54B (-65° F.).

Conclusions

Based on the results of the test presented in this section, it is concluded that:

(1) The coefficient of thermal expansion of the aluminum stringer is 13 x 10^{-6} in./in./°F.

(2) The coefficient of thermal expansion of the boron/epoxy composite reinforcement is 2.14 x 10^{-6} in./in./°F.

(3) Both experimentally determined coefficients of thermal expansion agree favorably with presently used design values.

(4) The discrepancy in the predicted versus tested induced thermal stresses at raised temperatures is attributed to the measurement of oven temperature and not specimen temperature.

(5) Thermal stresses can be predicted analytically for design.

It is recommended that in future temperature verification tests thermocouples be placed on the specimen to assure correct temperature and strain gage correlation.

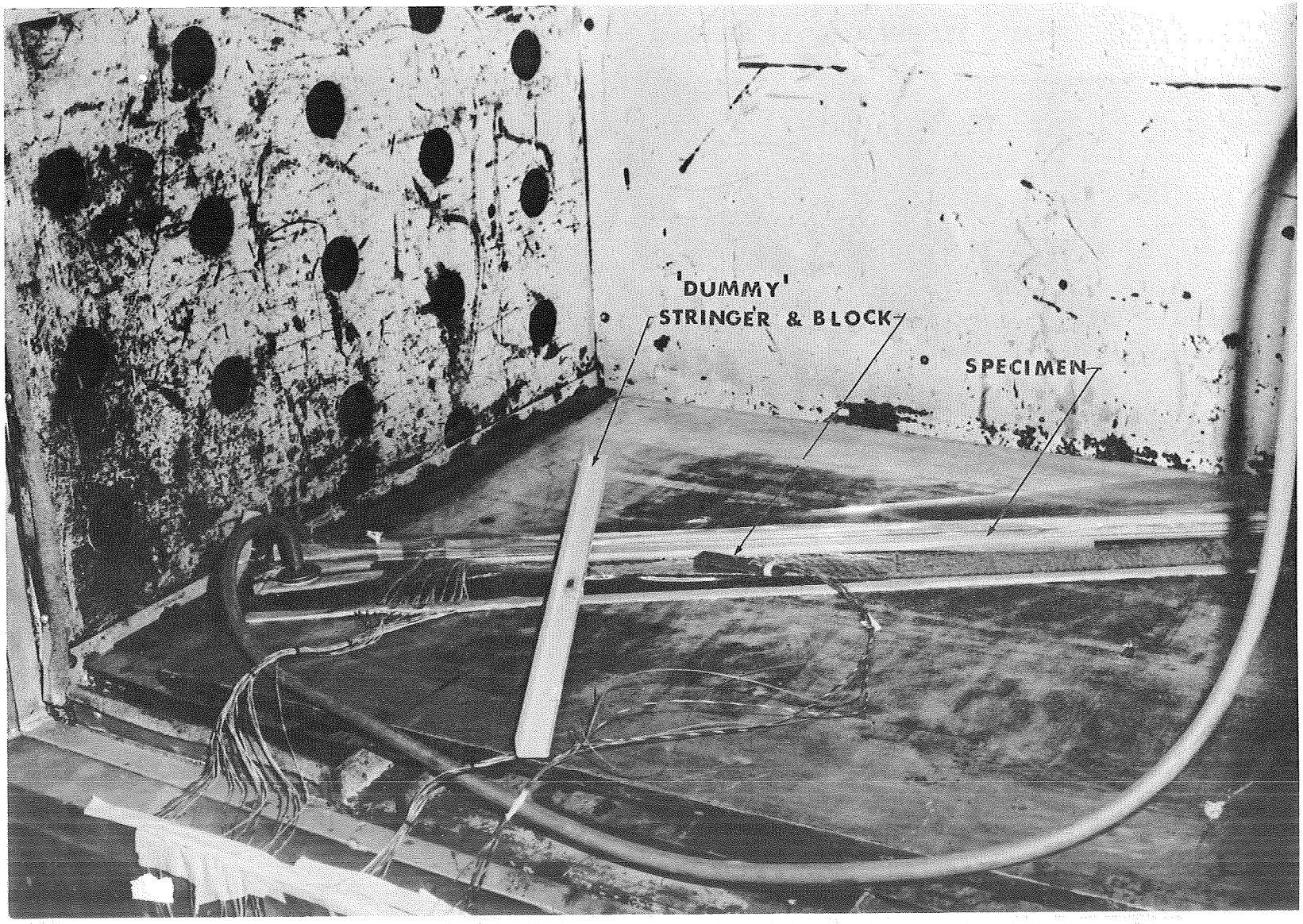

FIGURE 6-1. THERMAL TEST SPECIMEN.

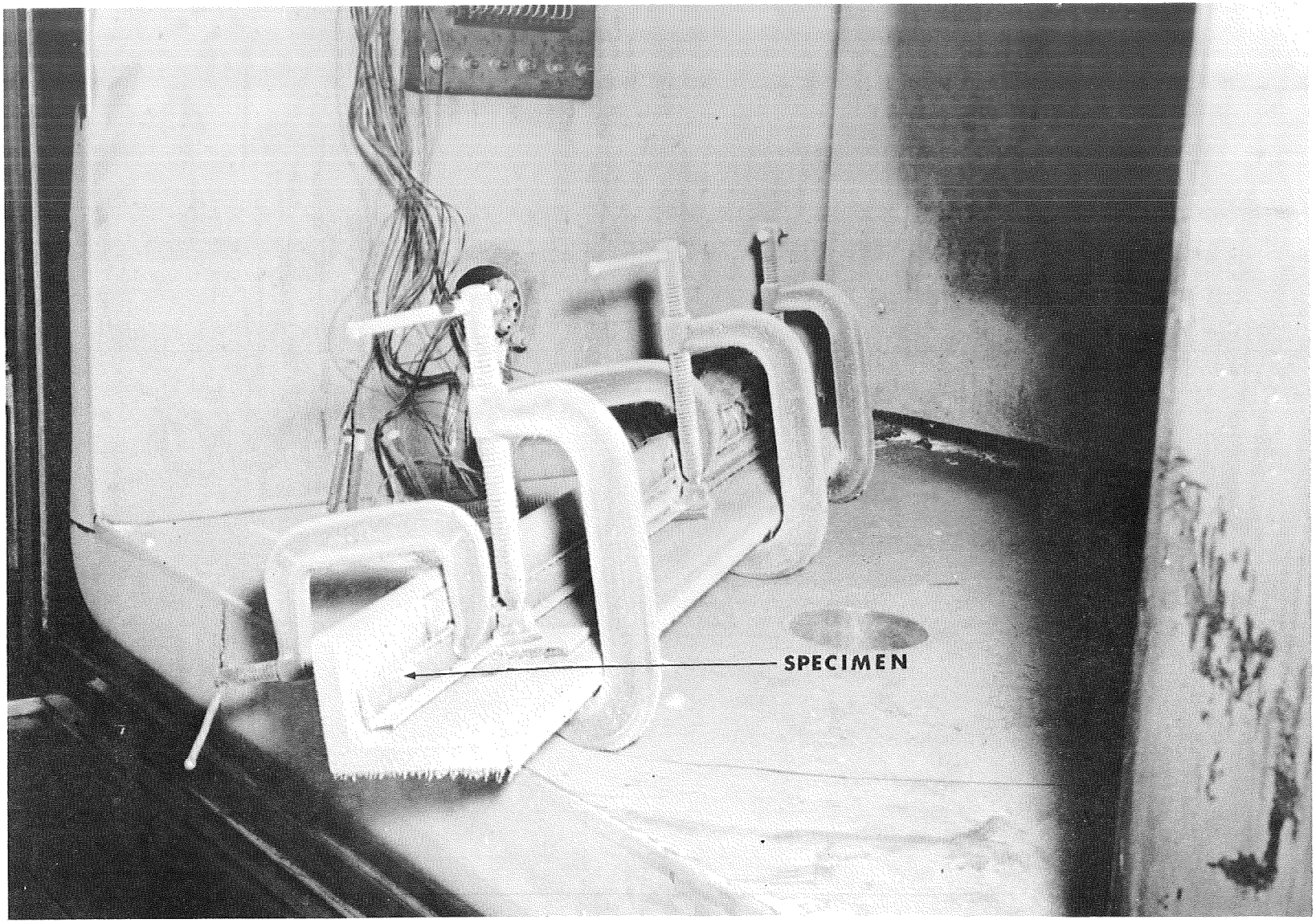

FIGURE 6-2. THERMAL TEST SPECIMEN IN ENVIRONMENTAL CHAMBER.

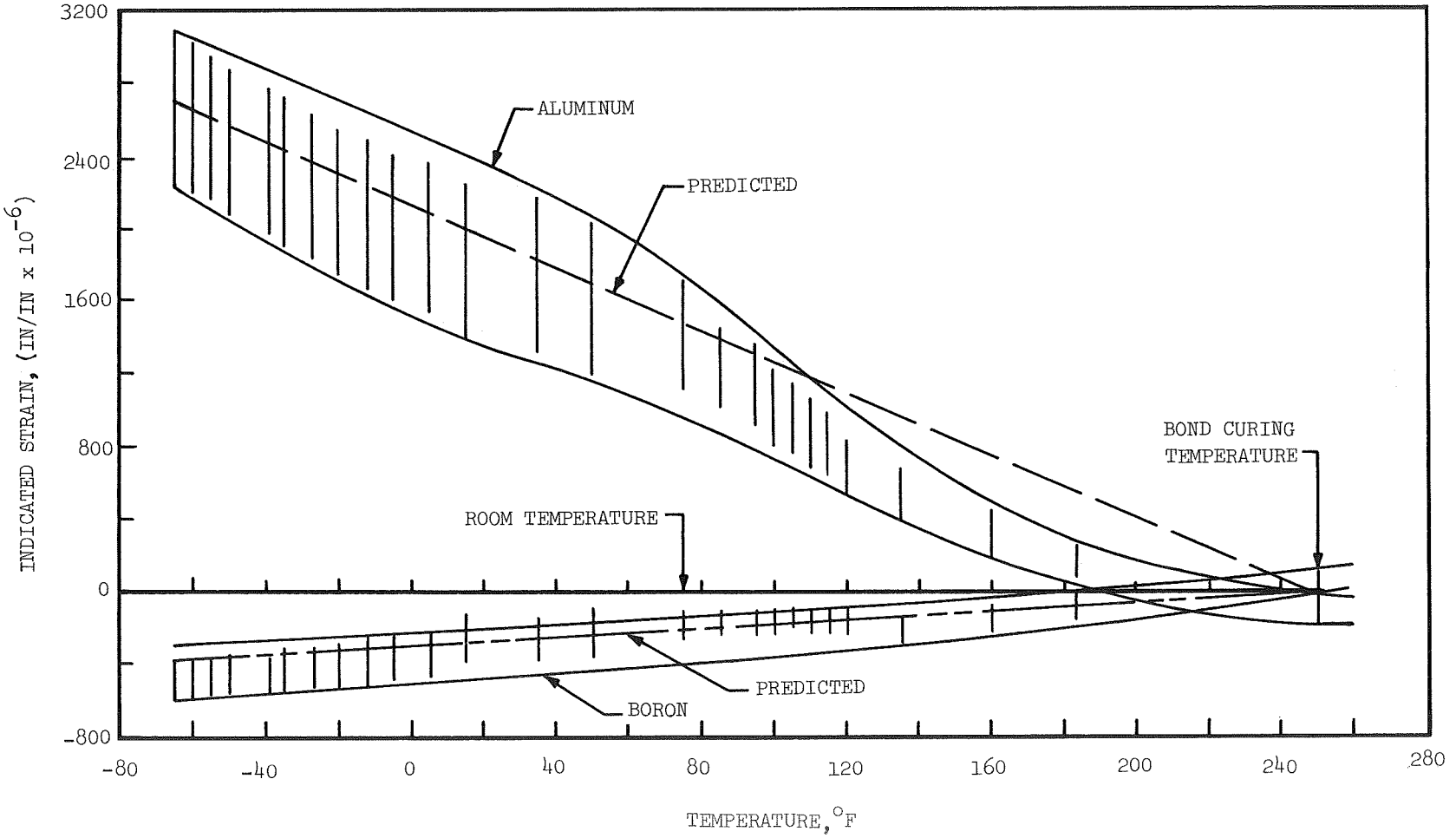

FIGURE 6-3. CALCULATED AND TEST RESULTS OF INDUCED THERMAL STRAINS IN BORON/EPOXY REINFORCED STRINGERS.

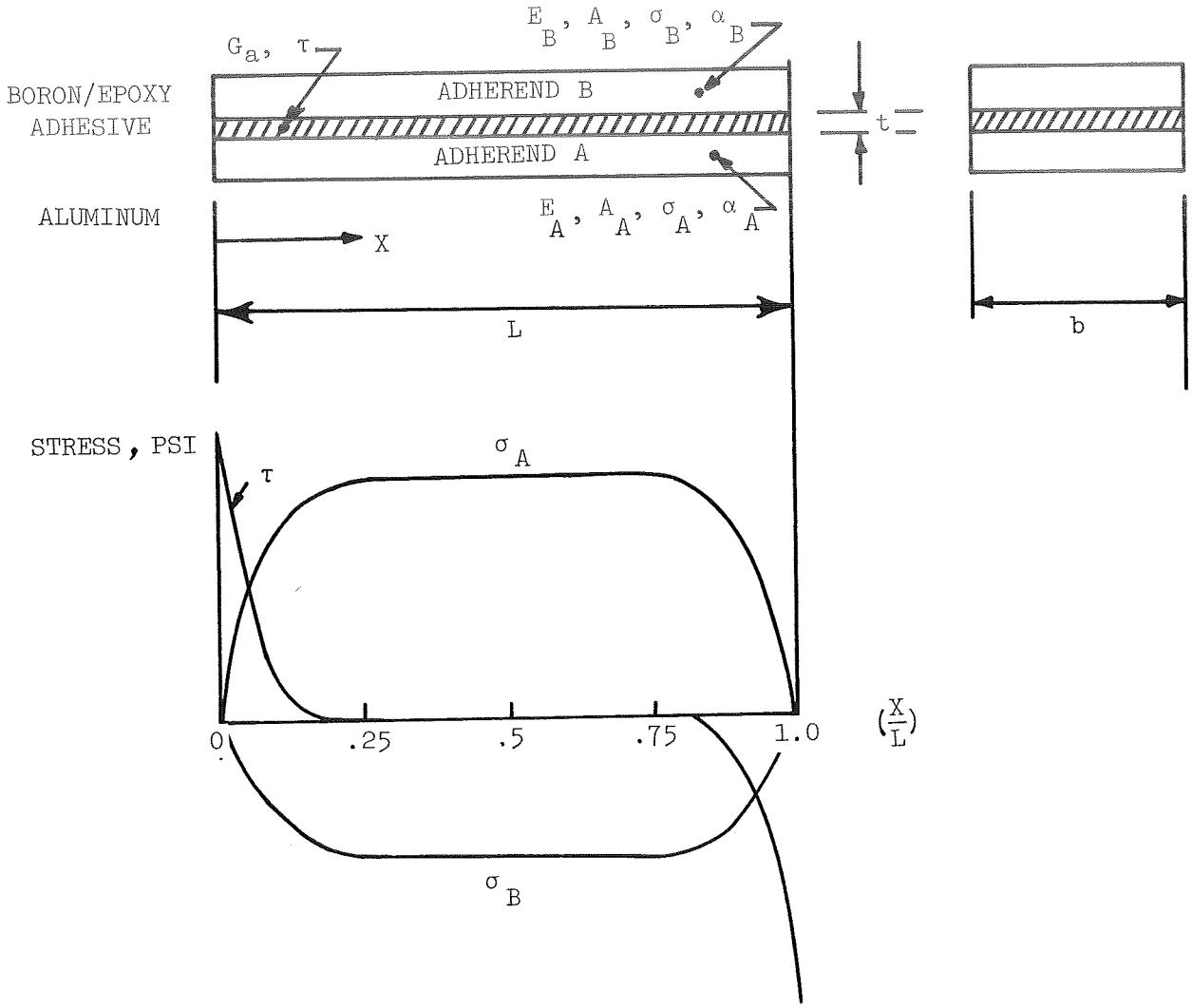

FIGURE 6-4. INDUCED THERMAL SHEAR STRESS DISTRIBUTION.

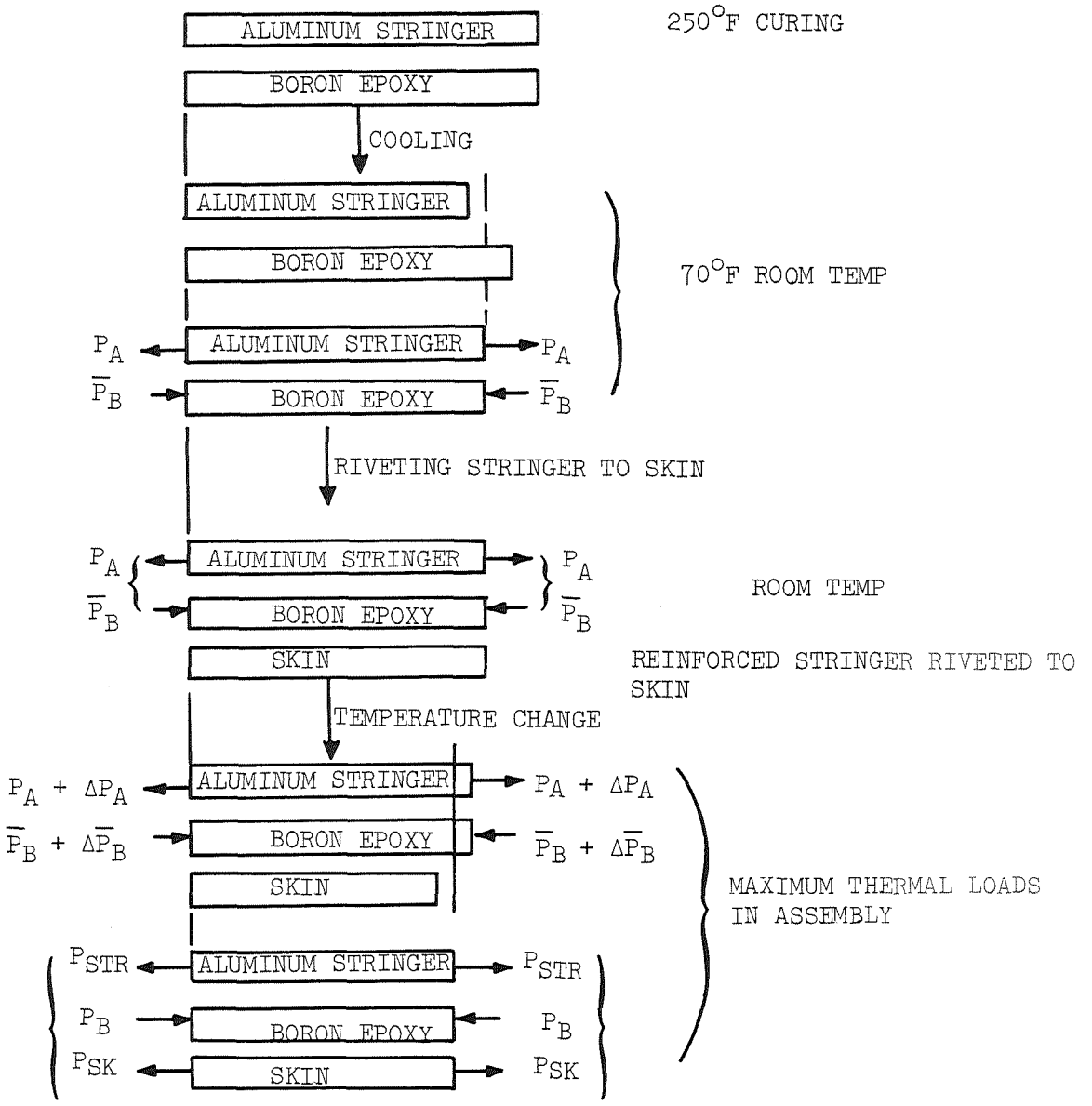

FIGURE 6-5. FABRICATION/TEMPERATURE SEQUENCE FOR BORON/EPOXY REINFORCED STRUCTURES.

7.0 SHEAR AND COMPRESSION TESTS

Objective

The objective of these tests was to obtain comparative shear and compression test data on production aluminum and boron/epoxy reinforced skin stringer panels.

Approach

Shear and compressive axial loads were applied to the specially designed shear and compression reinforced and nonreinforced specimens, and the resulting failure loads and modes of failure were recorded and compared.

Test Specimens

The shear and compression test specimens were basically 20-inch by 30-inch panels as shown in Figures 7-1 and 7-2. The boron/epoxy reinforced specimens were fabricated with fiberglass inserts on one tapered end and all boron on the other.

Two shear test specimens were fabricated with boron/epoxy reinforced stringers and two were of conventional construction.

Two compression test specimens were fabricated with boron/epoxy reinforced stringers and two were of conventional construction. The ends of these specimens were potted to facilitate load introduction. The boron/epoxy reinforcement was terminated before the potted end to simulate the proposed aircraft construction.

The potted ends were milled parallel with each other to within a tolerance of -0.000 to +0.005 inches.

Tests and Results

Shear panel tests were performed on both the production and the boron/epoxy reinforced stringer panels using a picture frame shear test fixture

mounted in the Statec Testing Machine as shown in Figure 7-3. The test loads were applied in increments to failure. The test results are summarized in Table 7-1.

Compression tests were performed on both the production and the boron/epoxy reinforced stringer panels in the Statec Testing Machine as shown in Figure 7-4. A photograph of an untested compression panel with the strain gage locations is shown in Figure 7-5. Incremental test loads were applied to failure. The test results are tabulated in Table 7-2. The photographs of tested panels are identified in Figures 7-6 through 7-11 and are cross referenced with the test results in Tables 7-1 and 7-2.

Discussion

Both the current production aluminum and boron/epoxy reinforced shear panels experienced skin shear failures at the edge rivet holes and at the point of load introduction. The failure mode and load magnitude for both types of panels were essentially the same. The average failing load for the conventional aluminum shear panel was 25,500 pounds while that predicted by analysis was 28,800 pounds.

The two conventional design compression panels failed at loads of 23,300 and 22,900 pounds with failure resulting from local crippling near the midpoint of the nonreinforced stringers. The two boron/epoxy reinforced stringer panels failed at loads of 34,500 and 29,500 pounds with failure resulting from local crippling of the reinforced stringer at the tapered end of the boron/epoxy reinforcement.

The predicted loads for the nonreinforced assemblies were 25,500 pounds and 29,400 pounds respectively. The failure mode of the reinforced panel was predicted to be in the aluminum stringer at the termination of the boron/epoxy reinforcement, thereby permitting the use of conventional analytical formulas.

Conclusions and Recommendations

Based on the results of the tests presented in this section, it is concluded that:

(1) The shear strength of the boron/epoxy reinforced stringer panels is equivalent to the shear strength of the nonreinforced stringer panels.

(2) The compressive strength of the boron/epoxy reinforced stringer panel is equal to or greater than the compressive strength of the nonreinforced stringer panels.

(3) Failure of the compression and shear panels was such that no conclusions can be made as to the performance of the fiberglass inserts in the tapered ends.

TABLE 7-1: SHEAR PANEL TEST RESULTS

Specimen Number	Boron/Epoxy Reinforced	Failure Load (lb.)	Remarks
SP-A1	no	26,000	Figure 7-6
SP-A2	no	25,000	
SP-B1	yes	26,600	
SP-B2	yes	27,600	Figures 7-7, 7-8

TABLE 7-2: COMPRESSION PANEL TEST RESULTS

Specimen Number	Boron/Epoxy Reinforced	Failure Load (lb.)	Remarks
CP-A1	no	23,300	
CP-A2	no	22,900	Figure 7- 9
CP-B1	yes	34,500	Figures 7-10
CP-B2	yes	29,500	Figures 7-11

S = shear

P = panel

A = aluminum

B = boron/epoxy

C = compression

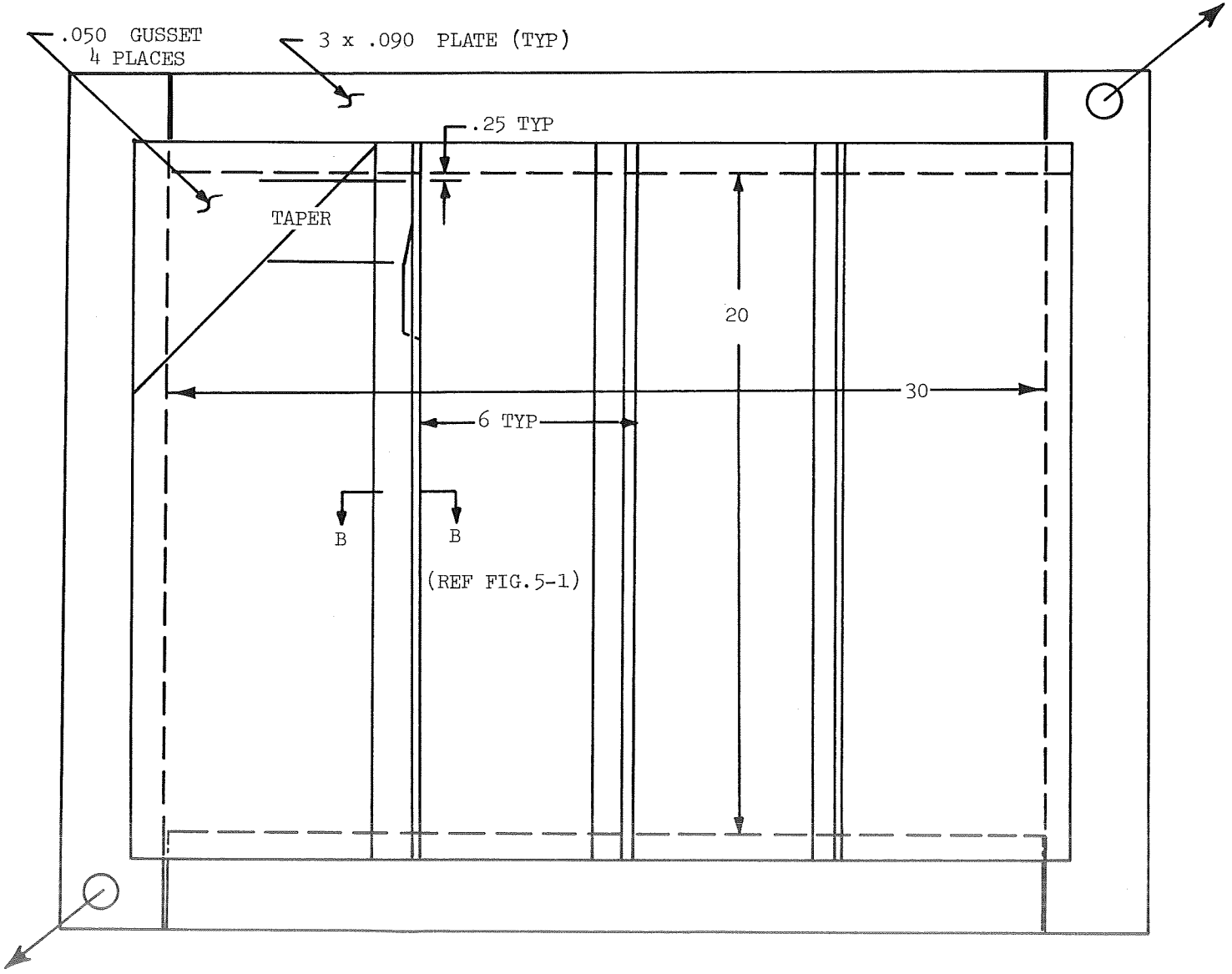

FIGURE 7-1. SHEAR TEST SPECIMEN GEOMETRY.

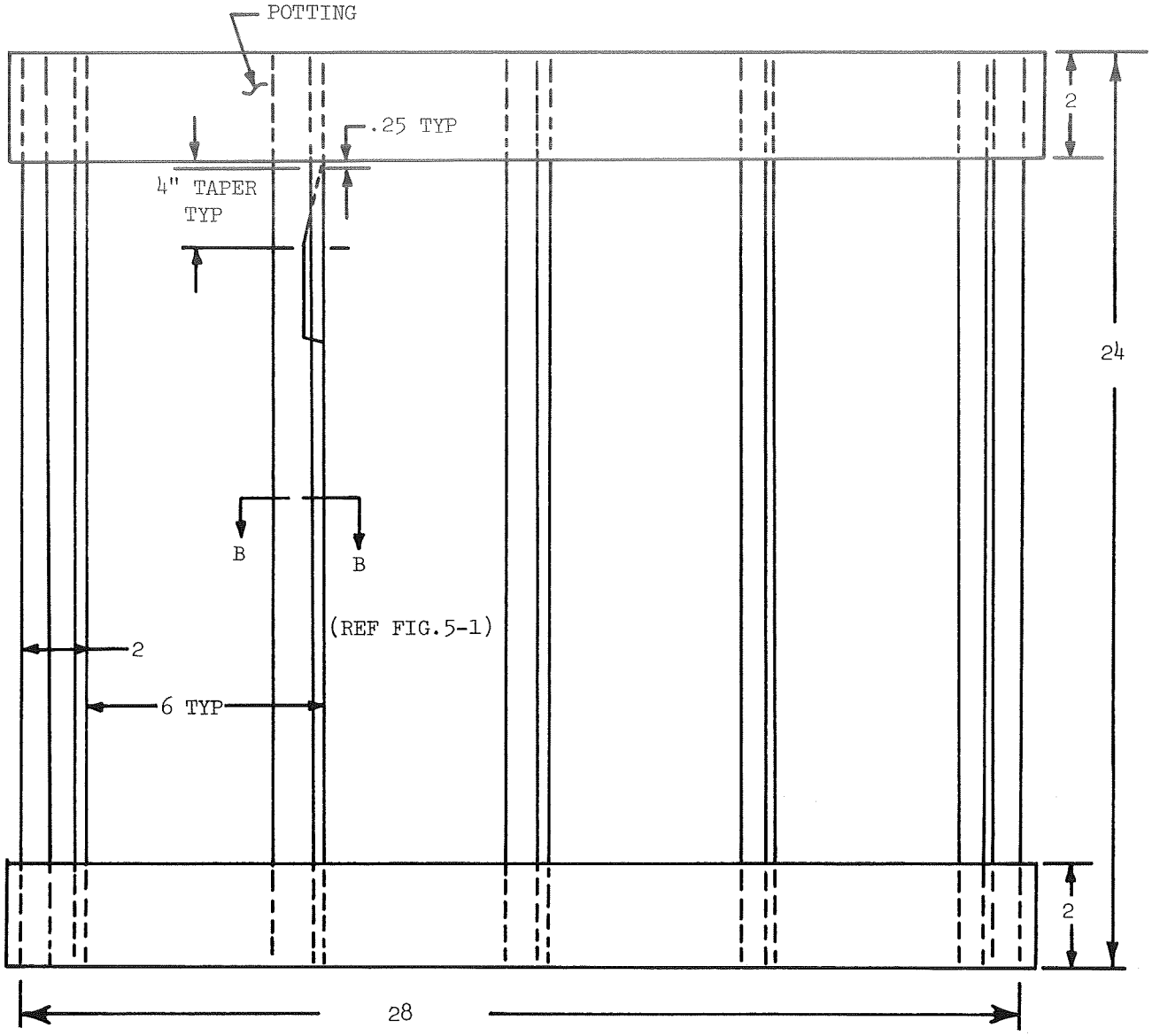

FIGURE 7-2. COMPRESSION TEST SPECIMEN GEOMETRY.

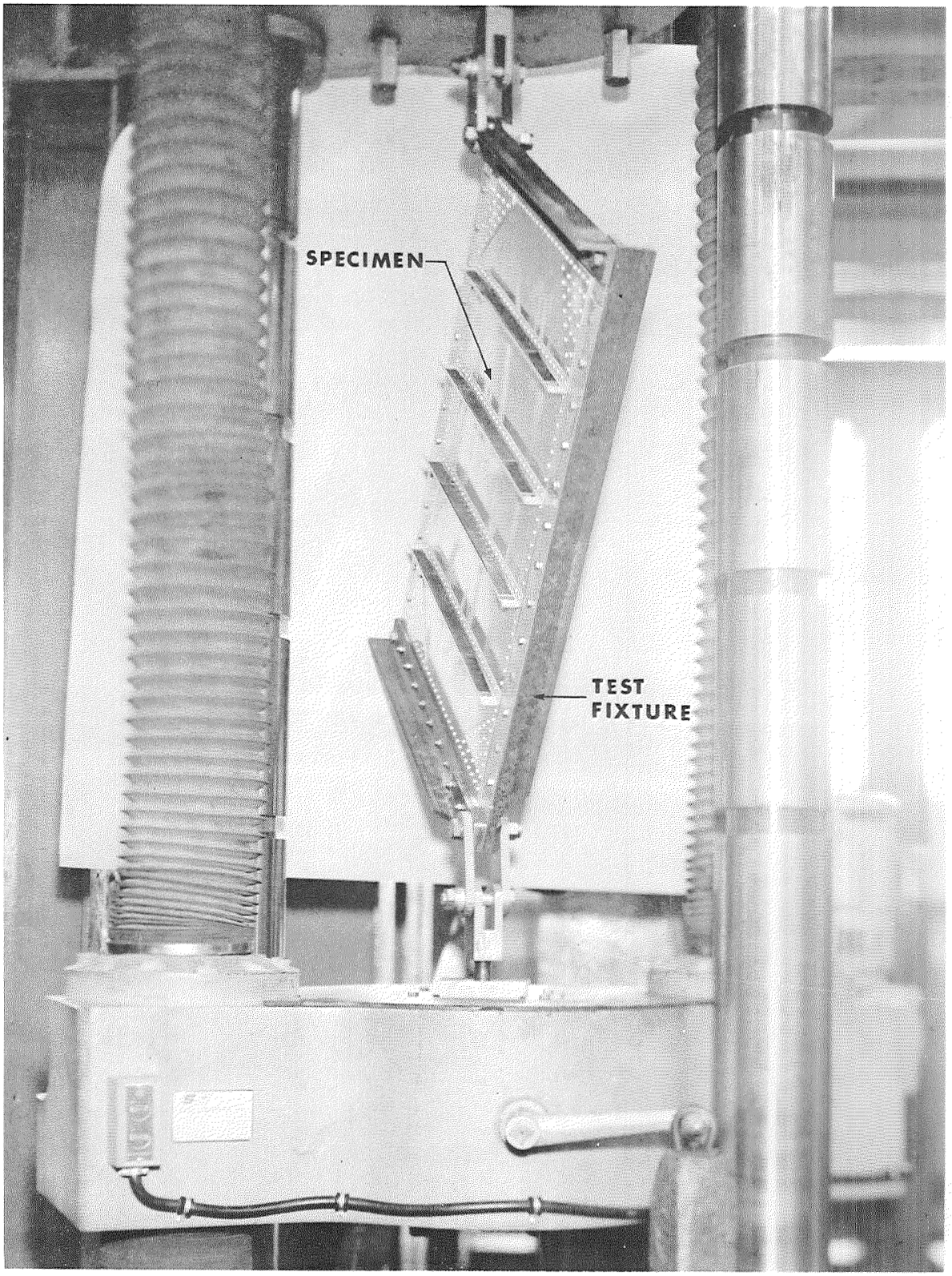

FIGURE 7-3. SHEAR PANEL TEST SET-UP.

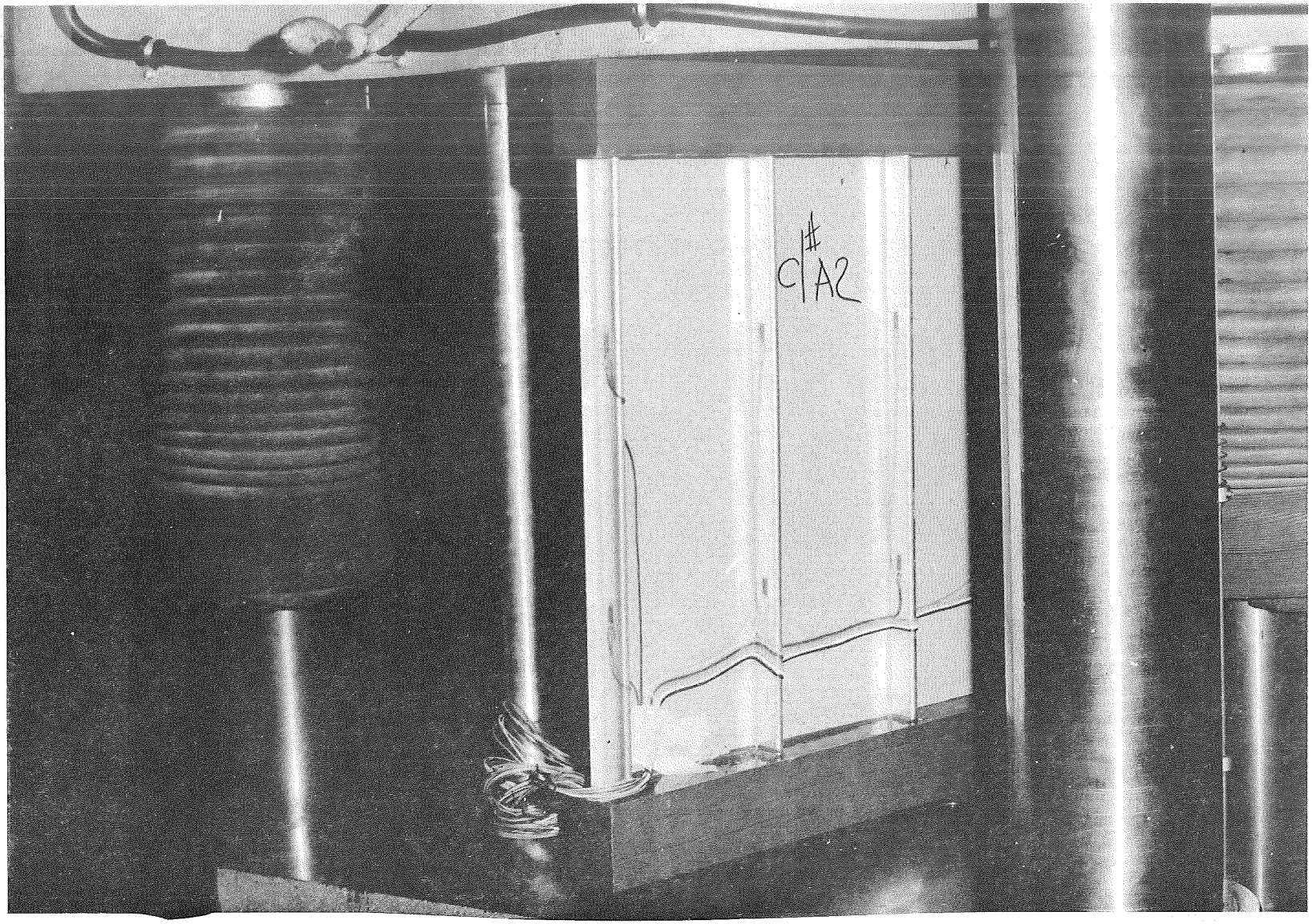

FIGURE 7-4. COMPRESSION PANEL TEST SET-UP.

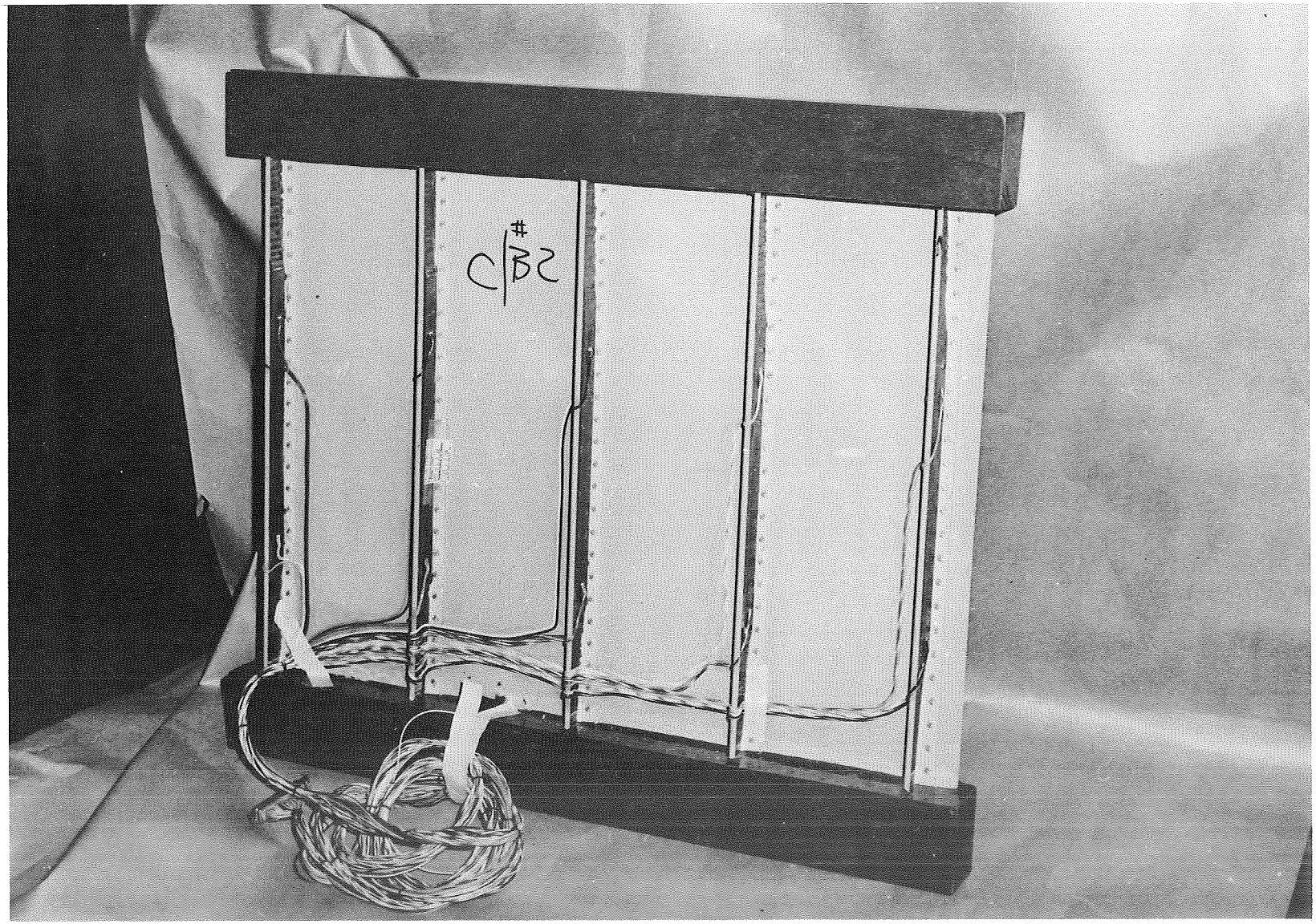

FIGURE 7-5. REINFORCED COMPRESSION TEST PANEL.

FIGURE 7-6. SHEAR FAILURE OF NONREINFORCED TEST PANEL.

FIGURE 7-7. SHEAR FAILURE OF BORON/EPOXY REINFORCED STRINGER TEST PANEL.

FIGURE 7-8. DETAIL OF SHEAR FAILURE OF BORON/EPOXY REINFORCED STRINGER TEST PANEL.

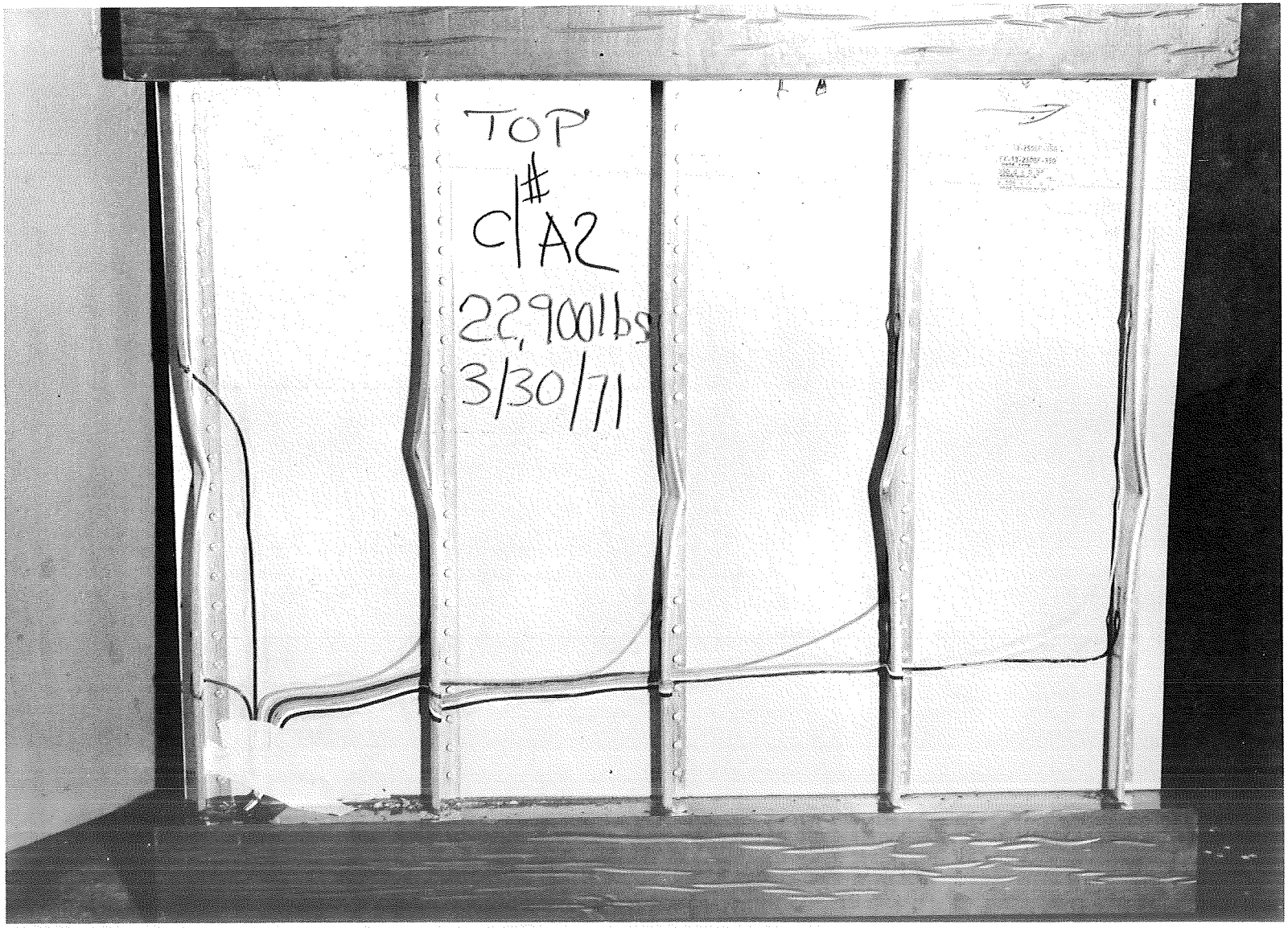

FIGURE 7-9. COMPRESSION FAILURE OF NONREINFORCED TEST PANEL.

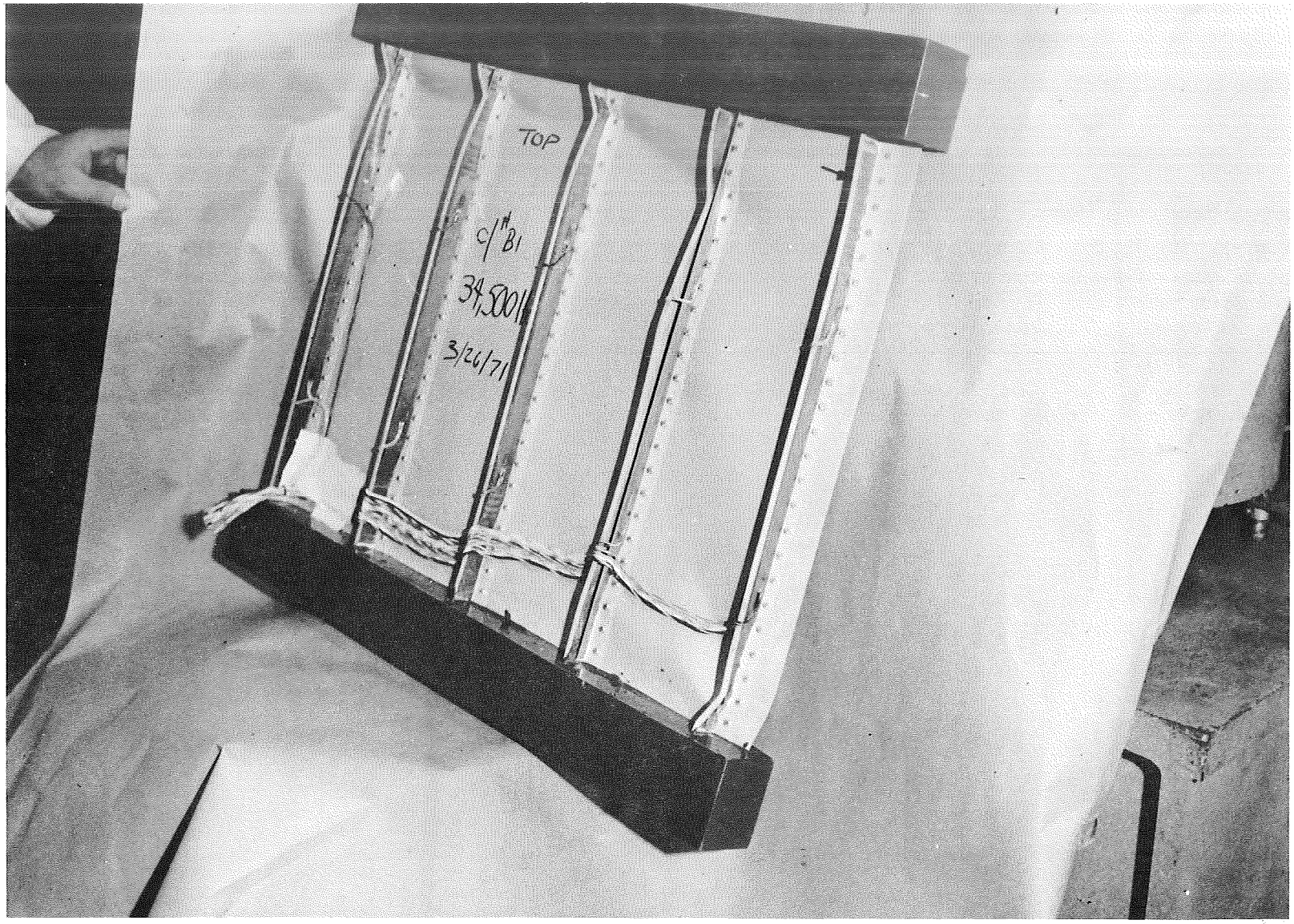

FIGURE 7-10. COMPRESSION FAILURE OF BORON/EPOXY REINFORCED STRINGER TEST PANEL.

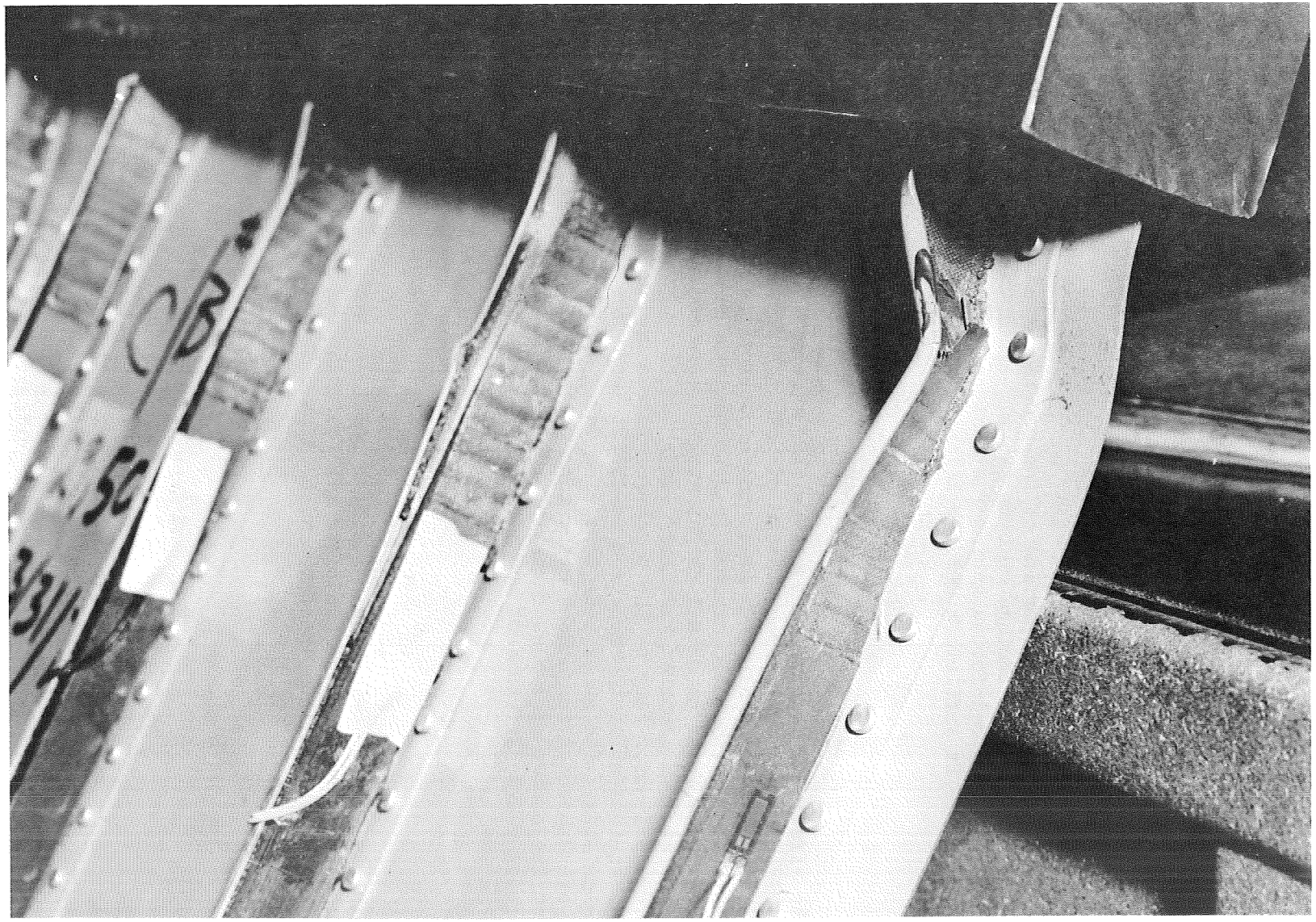

FIGURE 7-11. DETAIL OF COMPRESSION FAILURE OF BORON/EPOXY REINFORCED STRINGER TEST PANEL.

8.0 FATIGUE

Objective

The objectives of this portion of the program were: (1) to evaluate the effect of repeated loadings on both the all-aluminum stringer structure and the boron/epoxy reinforced stringer structure, and (2) to assure that the fatigue life is sufficient for the lifetime of the aircraft.

Approach

The effects of repeated loads were investigated by fatigue testing skin-stringer specimens representative of both the all-aluminum and the boron/epoxy reinforced aluminum tail cone construction. All tests were tension-tension (with ratio minimum load to maximum load R = +.10). The test loads were based on actual flight strain gage measurements and included the maximum measured vibratory loads and the maximum ground-air-ground cycle loads. Four of the boron-reinforced specimens were subjected to loads equivalent to the measured in-flight loads for at least four times the design life. The other specimens, including the three all aluminum ones, were subjected to loads greater than the measured in-flight loads to at least the number of cycles occurring in the anticipated 10,000 hours or the fifteen years lifetime of the aircraft.

Test Specimens

Nine 24-inch by 6-inch skin-stringer specimens were fabricated and tested: three boron/epoxy reinforced with clips; three boron/epoxy without clips; and three aluminum specimens with clips. The test specimen is shown in Figure 5-1.

Test and Results

The test load schedules are listed in Table 8-1, and a summary of the test results is included in Table 8-2. The results are also shown in the S-N diagram of Figure 8-1 which illustrates that the specimens subjected to loads equivalent to the measured in-flight loads (load schedules C and D) meet or exceed the life factor criteria of four (4). Figure 8-1

also shows that the specimens subjected to loads greater than the measured in-flight loads (load schedules A and B) exhibited lives equivalent to 10,000 hours or fifteen years of aircraft service.

Strain-gaged aluminum and boron/epoxy reinforced skin-stringer specimens were subjected to cyclic tensile (fatigue) loading for a predetermined number of cycles as shown in Table 8-1. The specimens were tested in an Ivy-20 Fatigue Test Machine as shown in Figure 8-2. Steady and vibratory tensile loads were applied, and the resulting strain measurements were recorded. As discussed previously, it was not possible to eliminate all bending in the reinforced specimens (see Section 5.0). These specimens were tested in the same manner as the static specimens by eliminating bending in the aluminum and accepting bending in the boron reinforcement. Vibratory strain readings and periodic inspections of the boron/epoxy reinforced stringer with a Fokker Bond Tester were used as an indication of bond deviation. A typical plot of strain reading versus number of cycles is shown in Figure 8-3.

Bond deviations were detected in all fatigue tests, in some cases well before strain deviations occurred. In test panel BCF-3, a bond deviation was detected before testing of the stringer. The bond deviation did not propagate or cause further problems during the testing of the specimen. The number of cycles at which a change in strain occurred was noted, although the load was maintained by the specimen for many more cycles. The number of cycles to strain deviation and to specimen failure or test termination and their ratios to the actual number of cycles applied in 10,000 hours of operation are included in Table 8-3. The boron/epoxy test specimens and their failure modes are shown in Figures 8-4 through 8-9 and are cross-referenced in Table 8-2.

Discussion

Previous experience shows that the CH-54B aircraft flies 600 - 700 hours per year. The airframe life was thus conservatively estimated at 10,000 hours or approximately fifteen years of operations. The test loads used were based on the measured-in-flight stresses. The envelope of these stresses is shown in Figure 8-10. The in-flight vibratory stresses in level flight are generally less than ±1,000 psi, and the highest recorded vibratory stress is ±1,750 psi occurring in an autorotational condition at 100 knots with the maximum rotor rpm. This flight condition occurs for .24% of the aircraft time with a frequency of 4.2 cycles per second. Thus, the low stress/high cycle flight condition produces 364,000 load cycles in 10,000 hours of aircraft operation.

The high stress/low cycle repeated stress is obtained from the condition of lift-off (5,640 psi) to a climb at 70 knots and 9,000 feet (-9,500 psi), thus the repeated load ranges from 5,640 to -9,500 psi (-1,930 ±7,570 psi). The ground-air-ground frequency is 2.38

cycles per flight hour, which in 10,000 hours of aircraft service produces 23,800 cycles of repeated loading.

The gross area of the aluminum skin and stringer is .331 square inches, and the test loads were therefore the stresses times the stringer area of .331.

The vibratory stress versus steady stress diagram of Figure 8-11 indicates the actual stresses and the stresses used for test. The R = +.10 line was used for testing. The test schedule is shown in Table 8-1, and the loading cases denoted by conditions A through D. Schedule A is more severe than the actual ground-air-ground cycles because of its higher steady stress. The Goodman Diagram included in Fig. 8-11 is a line of constant fatigue damage for aluminum alloy structure with a yield strength of 47,000 psi. Thus Schedule C, which is the point on the Goodman Diagram for R = +.10, is equivalent to the measured ground-air-ground cycle stresses. The high cycle-low stress in-flight fatigue stresses are close to the R = +.10 line and thus the vibratory stress of Schedule D is maintained at the level of the in-flight vibratory stress of 1,750 psi. Fatigue tests of aluminum alloy structures show considerable scatter of the fatigue strength. Statistical analysis shows that the strength for a high reliability (.999) is only 61% of the mean strength. Thus, the loads of test Schedule B are those of Schedule D increased by a factor of 1/.61 or 1.64.

The ground-air-ground stress cycle includes the most severe take off, in-flight, and landing conditions and the in-flight vibratory stresses are the maximum measured. It would thus be too severe a condition to subject each specimen to both type load schedules. Thus since each test specimen is subjected to constant loading only, no cummulative damage due to variable load levels occurs.

Initially, the concept of testing was to provide a statistical com parison with the known fatigue data for aluminum construction. However, there is insufficient statistical information on bonded joints to make a valid criteria, and it was decided that a criteria of a life factor of 4 would be more than sufficient to assure the integrity of the structure.

All of the nonreinforced stringers completed the required fatigue testing and were retired at the completion of each test.

All of the reinforced specimens experienced changes in the integrity of the boron composite-to-stringer bond during testing. These changes ranged from a deviation of the bond in the tapered load transfer region of the boron to disbond of some areas of the boron reinforcement.

It was difficult to determine where the bond deviations initiated within the boron composite; however, most of the changes were initially detected in the tapered load transfer region at the end of the constant boron composite section.

No bond failures were detected in the area of the clip attachment holes. For these reasons the tapered load transfer region was considered the critical section in fatigue. From Table 8-3 for the tests with equivalent tail cone stresses and increased number of cycles (Load Schedules C and D), it is seen that:

(1) The ratio of applied test cycles to service cycles ranged from 4.1 to 7.3 with no strain deviation occurring.

(2) For the tests with increased loads (Load Schedules A and B), the number of applied cycles exceeded the service cycles, though in the case of specimens BF-1 (Test No. 4) and BF-2 (Test No. 5), strain deviations did occur. It is emphasized that, even though strain deviations indicating some loss of load transfer capability within the bond were detected, all the boron reinforced stringers successfully carried the fatigue loads, thus showing that a service life of 10,000 hours or approximately fifteen years is attainable.

Conclusions and Recommendations

Based on the results of the fatigue tests it is concluded that:

(1) Both the all-aluminum and the boron-reinforced structures have satisfactory service life.

(2) The attachment of clips to the reinforced stringers has no adverse effect on the reinforcement bond integrity.

(3) The boron/epoxy composite reinforced stringer specimens experienced bond deviations as a result of fatigue testing.

(4) Location of bond deviation origin is difficult; however, the tapered load transfer region of the boron composite appears to be the critical section in fatigue.

(5) The deviations of the bond strength did not reduce the overall fatigue strength of the structure below the anticipated 10,000 hours of service usage.

Based on the results of the tests presented in this section, it is recommended that design analysis and testing be performed to determine more specifically the load transfer characteristics of a typical tapered boron/epoxy joint.

TABLE 8-1 FATIGUE TEST LOAD SCHEDULES.

SCHEDULE	CONDITION	APPLIED STRESS psi	APPLIED LOAD lbs.	MAXIMUM LOAD lbs.	NUMBER OF CYCLES x 10^{-6}
A	Ground-Air-Ground, Actual Amplitude, Increased Cycles	9250 ± 7570	3080 ± 2520	5600	.173
B	In-Flight Vibratory, Increased Load, Actual Cycles.	3510 ± 2870	1180 ± 960	2140	.364
C	Ground-Air-Ground Equivalent Amplitude, Increased Cycles.	7460 ± 6120	2475 ± 2025	4500	.173
D	In-Flight Vibratory, Actual Load, Increased Cycles.	2140 ± 1750	710 ± 580	1290	1.50

TABLE 8-2. FATIGUE TEST RESULTS

Test No.	Specimen No.	Boron/Epoxy Reinforced	Clips at Midpoint	Load Schedule	Applied Test Cycles x 10^{-6}	Remarks
1	Al F-1	no	yes	A	0.175	Test stopped after reaching required cycles.
2	Al F-2	no	yes	B	0.365	Test stopped after reaching required cycles.
3	Al F-3	no	yes	A	0.175	Test stopped after reaching required cycles.
4	B F-1	yes	no	A	0.159	Cracked stringer through attachment bolt hole. Figure 8-4.
5	B F-2	yes	no	B	1.541	Test stopped at 1.5×10^6 cycles. Figure 8-5.
6	BC F-1	yes	yes	C	0.175	Test stopped at required cycles. Figure 8-6.
7	BC F-2	yes	yes	D	1.500	Test stopped at required cycles. Figure 8-7.
8	BC F-3	yes	yes	C	0.127	Cracked stringer through attachment bolt hole. Figure 8-8.
9	BC F-4	yes	yes	D	1.500	Test stopped at required cycles. Figure 8-9.

Al - aluminum
F - fatigue
B - boron reinforced
BC - boron reinforced with clip

TABLE 8-3. FATIGUE CYCLE RATIOS

Test No.	Specimen No.	Load Schedule	Service Cycles (in 10,000 hrs.)	Cycles to Strain Redistribution	Applied Test Cycles	Ratio Applied Test Cycles/ Service Cycles
1	A1 F-1	A	$.024 \times 10^6$	b	$.175 \times 10^6$	7.3
2	A1 F-2	B	$.364 \times 10^6$	b	$.365 \times 10^6$	1.0(a)
3	A1 F-3	A	$.024 \times 10^6$	b	$.175 \times 10^6$	7.3
4	BF-1	A	$.024 \times 10^6$	$.045 \times 10^6$	$.159 \times 10^6$	6.6
5	BF-2	B	$.364 \times 10^6$	$.200 \times 10^6$	1.541×10^6	4.2(a)
6	BCF-1	C	$.024 \times 10^6$	b	$.175 \times 10^6$	7.3
7	BCF-2	D	$.364 \times 10^6$	b	1.500×10^6	4.1
8	BCF-3	C	$.024 \times 10^6$	b	$.127 \times 10^6$	5.3
9	BCF-4	D	$.364 \times 10^6$	b	1.500×10^6	4.1

a With Load Schedule B, a cycle ratio of 1.0 is satisfactory since the test is run at increased load rather than increased cycles.

b No strain redistribution in test life

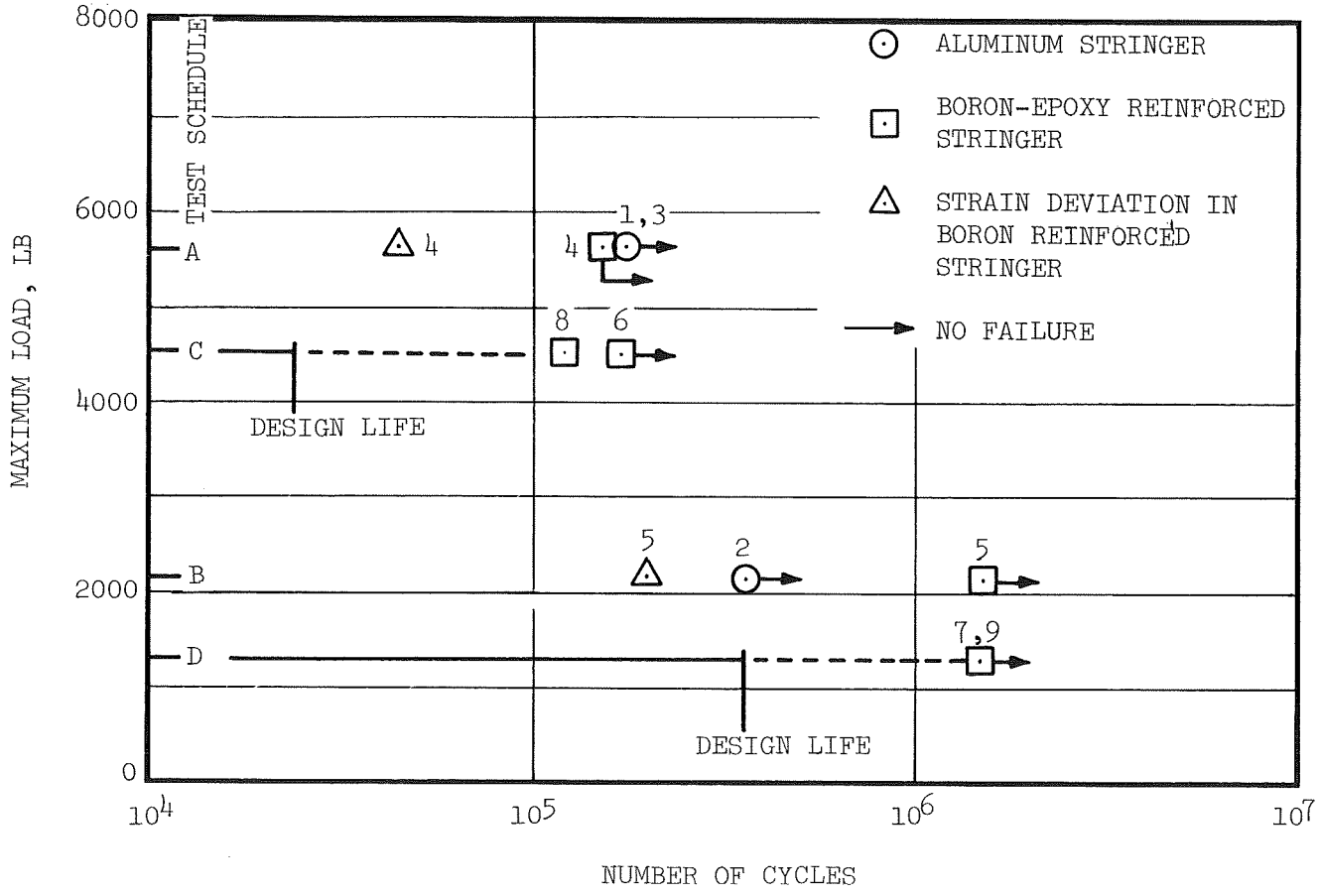

FIGURE 8-1. LOAD/CYCLE TEST RESULTS FOR BORON/EPOXY REINFORCED STRINGERS.

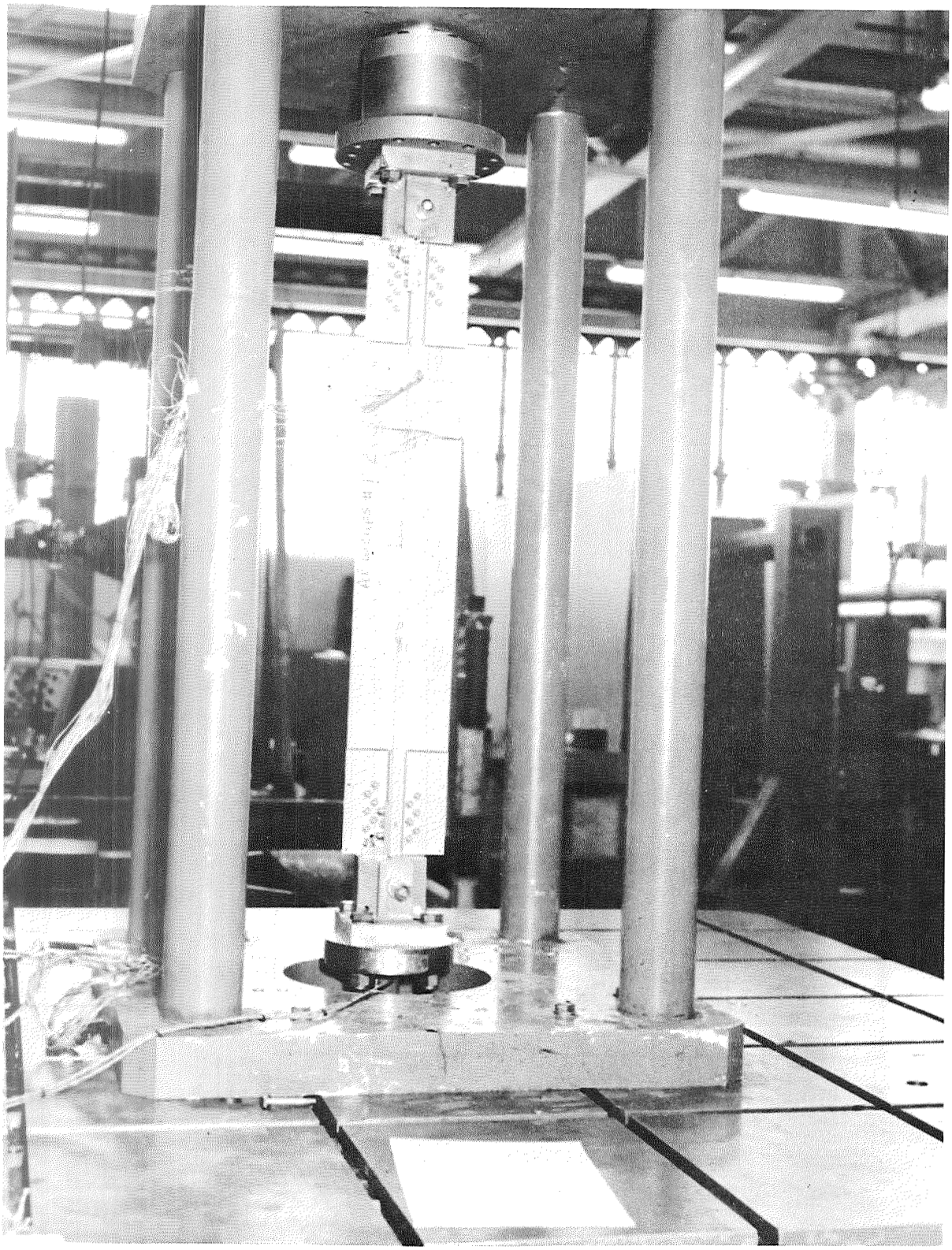

FIGURE 8-2. FATIGUE TEST SET-UP.

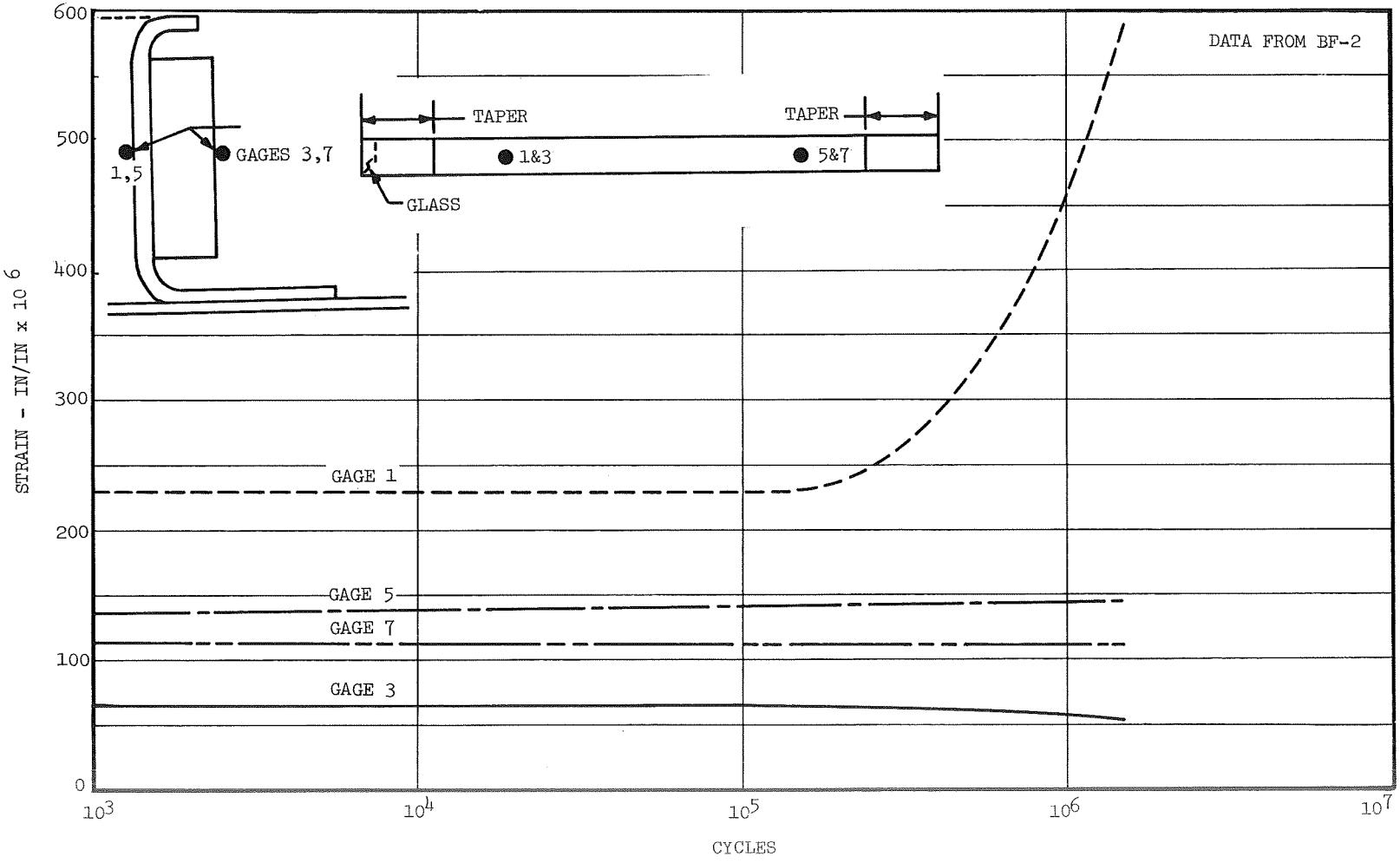

FIGURE 8-3. MEASURED VIBRATORY STRAIN VERSUS CYCLES FOR BORON/EPOXY REINFORCED STRINGER.

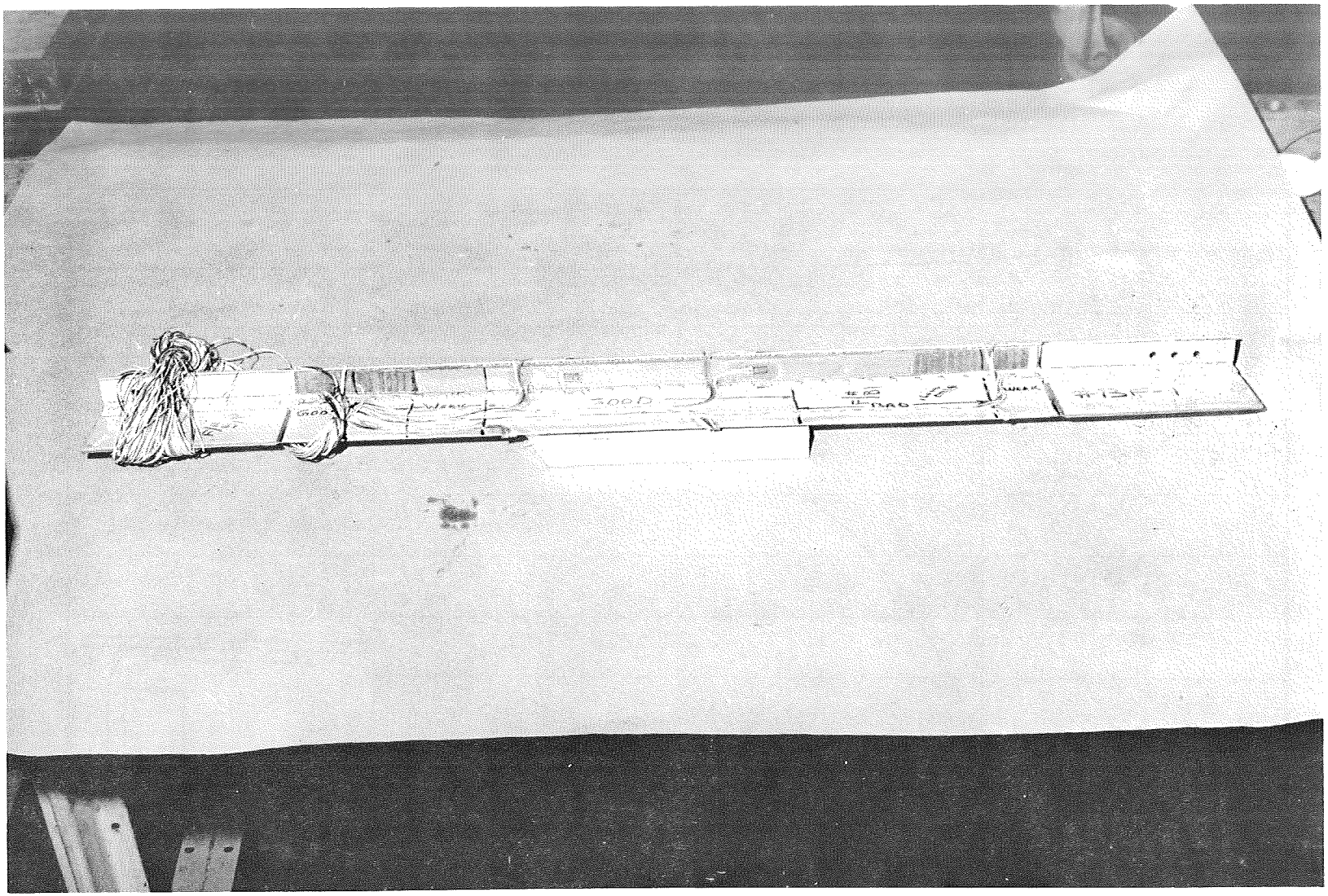

FIGURE 8-4. REINFORCED FATIGUE TEST SPECIMEN AT COMPLETION OF TESTING - NO CLIPS - APPLIED CYCLES 0.159×10^{-6}.

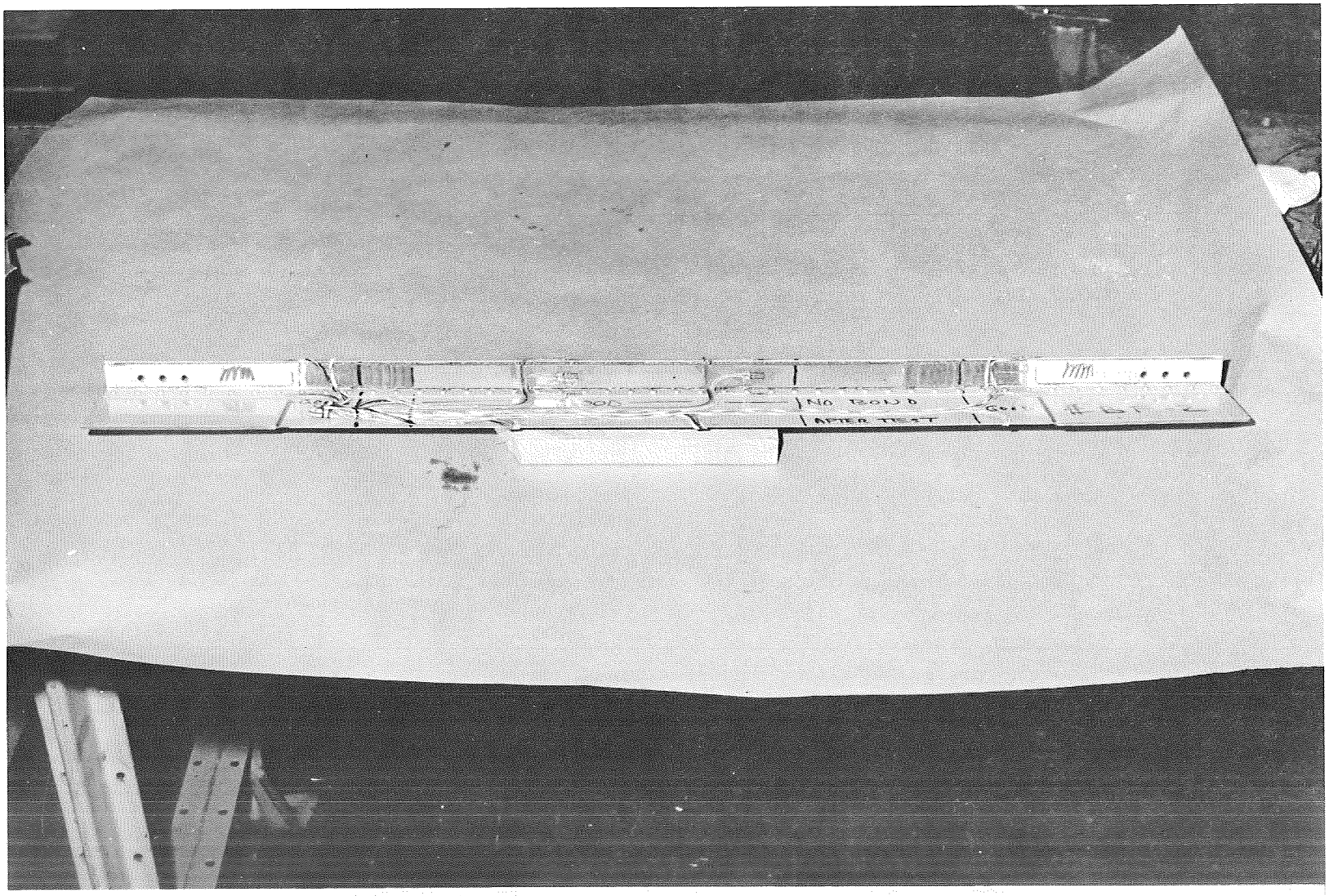

FIGURE 8-5. REINFORCED FATIGUE TEST SPECIMEN AT COMPLETION OF TESTING - NO CLIPS - APPLIED CYCLES 1.54×10^{-6}.

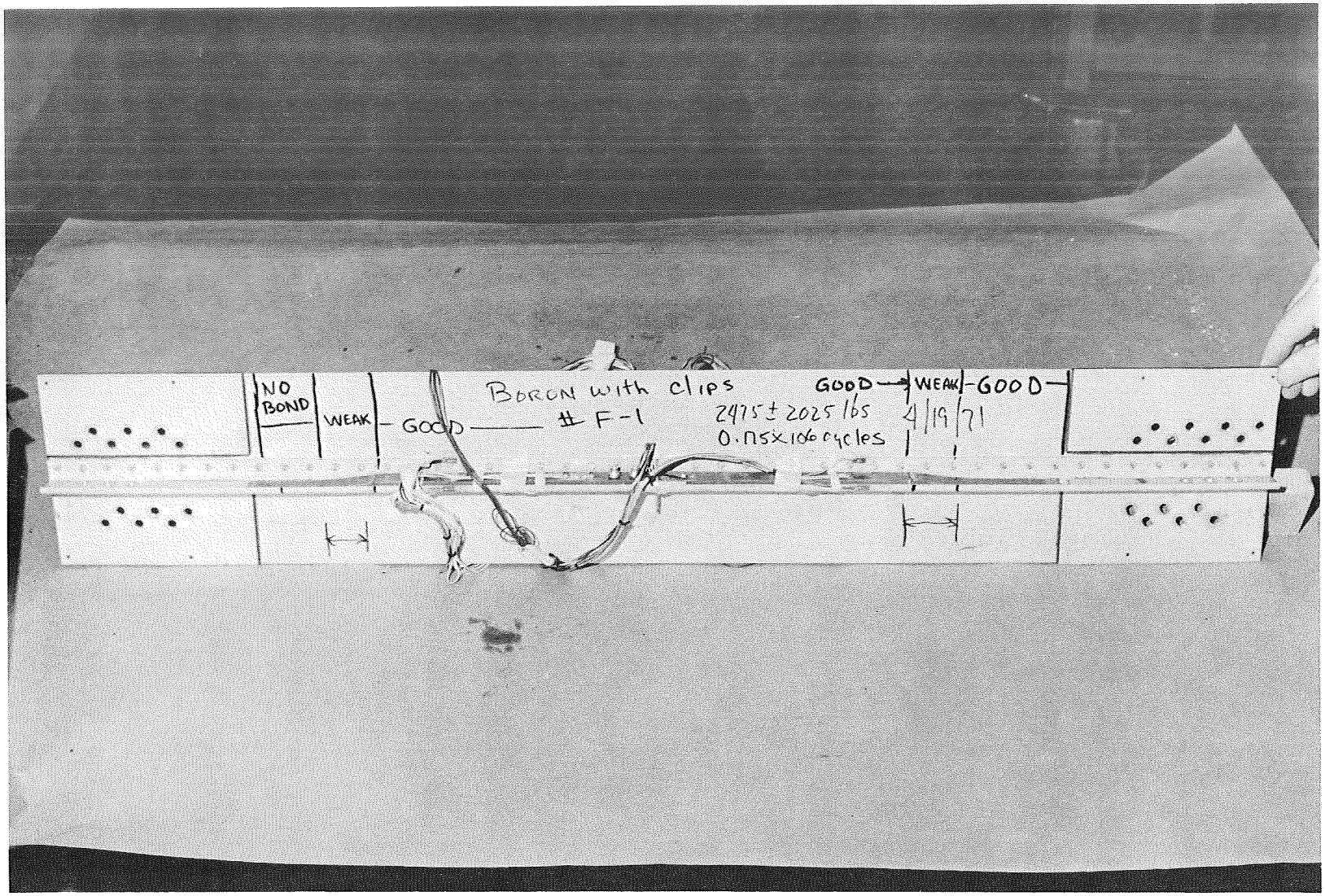

FIGURE 8-6. REINFORCED FATIGUE TEST SPECIMEN AT COMPLETION OF TESTING - WITH CLIPS - APPLIED CYCLES 0.175 x 10^{-6}.

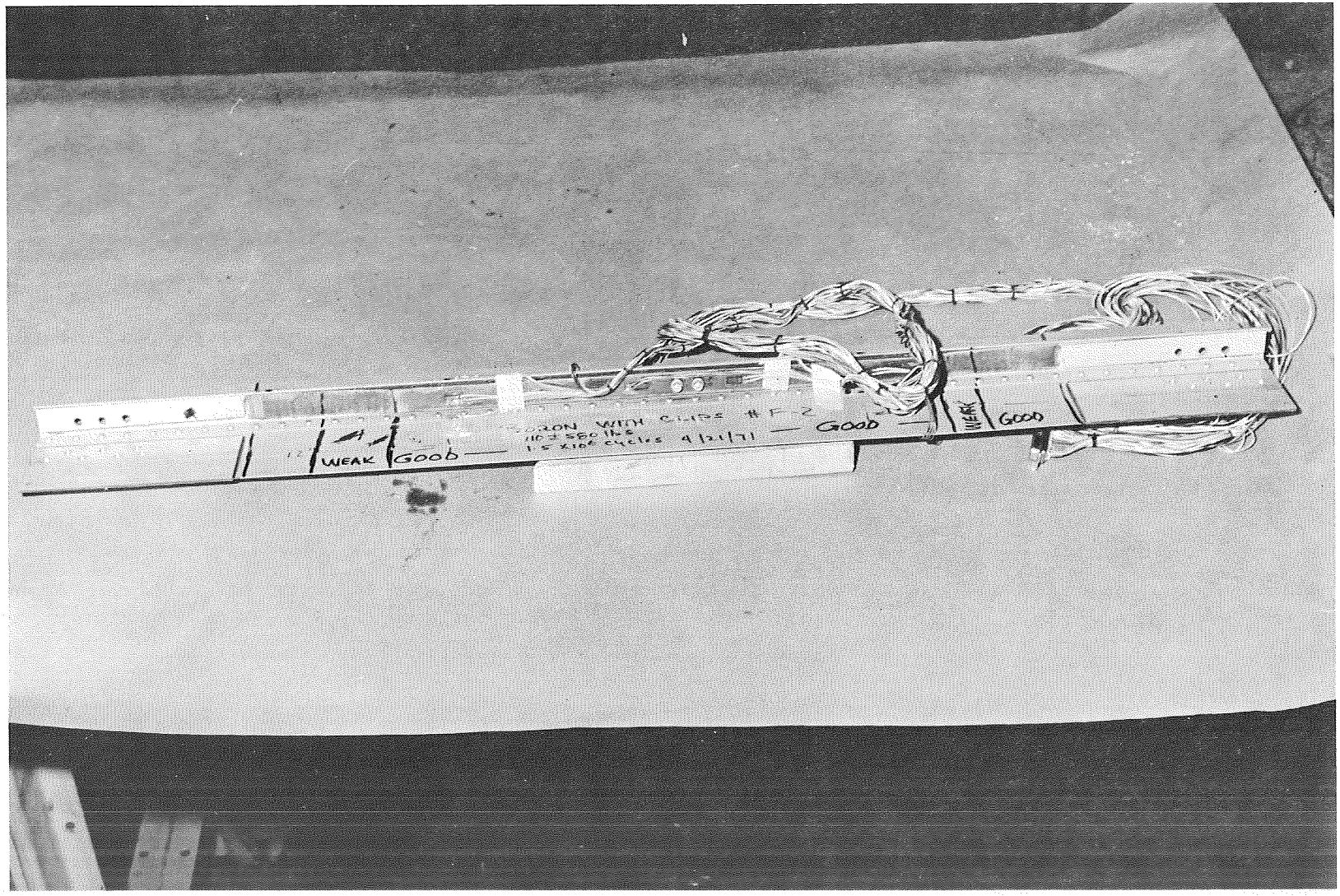

FIGURE 8-7. REINFORCED FATIGUE TEST SPECIMEN AT COMPLETION OF TESTING - WITH CLIPS - APPLIED CYCLES .127 x 10^{-6}.

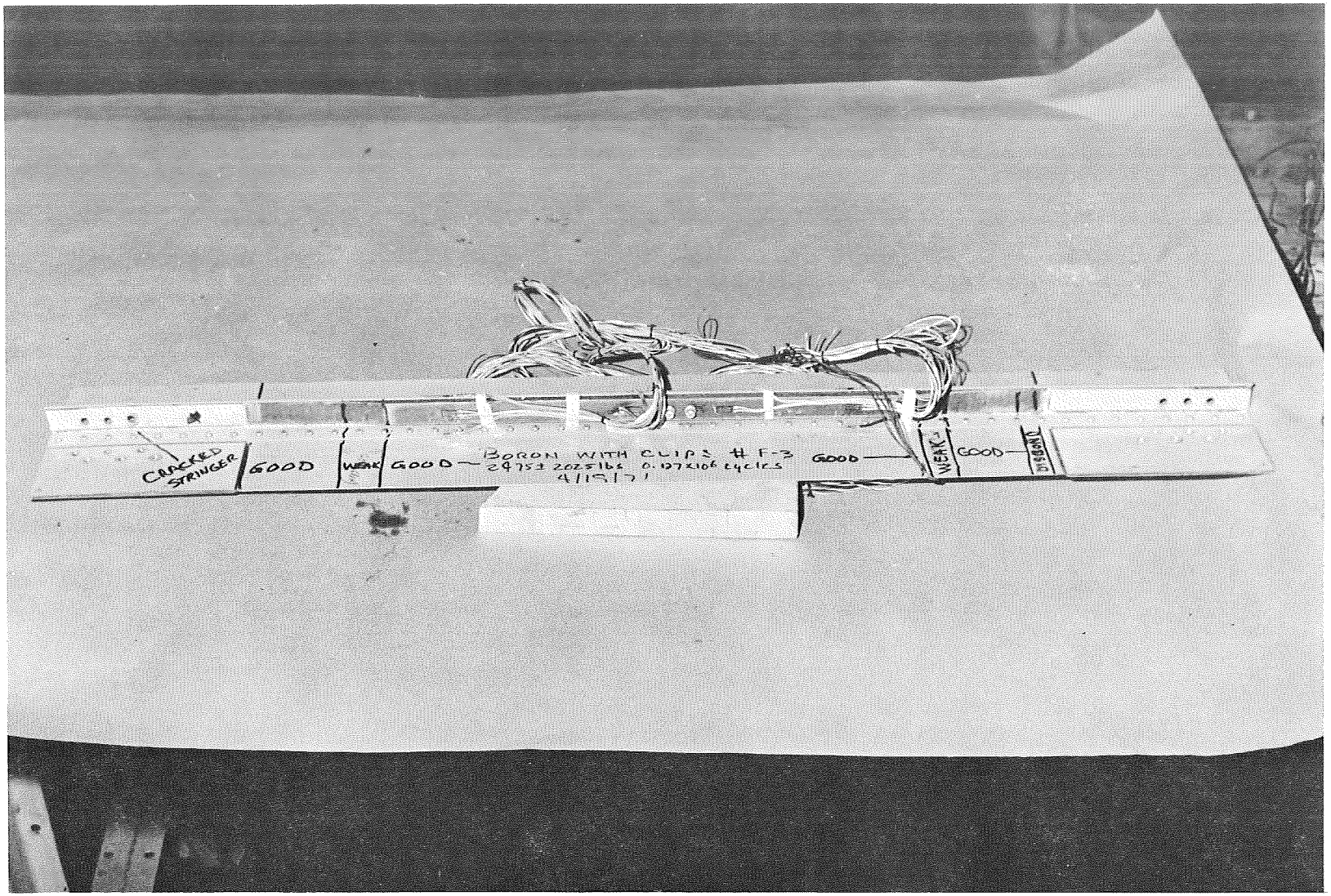

FIGURE 8-8. REINFORCED FATIGUE TEST SPECIMEN AT COMPLETION OF TESTING - WITH CLIPS - APPLIED CYCLES 1.5×10^{-6}.

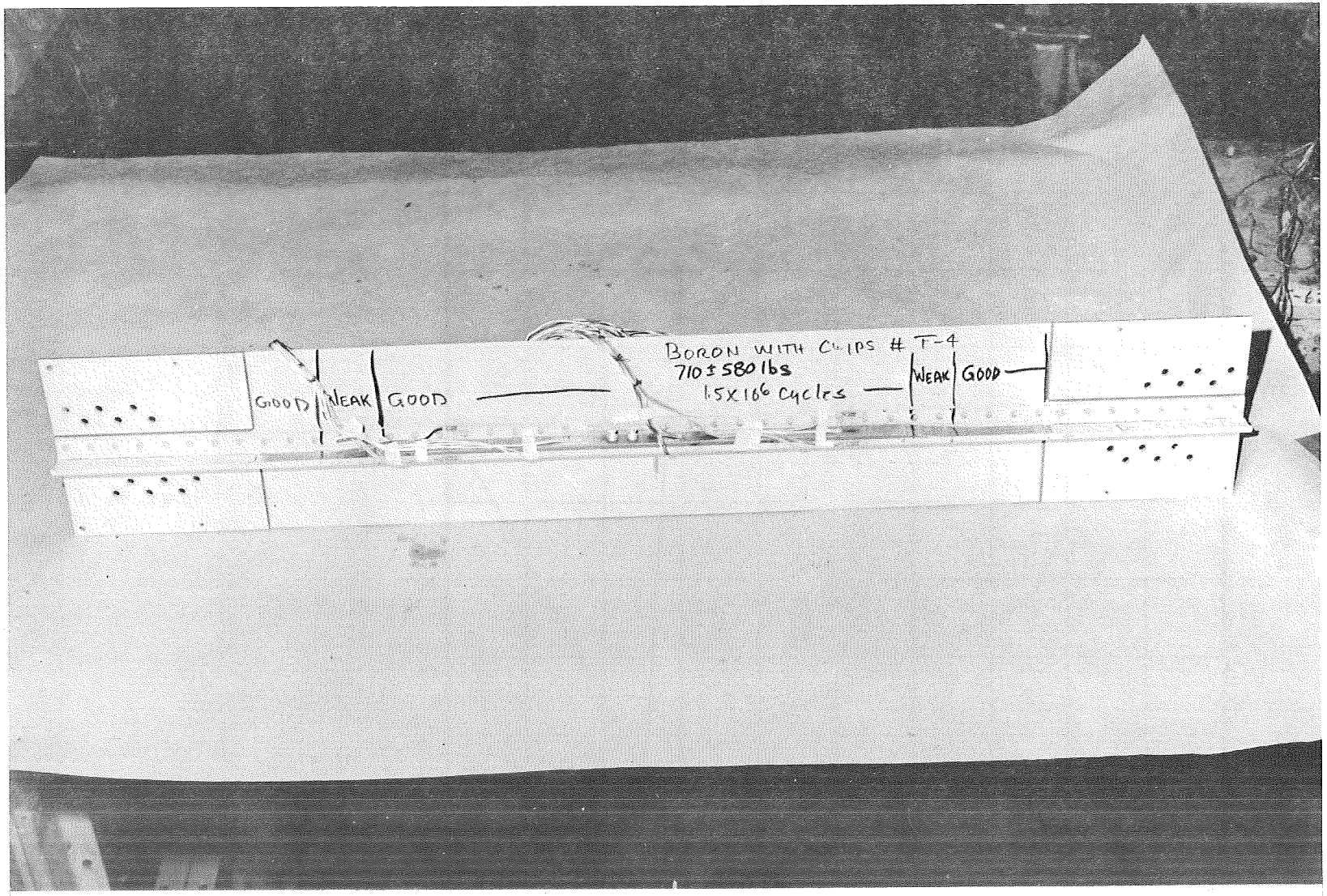

FIGURE 8-9. REINFORCED FATIGUE TEST SPECIMEN AT COMPLETION OF TESTING - WITH CLIPS - APPLIED CYCLES 1.5 x 10^{-6}.

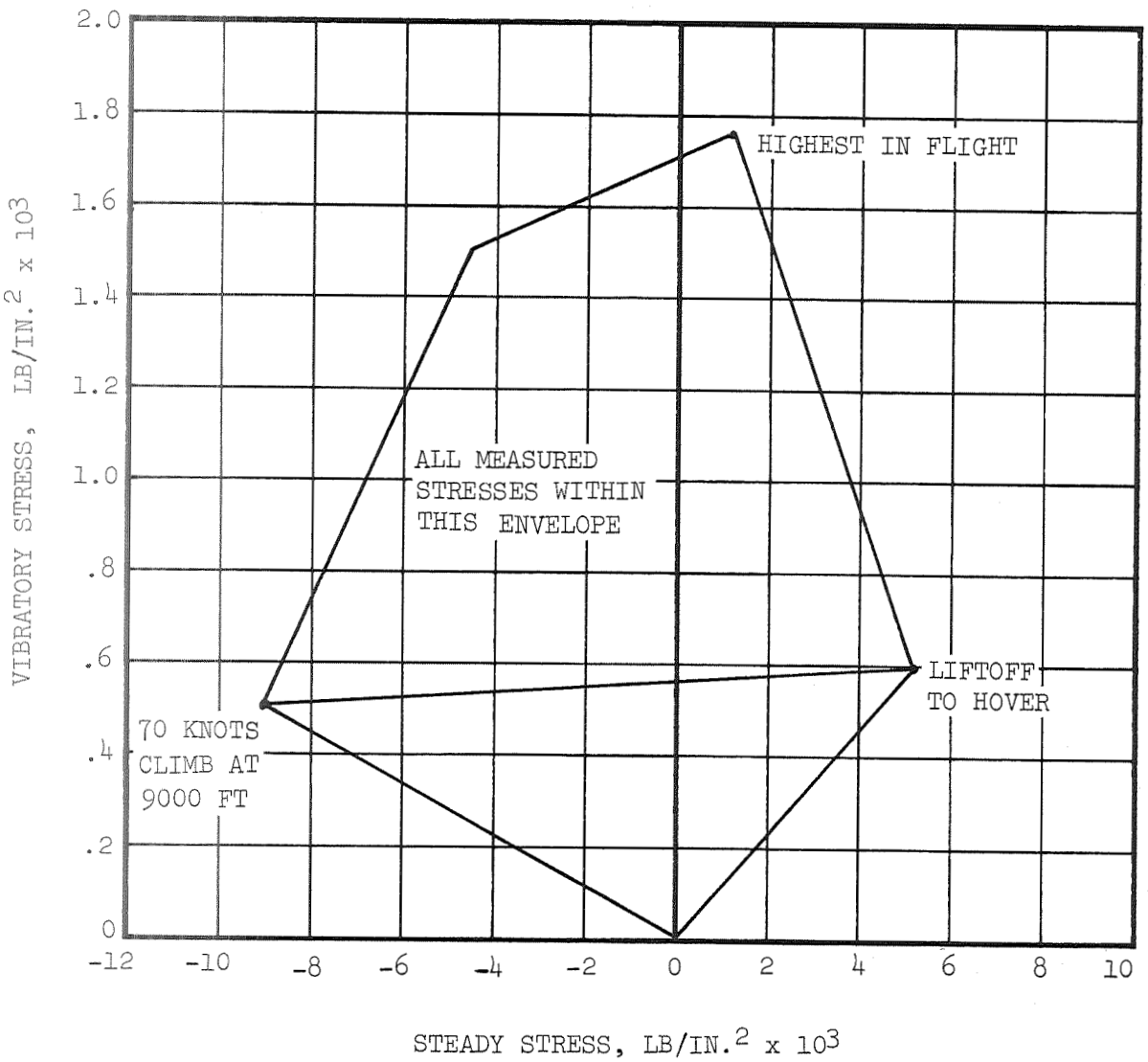

FIGURE 8-10. ENVELOPE OF MEASURED IN-FLIGHT STRESSES.

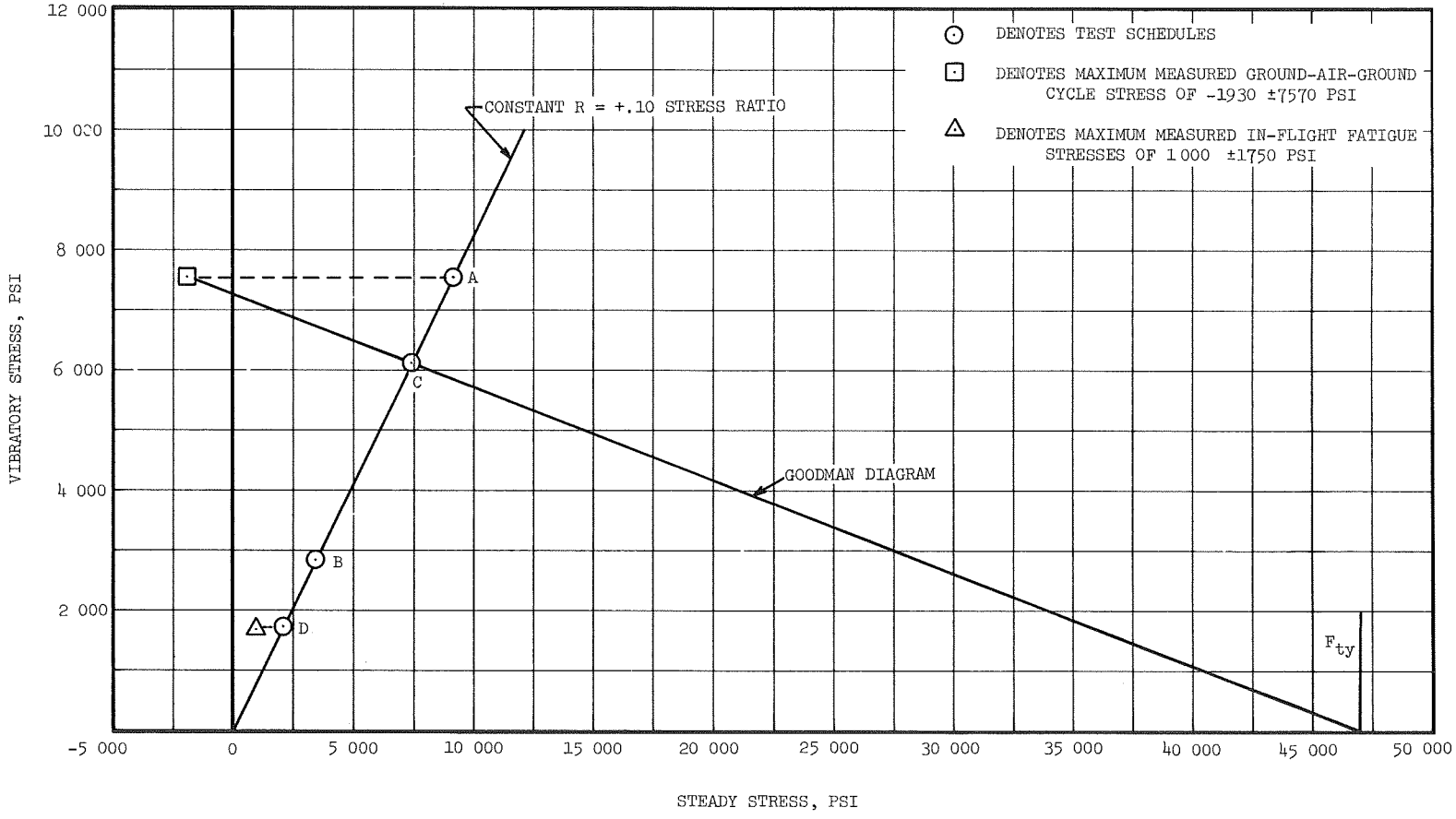

FIGURE 8-11. ACTUAL AND TEST VIBRATORY VERSUS STEADY STRESSES.

9.0 SERVICEABILITY

Objective

The objective of this study was to determine a method of inspecting the bond integrity of the boron/epoxy reinforced stringers in the field and to establish a field repair procedure to follow in the event of disbonds.

Approach

For field inspection, the coin tap method of determining bond deviations is recommended. This method has been used in this program for inspecting all test specimens before and after testing. The results have been confirmed by use of the Fokker Bond Tester.

Three types of disbond are assumed and their recommended field repairs outlined. The assumed disbond types are: complete stringer disbond over the entire length, no bond between frames, and no bond at a tapered end. The various assumed disbond cases are shown in Figure 9-1.

The static strength capability of the tail cone is maintained in the event of complete or partial disbond in one or all reinforced stringers as shown in the analysis of Reference 1.

Field Repairs

In the event of a disbond over the entire length of stringer, a steel strap one inch wide and 0.25 inches thick can be riveted to the skin and stringer. The strap material is to be 4130, 125,000 H.T. steel. A conventional primer, used with dissimilar metals, is to be used.

This type of repair will maintain the stiffness of the assumed disbond reinforcement. The repair is not needed for static strength. The loose boron strips will be held in place by the Hi-Lok fasteners at the fuselage frames.

In the event of a disbond between frames, it is recommended that a Hi-Lok fastener be inserted in the predrilled hole made in the boron/epoxy

reinforcement. A convetional drill is all that is required as the drill must go through only the aluminum stringer.

The boron/epoxy reinforcement has a critical column length of approximately ten inches. The Hi-Lok fastener will provide the necessary column support. The load transfer between the boron/epoxy reinforcement and aluminum stringer is low when away from the ends, and the disbond is not expected to propagate based upon the results of the fatigue test made with a debonded area, Reference Section 8.

In the event of a disbond at a tapered boron/epoxy end, a room temperature bond is to be made. A clamp is to be applied to the stringer at the frame and the boron/epoxy pried away from the stringer as shown in Figure 9-2. The surface is to be cleaned with trichlorethylene and bonded with ADX-372 Hysol adhesive. The stringer is to be clamped until the bond is cured. The recommended cure cycle varies from 15 minutes at 250° F. to 72 hours at room temperature.

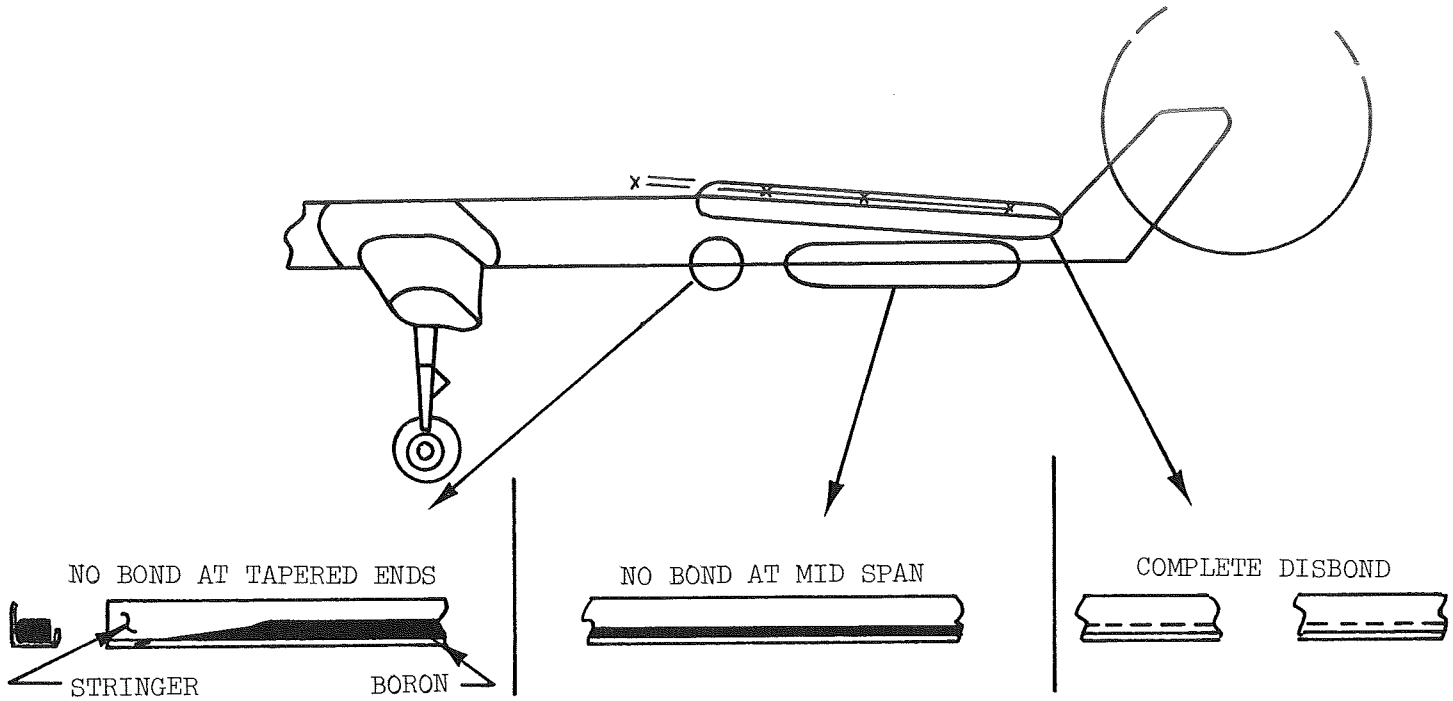

FIGURE 9-1. TYPES OF ASSUMED TAIL CONE NO-BOND AREAS.

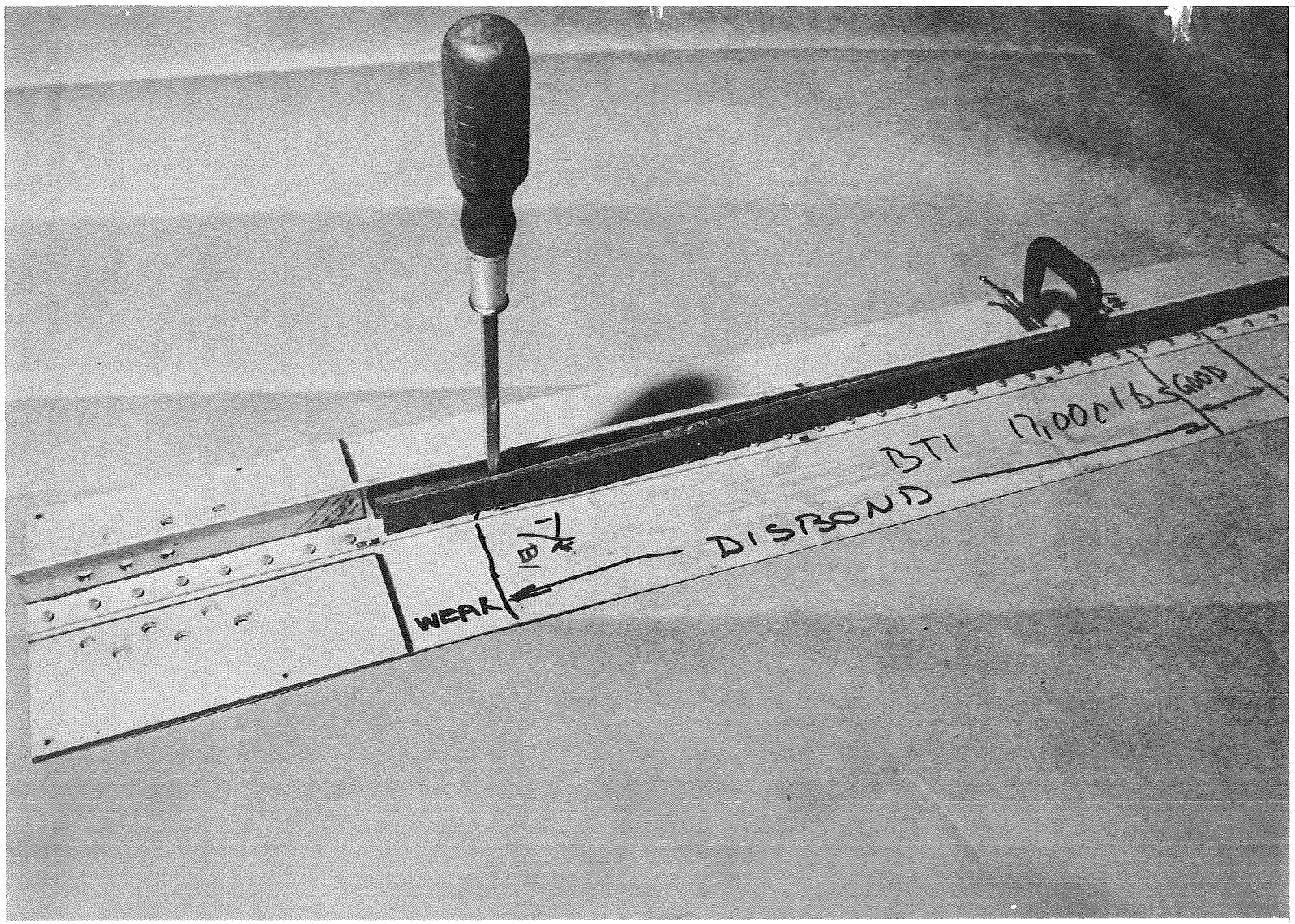

FIGURE 9-2. FIELD REPAIR PROCEDURE FOR TAPERED END.

10.0 SUMMARY OF CONCLUSIONS AND RECOMMENDATIONS

Tail Cone Design/Analysis

The tail cone of the CH-54B helicopter was redesigned to use bonded boron/epoxy stiffened aluminum stringers and reduced thickness skins. It was shown that positive margins of safety existed in all flight conditions even with complete and partially debonded reinforcement. Minor modifications to the original design, in the form of skin gages and panel breakers, were required. The structural stiffness of the present CH-54B was maintained with the boron/epoxy reinforced stringers.

A flight test program is planned for Phase II to confirm the structural integrity and tail cone stiffness analysis.

The taper geometry of the boron/epoxy reinforcement, developed in this study, was such that the adhesive shear stresses and adherend direct stresses were of an acceptable magnitude. The insertion of two layers of unidirectional fiberglass/epoxy at the ends of the tapered joint reduced the peak adhesive shear stress by approximately 53 per cent. The fiberglass insert is recommended for fabrication into the prototype reinforced stringers.

The maximum adhesive shear stress in the 12.5-inch-long taper recommended for the tail cone construction is equal to or less than the tested 4-inch taper.

Fabrication

The fabrication and assembly of representative boron/epoxy reinforced stringers have provided the technical information, tooling, and structural confidence for the production of prototype parts.

The residual stresses in the hybrid boron epoxy/aluminum stringers were found to be readily predictable by analysis. These stresses were included in the structural analysis of the tail cone.

Bond deviations were determined by the coin tap and Fokker bond test method of inspection. Although some of these deviations were identified with specific types of bond discrepancies (voids, peel ply), considerable R&D is needed in this area to positively relate adhesive bond structural integrity to specific ultrasonic indications.

Field inspection and repair of the boron/epoxy reinforced stringer can be made using conventional equipment and materials.

Testing

The tensile strength of the boron/epoxy reinforced and nonreinforced stringers were found to be the same. The elastic strain of the reinforced specimens, however, was found to be one-third that of the aluminum specimens.

The experimentally determined area modulus product for the reinforced and nonreinforced stringer agreed with the predicted values. The proportions of the boron/epoxy reinforcement is such that the area modulus of the reinforced stringer is equivalent to that of the current production aluminum skin/stringer combination.

The shear and compression strengths of the tested boron/epoxy reinforced panels were found to be equal to or slightly better than conventional aluminum panels. The limiting factor in the hybrid panel tests was the basic aluminum structure. In the shear test, failure occurred by aluminum skin tearing at the rivets. In the compression test, local crippling of the aluminum stringers was the failure mode.

For future designs it is recommended that combined shear and axial load tests be made and correlated with analysis.

Fatigue tests of the boron/epoxy reinforced stringers showed that these members when subjected to loads equivalent to the measured in-flight loads meet or exceed a life factor of four. The specimens subjected to loads greater than the measured in-flight loads exhibited lives equivalent to 10,000 hours or fifteen years of aircraft service.

The noted bond deviations did not reduce the overall fatigue strength of the structure below the anticipated service useage.

The attachment of clips to the reinforced stringers had no adverse effect on the fatigue behavior of the stringers.

11.0 REFERENCES

1. Lowry, D. W., Ciardullo, S., "CH-54B Boron/Epoxy Reinforced Tail Cone Detailed Structural Substantiation," (NASA-CR-111930), May 1971.